



Fall 2022

Elucidating the Mechanisms Underlying How VMP1 Regulates Inflammatory Responses

Stephanie Zack

Follow this and additional works at: https://ecommons.luc.edu/luc_diss

 Part of the [Immunity Commons](#)

Recommended Citation

Zack, Stephanie, "Elucidating the Mechanisms Underlying How VMP1 Regulates Inflammatory Responses" (2022). *Dissertations*. 3969.

https://ecommons.luc.edu/luc_diss/3969

This Dissertation is brought to you for free and open access by the Theses and Dissertations at Loyola eCommons. It has been accepted for inclusion in Dissertations by an authorized administrator of Loyola eCommons. For more information, please contact ecommons@luc.edu.



This work is licensed under a [Creative Commons Attribution-NonCommercial-No Derivative Works 3.0 License](#).
Copyright © 2022 Stephanie Zack

LOYOLA UNIVERSITY CHICAGO

ELUCIDATING THE MECHANISMS UNDERLYING HOW VMP1 REGULATES
INFLAMMATORY RESPONSES

A DISSERTATION SUBMITTED TO
THE FACULTY OF THE GRADUATE SCHOOL
IN CANDIDACY FOR THE DEGREE OF
DOCTOR IN PHILOSOPHY

PROGRAM IN MICROBIOLOGY AND IMMUNOLOGY

BY

STEPHANIE R. ZACK

CHICAGO, ILLINOIS

DECEMBER 2022

Copyright by Stephanie Zack, 2022
All rights reserved.

ACKNOWLEDGEMENTS

I would like to thank my mentor, Dr. Ed Campbell, for helping me to grow as an individual and to develop as a scientist. He has challenged me to think critically and creatively read the literature to identify holes that can be filled by the scientific approaches we excel in. I am very grateful for his mentorship, and I will always remember his advice and guidance both of which I think I could have only gotten from him. I was first interested in joining his lab because my Grandpa Jirus suffered from Parkinson's disease, and it feels like now my work has come full circle by me ultimately studying a protein that very recently has been connected to Parkinson's disease. I would like to thank the members of my committee, Drs. Andy Ulijasz, Tom Gallagher, Mashkoor Choudhry, and Fletcher White for their guidance. Their insight pushed my project in the direction that ultimately led to some of the most interesting findings. I would like to thank Drs. Aleksey Zima and Roman Nikolaienko for their input and assistance with calcium imaging experiments. I would like to acknowledge the past and current members of the lab who have created a supportive and friendly environment. I would especially like to thank Dr. Adarsh Dharan who is a scientist I admire and a mentor that I couldn't have done without. I would also like to thank Dr. Sevnur K m rl  Keceli for her support, guidance, and friendship. I would like to acknowledge the Department of Microbiology and Immunology led by Dr. Katherine Knight for providing many opportunities to development our scientific communication skills.

I would like to acknowledge Dr. Kevin Morris, my undergraduate research mentor, without whom I would not be a scientist.

I would like to thank my parents, Steven and Linda Zack, for their unwavering love and support all these years. I couldn't have achieved this dream without you. I especially appreciate your dedication and encouragement towards my education.

I would like to acknowledge my brother, Michael Zack, who has always been competitive with me, but that has encouraged me to pursue my dreams. I hope I have been someone you could look up to, and I would like to thank you for being the best brother I could ask for.

I would like to thank my grandparents, Edward and Bernadine Zack and Robert and Rosemarie Jirus, and my great grandmother, Marie Chovanec. Being your granddaughter has been one of the best things in my life. You all have been an inspiration to me and have instilled in me a strong work ethic.

I would like to thank my friends and family for their support all these years. I would especially like to thank my college roommate, Marisa Matheson, for her continued friendship and support.

To my Grandma Rose who has been everything to me.

TABLE OF CONTENTS

ACKNOWLEDGEMENTS.....	iii
LIST OF FIGURES.....	ix
LIST OF ABBREVIATIONS.....	xi
ABSTRACT	xvi
CHAPTER ONE: REVIEW OF THE LITERATURE	1
The Function of VMP1 in Cells.....	1
VMP1 and SERCA	2
VMP1 and Autophagy	4
VMP1 Expression Levels and Disease.....	6
VMP1 and Cancer.....	6
VMP1 and Parkinson’s Disease	7
VMP1 and Multiple Sclerosis.....	12
Inflammation and Disease.....	17
Toll-like Receptor Signaling.....	17
Canonical NLRP3 Inflammasome Signaling.....	20
Gal-3 and Unconventional Protein Secretion	23
Regulation of Inflammatory Signaling.....	25
Regulation of Toll-like Receptor Signaling.....	26
TLR Activation and Calcium Signaling	27
The Role of Ca ²⁺ Signaling on NF-κB Activation.....	29
Calcium Flux and Inflammasome Activation.....	30
Mitochondrial Homeostasis	34
Mitochondrial Fission and Fusion.....	35
Mitochondria-derived Danger Signals and Inflammasome Activation.....	36
cGAS-STING and Inflammasome Activation.....	39
Autophagy	40
Ca ²⁺ Modulation of IM Association with the ER	41
Ca ²⁺ Homeostasis and Mitochondrial Membrane Potential	42
VMP1 and Mitophagy.....	44
Secretory Autophagy.....	44
Concluding Remarks.....	46
CHAPTER TWO: MATERIALS AND METHODS	48
Cell Culture, Differentiation, and Treatments	48
Cloning and Generation of Stable Cell Lines.....	49
Sandwich ELISAs.....	50
Quantitative Real-Time PCR	51
RNA-Sequencing and Pathway Analysis.....	52

Western Blotting	52
Caspase-1 Activation Assays	54
Lactate Dehydrogenase Assay	55
Purification of Extracellular Vesicles.....	55
Extracellular Vesicle Immunofluorescence Staining and Imaging	56
Calcium Live Cell Imaging.....	57
MitoTracker Live Cell Imaging.....	59
Immunofluorescence Imaging	59
Wide-field Fluorescence Deconvolution Microscopy	60
Image Analysis.....	61
Quantification of Cellular and Cell-free mtDNA using qPCR	62
Lysosome Dysfunction Assay	63
Statistical Analysis.....	63
CHAPTER THREE: RESULTS	64
SECTION ONE: THE UNCONVENTIONAL SECRETION OF GAL-3 FOLLOWING INFLAMMATORY STIMULATION.....	64
Rationale.....	64
Results	66
Gal-3 is Predominantly Released through GSDMD Pores under Inflammatory Conditions	66
Discussion.....	70
SECTION TWO: VMP1 RESTRICTS INFLAMMASOME ACTIVATION THROUGH ITS MODULATION OF SERCA ACTIVITY AND AUTOPHAGY	71
Rationale.....	71
Results	73
VMP1 Negatively Regulates the Release of Proinflammatory Molecules.....	73
VMP1 KO Cells have Increased Caspase-1 and Caspase-3 Activation depending on the Stimuli.....	77
VMP1 KO Cells have Depleted ER Ca ²⁺ Stores but Elevated Intracellular [Ca ²⁺] with ATP Activation	80
VMP1 KO Cells have an Increased Rate of Ca ²⁺ Influx into Mitochondria upon ATP Stimulation.....	85
VMP1 KO Cells have More and Smaller Mitochondria that Lose their Membrane Potential with LPS and ATP Treatment.....	88
VMP1 KO Cells have Increased Levels of Exposed Cytoplasmic mtDNA and Extracellular mtDNA.....	92
VMP1 KO Cells have Disrupted Autophagic Flux and Increased Lysosomal Activity.....	96
VMP1 KO Cells have Several Global Pathway Gene Expression Changes that Prime them for Proinflammatory Responses.....	99

CHAPTER FOUR: DISCUSSION.....	108
Concluding Remarks	120
REFERENCES.....	122
VITA	154

LIST OF FIGURES

Figure 1. VMP1 Interacts with SERCA	3
Figure 2. Overview of Autophagy	5
Figure 3. Inflammation in PD	10
Figure 4. Mechanism of Disease Pathogenesis in MS	13
Figure 5. Overview of TLR Signaling Pathways	19
Figure 6. Mechanisms of Canonical, Noncanonical, and Alternative NLRP3 Inflammasome Activation	21
Figure 7. Crosstalk between TLRs and Ca ²⁺ Signaling.....	28
Figure 8. Crosstalk between NF-κB and Ca ²⁺ Signaling	31
Figure 9. Crosstalk between NLRs and Ca ²⁺ Signaling	33
Figure 10. Mitochondrial Stress can Trigger Innate Immune Responses.....	37
Figure 11. Gal-3 is Predominantly Secreted through GSDMD Pores under Inflammatory Conditions.....	67
Figure 12. VMP1 Negatively Regulates the Release of Proinflammatory Cytokines and Gal-3 under Inflammatory Conditions.....	74
Figure 13. VMP1 Negatively Regulates the Expression Levels of Canonical Proinflammatory Cytokines but has no Effect on Gal-3 Expression in Macrophages.....	76
Figure 14. VMP1 KO Cells have Increased Caspase-1 and Caspase-3 Activation with Inflammatory Stimulation.....	79
Figure 15. VMP1 KO cells have Depleted ER Ca ²⁺ Stores but Elevated Intracellular [Ca ²⁺] with ATP Activation	82

Figure 16. VMP1 KO Cells Release More Proinflammatory Molecules when Extracellular $[Ca^{2+}]$ Are Depleted Prior to the Release of Intracellular Ca^{2+} Stores	84
Figure 17. VMP1 KO Cells have an Increased Rate of Influx of Ca^{2+} into Mitochondria upon ATP Activation.....	86
Figure 18. VMP1 KO Cells have More Mitochondria and Almost All Lose Their Membrane Potential with LPS and ATP Treatment	89
Figure 19. Mild Detergent Conditions Allow for Detection of Exposed Cytoplasmic mtDNA	93
Figure 20. Imaris Algorithm Built around a Phalloidin Stain Allows for Quantification of DNA Puncta Inside and Outside of the Cell	94
Figure 21. LPS and ATP Treated VMP1 KO Cells have More Exposed Cytoplasmic and Released Extracellular mtDNA than Control Cells.....	95
Figure 22. VMP1 KO Cells have Disrupted Autophagic Flux and Increased Cathepsin B Activity.....	98
Figure 23. RNA-Seq Samples Demonstrate that VMP1 Negatively Regulates Gal-3 Release and Proinflammatory Cytokine Gene Expression	100
Figure 24. Heatmaps Representing Changes in Toll-like Receptor Signaling and Nod-like Receptor Signaling in VMP1 KO vs. Control Cells.....	101
Figure 25. Heatmaps Representing Changes in Calcium Signaling and the Cytosolic DNA-sensing Pathway in VMP1 KO vs. Control Cells.....	104
Figure 26. Heatmaps Representing Changes in Genes Involved in Regulating Autophagy and Lysosome Associated Genes in VMP1 KO vs. Control Cells	106
Figure 27. Working Model for How VMP1 Regulates Inflammatory Responses.....	109

LIST OF ABBREVIATIONS

4-parameter logistic	4PL
α -synuclein	α -syn
Adenosine 5-triphosphate disodium salt hydrate	ATP
Alzheimer's disease	AD
American type culture collection	ATCC
Antigen presenting cells	APCs
Apoptosis-associated speck-like protein containing a CARD	ASC
Autophagic secretion of mitochondria	ASM
Autophagosome-lysosome pathway	ALP
Beclin-1	BECN1
Blood brain barrier	BBB
Bone marrow-derived macrophages	BMDMs
Bovine serum albumin	BSA
Calcium/calmodulin-dependent protein kinase II	CaMKII
Calcium induced calcium release	CICR
Calmodulin	CaM
Cell-free mitochondrial DNA	cfmtDNA
Central nervous system	CNS
Cerebrospinal fluid	CSF

Cyclic GMP-AMP synthase	cGAS
Cyclic guanosine monophosphate-adenosine monophosphate	cGAMP
Damage associated molecular patterns	DAMPs
Dopaminergic	DAergic
Double-stranded RNA	dsRNA
Dynamin-related protein 1	DRP1
Endoplasmic reticulum	ER
EV multiplex analysis of colocalization	EV-MAC
Extracellular vesicles	EVs
Fetal bovine serum	FBS
Fluorochrome-labeled inhibitors of caspases assay	FLICA
G-protein coupled receptors	GPCR
Galectin-3	Gal-3
Gasdermin D	GSDMD
Gasdermin E	GSDME
Geneticin	G418
H ⁺ -Ca ²⁺ exchangers	HCX
High mobility group box 1	HMGB1
Horseradish peroxidase	HRP
IκB kinase	IKK
Inner mitochondrial membrane	IMM
Inositol 1,4,5-trisphosphate receptor channels	IP3Rs

Interferon gamma	IFN- γ
Interleukin 1 β	IL-1 β
Interleukin 18	IL-18
Interleukin 6	IL-6
Isolation membranes	IMs
Knock out	KO
Lactate dehydrogenase	LDH
Leucine-rich repeat	LRR
Lipopolysaccharide	LPS
Lysosome-associated membrane protein 1	LAMP1
Major Histocompatibility Complex	MHC
Mammalian target of rapamycin	mTOR
Membrane contact sites	MCSs
Microtubule-associated protein 1A/1B-light chain 3	LC3
Mitochondria-associated membrane	MAM
Mitochondrial Ca ²⁺ Uniporter	MCU
Mitochondrial DNA	mtDNA
Mitochondrial NCX	mNCX
Mitochondrial permeability transition pore	mPTP
Mitochondrial reactive oxygen species	mtROS
Mitofusin 1	MFN1
Mitofusin 2	MFN2

Mitogen-activated protein kinase	MAPK
MitoTracker Green FM	MTG
MitoTracker Red CMXRos	CMXRos
Multiple sclerosis	MS
Myeloid differentiation primary response protein 88	MyD88
Na ⁺ -Ca ²⁺ exchanger	NCX
NOD-like receptor	NLR
Nucleic acid-sensing	NA-sensing
Nucleotide-binding domain	NACHT
Nucleotide-binding domain, leucine-rich repeats containing family, pyrin domain-containing-3	NLRP3
Optic atrophy protein 1	OPA1
Oxidative phosphorylation	OXPHOS
Pathogen associated molecular patterns	PAMPs
Pathogen recognition receptors	PRRs
Parkinson's disease	PD
Peripheral blood mononuclear cells	PBMCs
Phorbol 12-myristate 13-acetate	PMA
Phosphatase and tensin homolog deleted on chromosome 10 induced kinase 1	PINK1
Phospholambin	PLN
Piperazine- <i>N-N</i> bis[2-ethanesulfonic acid]	PIPES
Plasma membrane	PM

Polyethyleneimine	PEI
Primary progressive multiple sclerosis	PPMS
Principle component analysis	PCA
Prointerleukin-1beta	proIL-1 β
PTEN-induced kinase 1	PINK1
Pyrin domain	PYD
Reactive oxygen species	ROS
Ryanodine receptors	RyRs
Sarcolipin	SLN
Sarco/endoplasmic reticulum calcium ATPase	SERCA
Single nucleotide variants	SNVs
SQSTM1	p62
Stimulator of interferon genes	STING
Three-dimensional	3D
TIR domain-containing adaptor protein inducing IFN β	TRIF
Toll-like receptor	TLR
Transient receptor potential	TRP
Transient receptor potential melastatin-subfamily member 7	TRPM7
Tumor necrosis factor alpha	TNF- α
Vacuole membrane protein 1	VMP1
Voltage-dependent anion channels	VDACs

ABSTRACT

Inflammatory responses while beneficial when controlling infection need to be tightly regulated to prevent unnecessary damage to the host. Identifying novel regulators of inflammatory signaling is crucial to be able to fine-tune these responses during disease and mitigate unwanted responses under sterile or autoimmune conditions. One intriguing potential regulator of inflammatory signaling is vacuole membrane protein 1 (VMP1), an endoplasmic reticulum (ER)-resident protein known for its ability to regulate sarco/endoplasmic reticulum Ca^{2+} -ATPase (SERCA) activity and autophagy.

VMP1 was first characterized in acute pancreatitis models, an inflammatory disease that results in significant cell death. With connections to inflammatory disease, we sought to understand how VMP1 may regulate inflammatory signaling. For canonical inflammasome activation, two signals are required: the first signal induces upregulation of proinflammatory gene expression, and the second signal activates a multiprotein complex known as the inflammasome. Activation of these pathways ultimately results in the release of inflammatory mediators such as IL-6, IL-1 β , and galectin-3 (gal-3). Evidence in the literature demonstrated that both damaged mitochondria and calcium fluxes can act as signals to activate these proinflammatory pathways. Given its known functions, VMP1 may regulate these responses by degrading damaged mitochondria and buffering cytoplasmic Ca^{2+} concentrations.

To address the regulatory role of VMP1 in inflammatory responses, differentiated THP-1s, a model macrophage-like cell line, were depleted of VMP1 using CRISPR-Cas9. VMP1 KO cells released more proinflammatory cytokines and gal-3 in response to inflammatory stimuli. VMP1 negatively regulated inflammasome activation in response to lipopolysaccharide (LPS) and ATP, canonical activators of the NLRP3 inflammasome. In response to inflammatory stimuli, VMP1 KO cells have elevated intracellular $[Ca^{2+}]$ that are buffered by mitochondria. This excess Ca^{2+} resulted in the loss of membrane potential of almost all the mitochondria and the release of cytoplasmic mitochondrial DNA (mtDNA). Exposed mtDNA likely acted as a damage associated molecular pattern (DAMP) to increase activation of the NLRP3 inflammasome. Additionally, in VMP1 KO cells there was impaired autophagic flux at the stage of autophagosome/lysosome fusion which likely prevented the degradation of damaged mitochondria. There was also increased cathepsin B activity which potentially also contributed to inflammasome activation. Collectively, these data demonstrated that VMP1 restricts NLRP3 inflammasome activation through its modulation of SERCA activity and autophagy. Decreased expression of VMP1 has been found in the peripheral blood mononuclear cells (PBMCs) of Parkinson's disease (PD) patients suggesting that diminished expression of VMP1 may be contributing to the inflammatory sequelae associated with the disease and perhaps can be targeted therapeutically in the future.

CHAPTER ONE

REVIEW OF THE LITERATURE

The Function of VMP1 in Cells.

VMP1 was first identified as an upregulated transcript in pancreatitis, but it is also expressed in a variety of healthy tissues including brain, kidney, and intestine [9]. VMP1 is an ER-resident transmembrane protein that has been found to be essential for autophagosome formation suggesting that it promotes homeostasis in the cell, phagophore expansion and closure, lipid droplet formation, and is a crucial host factor for SARS-CoV-2 and pan-coronavirus infection [10-13]. Related to these functions, VMP1 has recently been identified to act as a phospholipid scramblase that facilitates the normal cellular distribution of cholesterol and phosphatidylserine [14]. Interestingly, VMP1 modulates contacts between the ER and mitochondria, lipid droplets, and endosomes through its interaction with SERCA such that the interaction between VMP1 and SERCA reduces cytosolic Ca^{2+} levels close to these membrane contacts [5, 15].

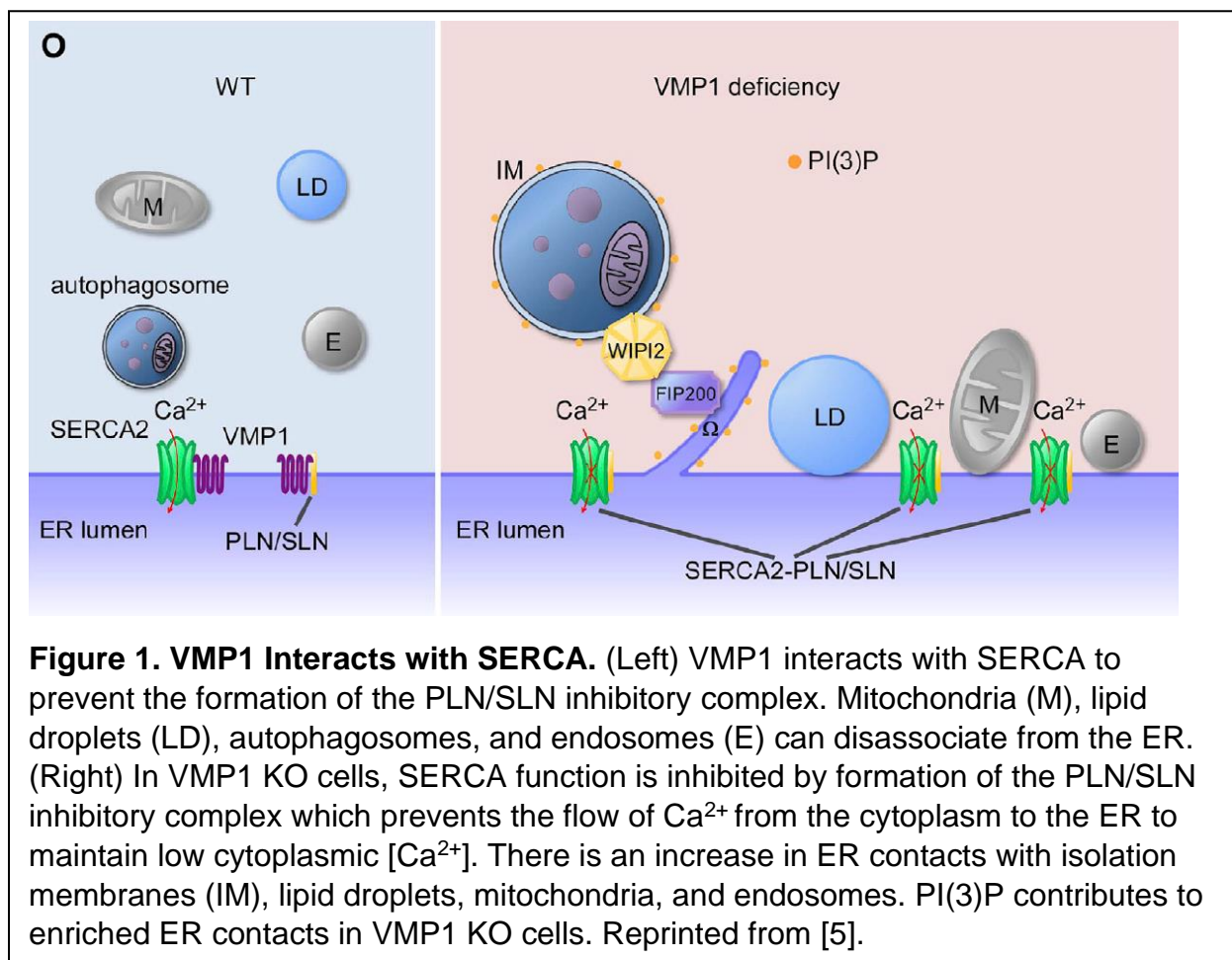
While VMP1 has primarily been characterized so far for its role in autophagy, studies in other organisms suggested that it may have diverse functions that include regulating protein secretion, endocytosis, phagocytosis, and regulating organelle function and morphology [16-19]. Surprisingly, in *Dictyostelium*, a versatile model organism, the secretion of a protein, AprA, through the classical ER-Golgi network was significantly reduced in wild type but attenuated from the VMP1 mutant (the VMP1 gene

was disrupted at amino acid 89) [16]. Phenotypes in this amoeba can be rescued by expressing mammalian VMP1 which suggested conservation of the function of this protein across species [16]. These findings were consistent with data showing that most autophagic structures colocalize with VMP1, but only 5% of VMP1 colocalizes with markers of autophagy [15]. Based on what is known so far, it seems incredible that one protein can regulate so many different cellular processes and the underlying mechanisms of this regulation are not yet well understood.

VMP1 and SERCA.

Recent work by Zhao et al. characterized a function for VMP1 in regulating the activity of SERCA, an ER-localized calcium channel that transports calcium from the cytoplasm into the ER lumen (Fig. 1) [5]. A mass spectrometry experiment revealed that VMP1 interacts with SERCA2, one of three major paralogs [5]. SERCA2 has differential Ca^{2+} affinity depending on its conformational state with the active form E1 conformation having high Ca^{2+} affinity and the E2 state having low Ca^{2+} affinity [20]. VMP1 acted as an activator of SERCA either by preventing formation of the SERCA/phospholamban (PLN)/sarcolipin (SLN) inhibitory complex or by stabilizing SERCA in its active form [21]. Interestingly, the interaction between SERCA and VMP1 modulates contact formation between the ER and mitochondria, lipid droplets, and endosomes [5]. The ER is connected to the PM, mitochondria, Golgi, and endosomes at membrane contact sites (MCSs) [22-24]. These ER contacts are important for mediating Ca^{2+} exchange, lipid transfer, and regulation of organelle dynamics such as fission, maturation, and

positioning [23, 24]. Formation of these contacts is dynamic and occurs in response to various stimuli. Global as well as local Ca^{2+} perturbations modulate ER contacts. Global cytosolic Ca^{2+} perturbations induce the ER-localized extended synaptotagmins to promote contacts between the ER and plasma membrane (PM) [25]. Due to the ability of VMP1 to modulate SERCA activity, VMP1 KO cells have decreased SERCA activity and an impaired ability to modulate changes in cytoplasmic $[\text{Ca}^{2+}]$.



Of particular interest here is the fact that local Ca^{2+} release from ER channels prevents the motility of mitochondria and promotes their association with the ER [26]. Around 70% of mitochondria were in contact with the ER in VMP1 KO cells compared to

20% in control cells and tended to have predominately spherical and swollen morphology in KO cells [5]. VMP1 preferentially binds with SERCA in its active form, and loss of VMP1 expression results in a loss of Ca^{2+} -ATPase activity in the microsomal fraction (mainly contains ER structures) compared to control cells which suggested that VMP1 promotes SERCA activity [5]. Proximity of VMP1 to SERCA competes with and prevents formation of the SERCA/PLN/SLN inhibitory complex. This inhibitory complex works by lowering the affinity of SERCA for cytosolic Ca^{2+} [27]. The interaction between VMP1 and SERCA reduces cytosolic Ca^{2+} levels close to these membrane contacts [5, 15]. Supporting the role for SERCA activity specifically in the persistence of membrane contacts is the fact that the presence of these ER contacts was increased by the non-competitive SERCA inhibitor, thapsigargin. Thapsigargin stabilized SERCA2 in its low Ca^{2+} affinity state, and the presence of thapsigargin interfered with the interaction between VMP1 and SERCA2 suggesting that VMP1 preferentially binds to the active form of SERCA2 [20]. ER contacts controlled by VMP1/SERCA are regulated by calmodulin (CaM), an intermediary protein that senses calcium levels and passes along signals to a number of calcium-sensitive enzymes, ion channels, and other proteins [5]. Overall, the interaction between VMP1 and SERCA serves to regulate the membrane contacts between the ER and various organelles by stabilizing SERCA in its active state.

VMP1 and Autophagy.

Autophagy is a cellular process that degrades and recycles cellular components. A portion of the cytosol is engulfed by a double-membrane autophagosome that is then

delivered to lysosomes for degradation (Fig. 2) [28, 29]. The initial step in autophagy induction is autophagosome formation. During this step, autophagosome precursors known as isolation membranes (IMs) have dynamic contact with the ER. Interestingly, it has been shown that in VMP1 KO cells there was stable association of IMs with the ER which prevented autophagosome formation [5].

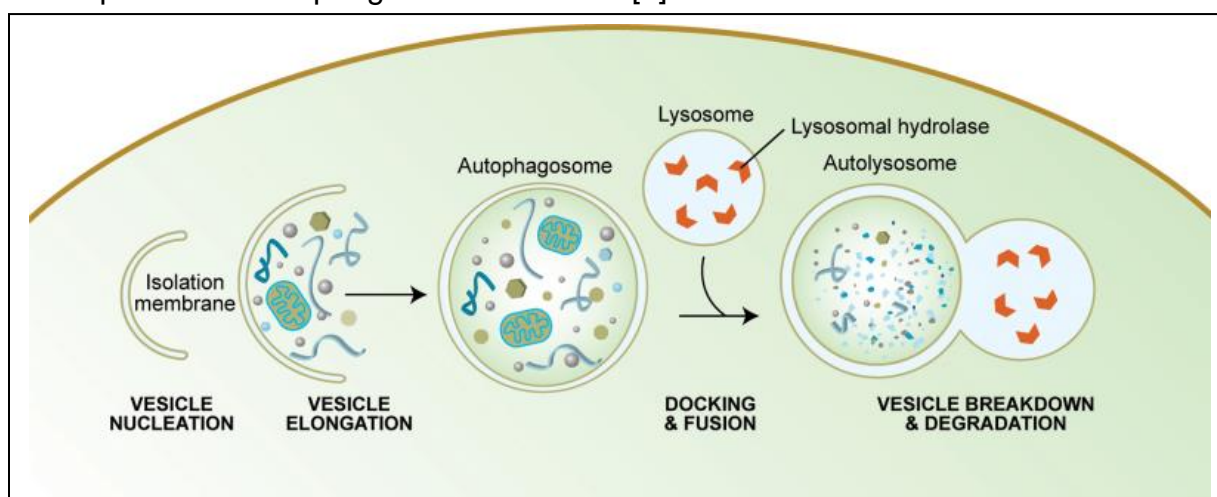


Figure 2. Overview of Autophagy. 1) Autophagy begins with the formation of the phagophore or isolation membrane (vesicle nucleation step). 2) Coordinated activity of autophagy core machinery proteins at the phagophore assembly site leads to the expansion of the phagophore into an autophagosome (vesicle elongation). The autophagosome can then engulf bulk cytoplasm nonspecifically, either specific cargo or entire organelles. 3) When the outer membrane of the autophagosome fuses with an endosome (forming an amphisome before fusing with the lysosome) or directly with a lysosome (docking and fusion steps), it forms an autophagolysosome. 4) The sequestered material is degraded inside the autophagolysosome (vesicle breakdown and degradation) and recycled. Reprinted from [2].

In addition to preventing autophagosome formation, VMP1 depletion also impaired autophagic flux at the step after LC3 lipidation evidenced by increased LC3II and p62 levels [5, 30]. Furthermore, in VMP1 KO cells, there was accumulation of LC3 puncta under both nutrient replete and starved conditions [5]. Some LC3 puncta were

larger than the ones in control cells. These LC3 puncta did not colocalize with LAMP1-labeled lysosomes suggesting that autophagic flux was impaired at the stage of autophagosome/lysosome fusion [5]. Additionally, in mice with the conditional KO of VMP1 in dopaminergic neurons, it was observed that there was accumulation of p62, more LC3 puncta, and less colocalization between LC3 and LAMP1 further supporting the idea that there was impaired autophagic flux in VMP1 KO cells [31]. Furthermore, an RFP-GFP-LC3 tandem reporter was used to determine the stage of autophagy of the LC3 puncta. In this construct, the GFP signal was quenched in acidic environments such that yellow vesicles were representative of IMs and immature autophagosomes and the red ones were acidified mature autophagosomes and autolysosomes [32]. Further supporting that autophagy was reduced in VMP1 KO cells, all of the LC3 puncta were yellow [5]. In VMP1 KO cells, disassociation of LC3-labeled autophagic structures from the ER was defective [5]. Overall, in VMP1 KO cells, there was compromised autophagosome formation and autophagic flux was stalled prior to autophagosome/lysosome fusion.

VMP1 Expression Levels and Disease.

VMP1 and Cancer.

In the last few years, altered VMP1 expression is increasingly being identified for its connection to disease. As the association between VMP1 expression levels and disease is better understood, measuring VMP1 expression levels could have potential prognostic value. Overexpression of VMP1 was associated with advanced glioma, an aggressive type of brain tumor, and poor prognosis [33]. Knockout of VMP1 expression

sensitized glioma cells to radiotherapy and chemotherapy. A model showed that VMP1 expression levels has prognostic value for determining survival in glioma patients [33]. Similarly, studies that measured VMP1 expression in patients with ovarian cancer and acute myeloid leukemia found that elevated VMP1 expression contributed to cancer progression and correlated with a poor prognosis [34, 35]. In contrast, in hepatocellular carcinoma and colorectal cancer, low VMP1 expression correlated with advanced cancer stage and shorter survival [36, 37]. Collectively, VMP1 expression levels were correlated with a variety of cancers, but whether increased or decreased expression correlated with cancer development and progression depended on the type of cancer. Yet what is known so far is that the link between VMP1 and cancer seemed to be related to the ability of VMP1 to regulate autophagy [33, 35, 37].

VMP1 and Parkinson's Disease.

Parkinson's disease (PD) is characterized by the progressive loss of dopaminergic (DAergic) neurons in the substantia nigra pars compacta accompanied by the accumulation of intracytoplasmic α -synuclein (α -syn) containing Lewy bodies [38, 39]. Expression of VMP1 was assessed in the PBMCs isolated from a cohort of PD patients [40]. In general, the PD group had significantly lower VMP1 expression compared to a healthy control cohort [40]. This disease affects 1% of the population over the age of 60 [38, 39]. Death of DAergic neurons affects dopamine transmission which results in the primary motor symptoms of the disease. These include tremor at rest, rigidity, and postural instability [41, 42]. Disease onset occurs decades before the first symptoms appear. Only about 5-10% of PD cases are associated with genetic

predisposition. Familial cases of PD can be caused by mutations in genes that encode for the proteins, α -syn, DJ-1, PINK, LRRK2, etc. However, most cases are idiopathic, but there tends to be increased risk with age. Other risk factors include exposure to environmental toxins, pesticides, heavy metals, traumatic lesions, and bacterial or viral infections which interestingly are all associated with inflammation [43].

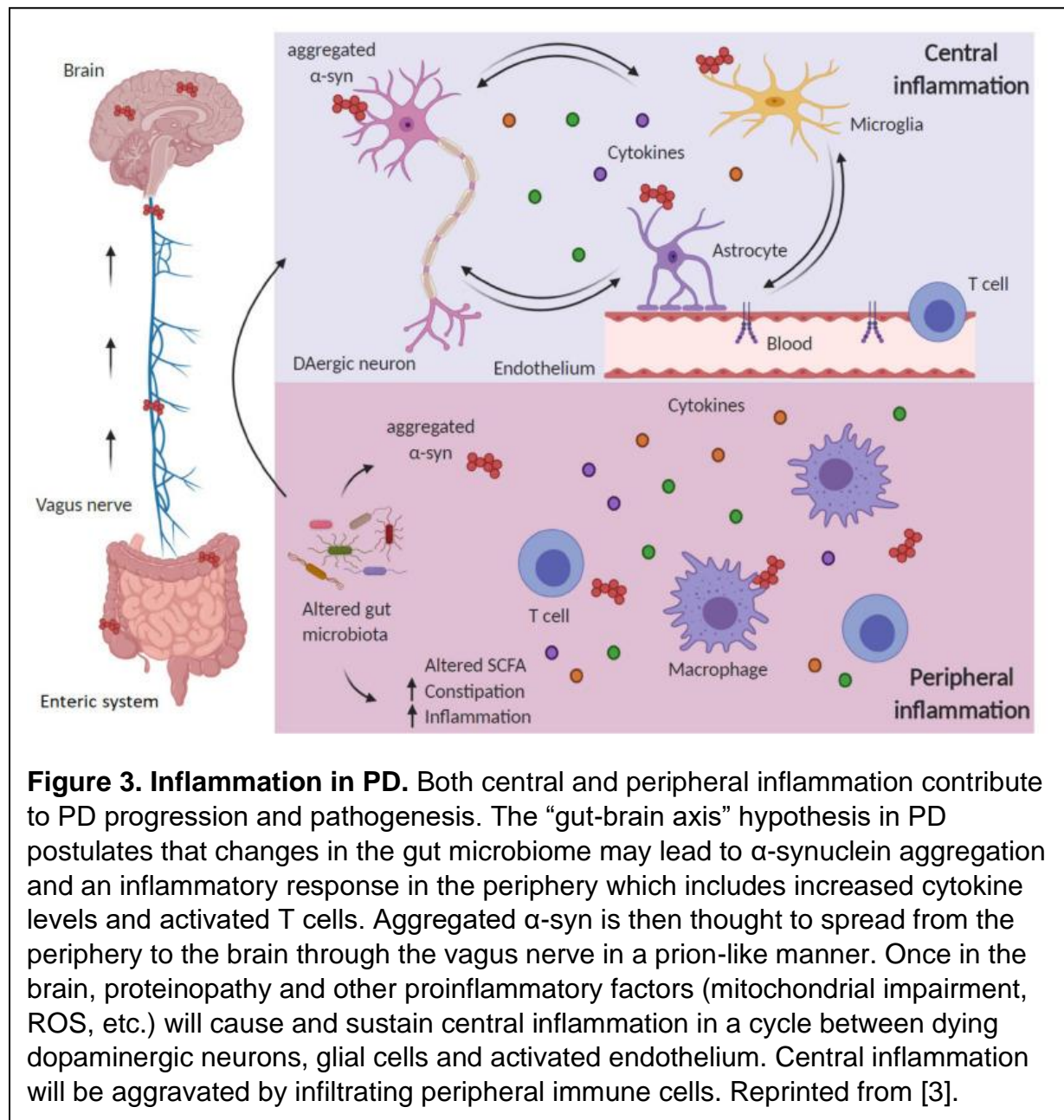
Inflammatory responses in both the periphery and the CNS contribute to PD disease pathogenesis (Fig. 3). The “gut-brain axis” hypothesis suggests that dysregulation in the gut can promote α -syn aggregation and inflammation in the periphery. This hypothesis was supported by elevated cytokine levels, including IL-1 β , IL-2, IL-6, IFN- γ , and TNF- α and increased CD4⁺ lymphocyte counts in the serum and cerebrospinal fluid (CSF) of PD patients supporting this idea for the presence of peripheral inflammation [44, 45]. It was then postulated that accumulation of α -syn in the intestine can spread through the vagus nerve to the brain in a fashion that mimics a prion-like disease [46]. Ultimately, glial cells in the CNS are activated by PAMPs and DAMPs secreted from damaged neurons or protein aggregates. This response results in chronic neuroinflammation that is thought to be critical to disease progression [47].

A recent study identified that there was significantly lower VMP1 expression in the PBMCs of a cohort of PD patients compared to a healthy control group [40]. In these patients, decreased VMP1 expression correlated with the length and severity of disease [40]. This decrease in VMP1 expression in PD patients could be ameliorated by the administration of a DAergic receptor agonist monotherapy or a combination of a

DAergic receptor agonist and L-dopa [40]. Furthermore, a recent study found that there was increased expression of the proinflammatory NLRP3 and procapase-1 genes in the PBMCs of PD patients as well as increased protein levels of NLRP3, caspase-1, and IL-1 β in the blood plasma which correlated with disease severity. Levels of IL-1 β and IL-6 also were elevated in the CSF of PD patients [48]. Interestingly, it has been found that the peripheral monocytes of PD patients have a hyperactive response to LPS [49]. These data support that PD is in fact a chronic systemic inflammatory disease and that there are likely novel regulators, potentially VMP1, that can attenuate inflammatory responses during the course of this disease [50].

In PD patients, pathological α -syn aggregates can act as a DAMP to trigger proinflammatory responses in the CNS [51-53]. Several studies have corroborating evidence that several toll-like receptors (TLRs), namely TLR2, TLR4, and TLR9, were involved prominently in the pathogenesis of PD [54, 55]. Oligomeric α -syn released from neuronal cells can act as a ligand for TLR2 expressed on microglia to induce an inflammatory response [56]. Furthermore, when TLR2 was activated, it has been observed that activation of this pathway can promote endogenous α -syn aggregation [57]. Studies of human postmortem brain showed that there was increased expression of TLR4 and its adaptor protein MyD88 particularly in the substantia nigra and putamen of PD patients [58-60]. Hughes et al. showed that oligomeric α -syn induced TNF- α production in WT mice at levels that were 10 to 100 times greater than in TLR4 knockout mice, yet the effect in TLR2 knockout mice was more modest suggesting that TLR4 was likely the primary TLR that recognized α -syn and initiated an inflammatory

response [59]. Collectively in the literature, the role of TLR4 seemed to vary depending on the stage of disease progression.



For example, in the acute phase of disease, TLR4 recognized α -syn causing it to be phagocytosed and cleared to delay disease progression. However, in the chronic phase

of PD, excessive stimulation of TLR4 resulted in proinflammatory cytokine production causing neuroinflammation and ultimately neurodegeneration which contributed to disease progression [61]. Supporting the “gut-brain” hypothesis were data demonstrating that there was higher TLR4 expression in the colonic samples of PD patients compared to control. In accordance with this higher expression, it was observed that there was disruption of the intestinal barrier, increased microbial markers, and a more proinflammatory gene profile in the colonic samples from these patients [62]. At this point, numerous studies have demonstrated that TLR signaling responses can be activated to contribute to PD pathology.

Prior work by Wang et al. utilized a mouse model with a conditional knockout of VMP1 in DAergic neurons, one of the key cell types involved in PD [31]. In this study, it was observed that in mice with conditional VMP1 KO in DAergic neurons there were motor defects, severe loss of DAergic neurons, and disturbance of autophagic flux [31]. In these mice, there was accumulation of α -syn in the striata suggesting that VMP1 expression may help to prevent misfolded protein aggregation which ultimately results in neuronal loss [31]. As mentioned, one of the hallmarks of PD pathology was the presence of α -syn aggregates. Clearance of α -syn aggregates by autophagy was dependent on p62/SQSTM1, a protein that binds polyubiquitinated proteins and can act as a scaffold for autophagic machinery by directly interacting with polyubiquitin and LC3 [63-66]. Previous work in *Dictyostelium*, a model organism often used to investigate human genes associated with disease and host/pathogen interactions, demonstrated

that VMP1 may help to mediate the clearance of α -syn aggregates in PD [67].

Dictyostelium have many conserved genes with humans including VMP1 [16]. In

Dictyostelium vmp1 mutant cells had an accumulation of large ubiquitin-positive protein aggregations that included the autophagy marker GFP-Atg8 and the putative

Dictyostelium p62 homologue [68]. Reduced colocalization between ubiquitin-positive aggregates and lysosomes suggested that VMP1 was required for the clearance of

ubiquitinated protein aggregates [68]. Given that it has been observed that VMP1

promotes autophagic flux, decreased expression of VMP1 in PD patients would likely

contribute to the accumulation of aggregated α -syn characteristic of disease pathology,

but the function of VMP1 has not yet been studied in macrophages.

VMP1 and Multiple Sclerosis.

Several studies have also linked changes in the VMP1 gene and its expression

to multiple sclerosis (MS). MS has a strong yet complex genetic component, and

several studies have identified single nucleotide variants (SNVs) in the VMP1 gene

associated with MS [69-71]. MS, an autoimmune disease of the CNS, has a

heterogenous clinical presentation that has been characterized by demyelination and

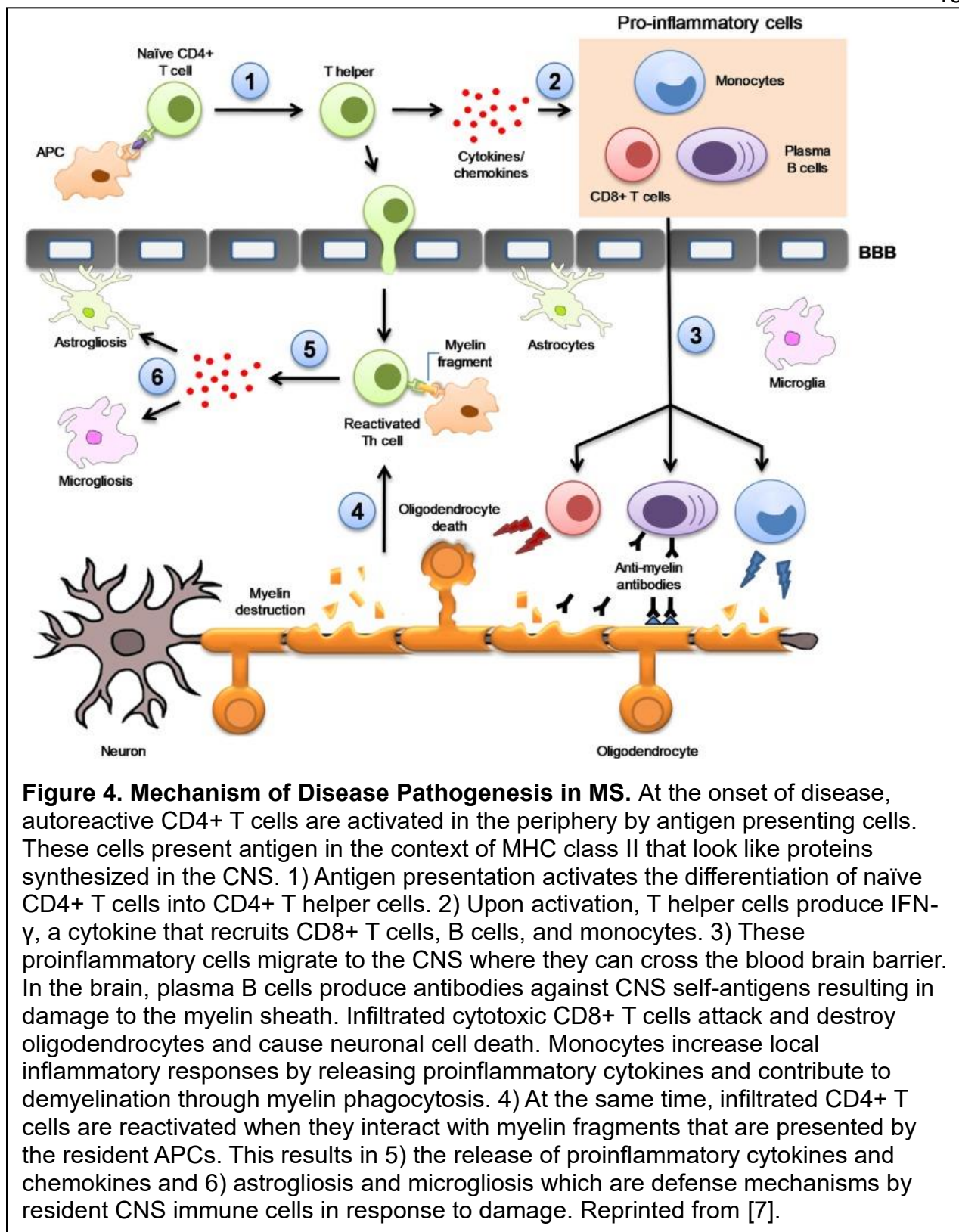
formation of neurological lesions [72]. Historically, the disease has been thought to have

a complex etiology likely due to a combination of genetic and environmental risk factors,

but in the last year, it has been identified that Epstein-Barr Virus infection is likely the

leading cause of MS [71-73]. The onset and development of MS has been characterized

by multiple inflammatory events (Fig. 4).



First, starting in the periphery, antigen presenting cells (APCs) presented peptides with similar structures to myelin found in the CNS via class II major histocompatibility complexes (MHC) to activate autoreactive CD4⁺ T cells [74]. Following this interaction, naïve CD4⁺ T cells differentiated into CD4⁺ T helper cells [75]. When these cells were activated, the Th1 subtype produced interferon gamma (IFN- γ), a cytokine that recruits CD8⁺ T cells, B cells, and monocytes to the periphery [76, 77]. These proinflammatory cells then can migrate through the bloodstream to the blood brain barrier (BBB) where they adhere to the endothelial cells [78]. In individuals suffering from MS, there was altered expression and organization of endothelial tight junctions that allowed for massive infiltration of immune cells into the brain [79, 80]. CD4⁺ T cells that infiltrated into the CNS were reactivated by the resident APCs [81]. The reactivated cells then released proinflammatory cytokines and chemokines that caused astrogliosis and microgliosis [82-84]. The damage was augmented by infiltrating CD8⁺ T cells that attack oligodendrocytes, destroying them and causing neuronal cell death [85]. At the same time, plasma B cells produced antibodies against self-antigens in the CNS which contributed to myelin sheath damage [86]. Plasma B cells along with monocytes exacerbated the local inflammatory response by reactivating the autoreactive CD4⁺ T cells [87]. Given that MS was characterized by a cascade of inflammatory events, it was likely that environmental and genetic risk factors that promote inflammatory responses likely played a key role in the development of this disease.

Many studies have been done to identify SNVs in the MS population. One of the goals of the International Multiple Sclerosis Genetics Consortium was to analyze the genetic data of MS and control subjects to create a reference map of variants in the MS population. Most of the susceptibility variants have been found in the MHC as expected given that it has been identified as an important contributor to disease pathology. This study prioritized about 500 genes outside of this region with most of the genes being related to the immune response [70]. The results of this analysis identified a SNV in the VMP1 gene. This change was located on chromosome 17 at base pair 59781849 with the base pair change of G to A (the SNP ID is rs2150879) [70]. The allele frequency was between 0.5-0.9 in different populations [70]. Other studies have focused on analyzing datasets from individuals in Europe given that the development of MS has been most prevalent in Northern Europeans between 0.1-0.2% of the population [72]. Three bioinformatics analyses found an association between disease and individuals that have a different SNV in the VMP1 gene located on chromosome 17 at base pair 59739396 with the base change of T to C (the SNP ID is rs8070345) [69, 71, 88]. The two SNVs identified in these studies were intronic which made it less clear how these SNVs might affect the amount of VMP1 protein. Additionally, the study that analyzed data from an Italian population identified 141 SNVs in the VMP1 gene [69-71]. These genetic analyzes together suggested that there was an increased frequency of SNVs in the VMP1 gene in people that develop MS. Furthermore, one study identified changes in the methylation of the *VMP1/MIR21* locus in CD4⁺ T cells [89]. Individuals with relapsing/remitting MS had higher methylation of the last two exons of these genes in

CD4⁺ T cells than individuals with secondary-progressive MS disease and healthy controls. These methylation changes seemed to not be correlated with known MS risk variants in *VMP1* [89]. Perhaps the most compelling data linking *VMP1* and MS was a recent study that used single cell RNA-sequencing to analyze gene expression changes in MS patients' cells. It was observed that there was decreased expression of *VMP1* in the monocytes of patients with primary progressive multiple sclerosis (PPMS), a form of the disease that was characterized by a progressively worsening condition [90]. Overall, these studies suggested that there were changes in the *VMP1* gene in MS patients compared to healthy controls that would need to be further studied.

Increasing evidence suggested that inflammasome activation played a critical role in MS pathogenesis [91]. Several studies have found that caspase-1 mRNA levels were elevated in the white matter of MS patients compared to control groups and that it was overexpressed in MS plaques, infiltrating perivascular mononuclear cells and parenchymal macrophages/microglia [92]. Another study showed that the expression of NLRP3, ASC, caspase-1, and IL-1 β was increased in reactive astrocytes and infiltrating macrophages/microglia of active demyelinating lesions of MS, but it was decreased in chronic inactive lesions of MS [93]. The inflammasome can potentially be used as a diagnostic biomarker with a cohort study showing higher levels of caspase-1 and ASC in the serum of MS patients. Specifically, ASC levels could differentiate disease severity with levels being higher in moderate MS patients compared to mild MS patients [94]. Furthermore, a recent study showed that PPMS patients (who have decreased

expression of VMP1 in their monocytes) have higher levels of NLRP3 compared to relapse-onset MS and healthy control subjects [90, 95]. Interestingly, when mice with experimental autoimmune encephalomyelitis, a common MS mouse model, were treated with the small molecule inhibitor of caspase-1, VX-765, there was reduced expression of inflammasome- and pyroptosis-associated proteins in the CNS, reduced axonal injury, and improved neurobehavioral performance suggesting a role for caspase-1 activation in MS pathogenesis [96]. Future work would need to characterize specifically the function of VMP1 in MS, but perhaps decreased VMP1 expression exacerbates the inflammatory responses associated with the disease.

Inflammation and Disease.

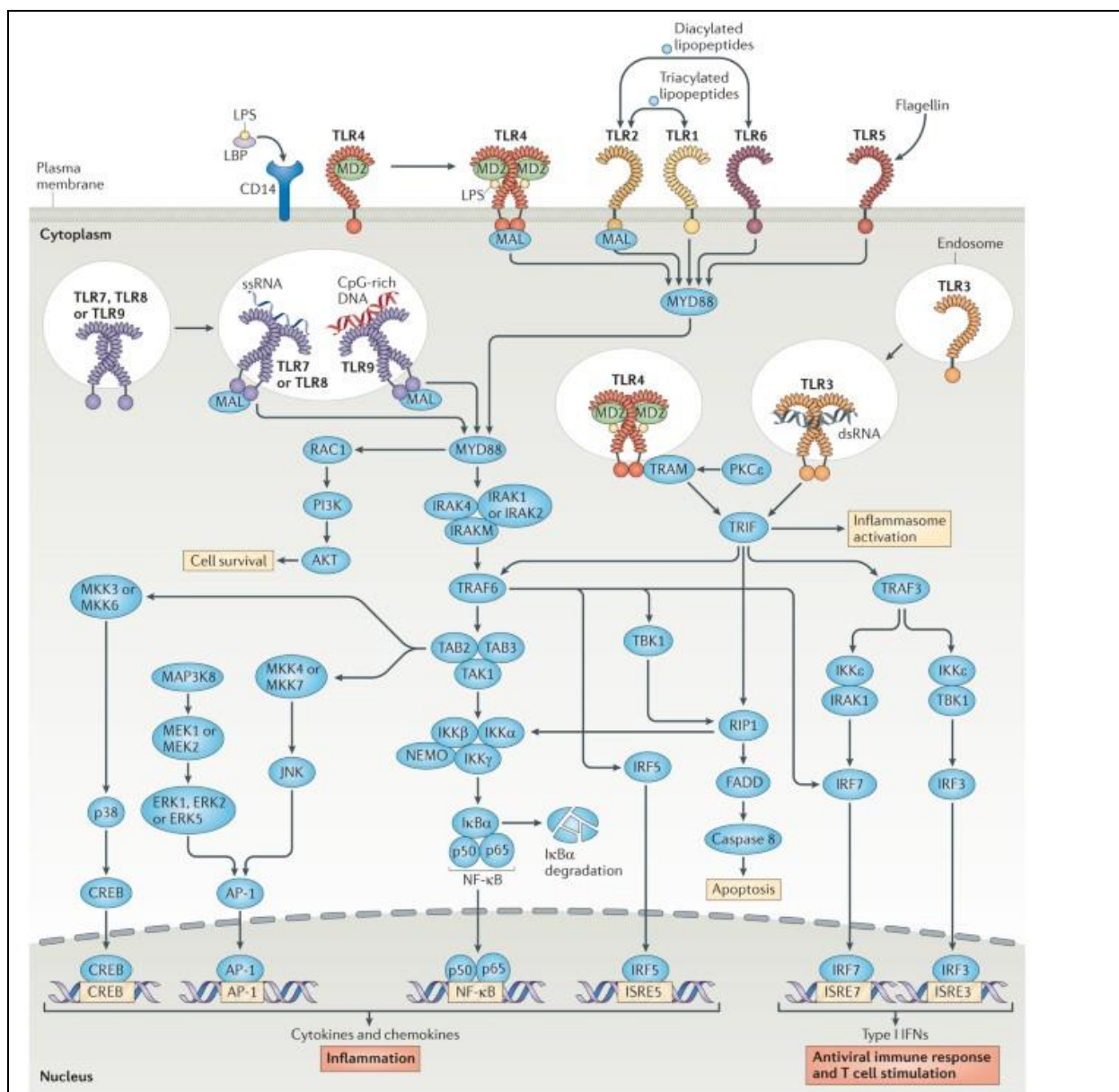
Innate immune cells such as macrophages play a critical role in the initial recognition of potential danger and mounting a response to protect against it. These cells express pattern recognition receptors (PRRs) that detect pathogen-associated molecular patterns (PAMPs) or signals indicating cellular stress termed damage associated molecular patterns (DAMPs) [97]. Unfortunately, if this response is not tightly regulated, there will be unnecessary or excessive inflammatory responses resulting in disease. Some of these inflammatory diseases include cryopyrin-associated periodic syndrome, arthritis, atherosclerosis, type 2 diabetes, Alzheimer's disease (AD), PD, MS, and cancers [98, 99].

Toll-like Receptor Signaling.

TLRs are the first line of defense for the immune system. TLRs are part of a family of PRRs [100]. They recognize molecules from both invading pathogens known

as PAMPs and endogenous danger signals released from dying cells known as DAMPs [101, 102]. Activation of TLRs leads to downstream signaling cascades that act to defend the host against invaders or to repair damaged tissue. These responses are mediated by the release of inflammatory cytokines and immune modulators [103]. The first TLR that was identified in humans was TLR4 which upon activation was shown to upregulate the expression of genes involved in inflammatory responses [104]. TLRs are expressed on the cell surface (heterodimers of TLR2 with TLR1 and TLR6 in addition to TLR4, TLR5, and TLR10) and inside of the cell either on the ER, endosomes, and lysosomes (TLR3, TLR7, TLR8, and TLR9) (Fig. 5) [1]. Of particular interest here are TLR4 and TLR3. TLR4 is activated by LPS found on the surface of gram-negative bacteria [105]. TLR3 is activated by double-stranded RNA (dsRNA) from viruses [106].

Downstream of TLR activation are adaptor proteins either myeloid differentiation primary response protein 88 (MyD88) for TLR4 or TIR domain-containing adaptor protein inducing IFN β (TRIF) which can act independently of MyD88 following TLR4 or TLR3 activation [107, 108]. This signaling results in activation of the transcription factor, NF- κ B, which leads to the upregulation of proinflammatory gene expression [109, 110]. Some of these proinflammatory cytokines include tumor necrosis factor alpha (TNF- α), interleukin-6 (IL-6), and prointerleukin-1 β (proIL-1 β) [111]. Ultimately, either proinflammatory cytokines or type I interferon are produced depending on the stimulus along with downstream signaling to promote the cellular response to invading pathogens [101].



Nature Reviews | Immunology

Figure 5. Overview of TLR Signaling Pathways. TLRs are expressed on the cell surface and in endosomes. They detect microbial cell-wall components, non-self nucleic acids or danger-associated self-molecules. Upon stimulation, TLRs activate two types of pathways that involve either MYD88 or TRIF. Crosstalk with other signaling pathways ensures that the TLR signal is properly regulated and leads to either apoptosis or cell survival, and the transcription of proinflammatory cytokines and chemokines and type I interferons. Reprinted from [1].

Cytokines are short-lived but can travel long distances to act on a variety of tissues and elicit a systemic response.

Canonical NLRP3 Inflammasome Signaling.

In the canonical NLRP3 inflammasome pathway, two signals are required: the first signal induces upregulation of proinflammatory gene expression mediated by TLR activation, and the second signal activates a multiprotein complex specifically the NLRP3 inflammasome. Activation of these pathways ultimately results in the release of inflammatory mediators such as IL-6, interleukin-1 β (IL-1 β), and gal-3. Inflammasome activation is a key component of the innate immune response and is modeled in Fig. 6 (left). The inflammasome consists of a ligand-sensing protein such as nucleotide-binding domain, leucine-rich repeats containing family, pyrin domain-containing-3 (NLRP3), an adaptor protein such as apoptosis-associated speck-like protein containing a CARD (ASC), and finally an effector protein such as caspase-1 [112, 113].

The key PRR of interest here is the cytoplasmic sensor, NLRP3, which is part of the NOD-like receptor (NLR) family. More specifically, NLRP3 has three domains: a carboxy-terminal leucine-rich repeat (LRR) that can recognize signals and has autoinhibitory functions, a central nucleotide-binding domain (NACHT) that mediates self-oligomerization and has ATPase activity, and an amino-terminal pyrin domain (PYD) needed to recruit ASC [114]. One thing that is unique about the NLRP3 inflammasome is that it is activated in response to a variety of stimuli including PAMPs such as viral and microbial components and DAMPs including ATP, uric acid crystals, and β -amyloid peptides. These signals induce K⁺ efflux, Cl⁻ efflux, mitochondrial

dysfunction, ROS release, mtDNA production, and lysosomal disruption to assemble and activate the NLRP3 inflammasome. NLRP3 senses these signals and self-oligomerizes via interactions between homotypic NACHT domains. Oligomerization of NLRP3 results in the recruitment of ASC through homotypic PYD-PYD domain interactions. This interaction results in the formation of a macromolecular complex with multiple copies of ASC, known as an ASC speck [115]. Following recruitment of ASC, this assembly recruits procaspase-1 through interactions between the homotypic CARD-CARD domains.

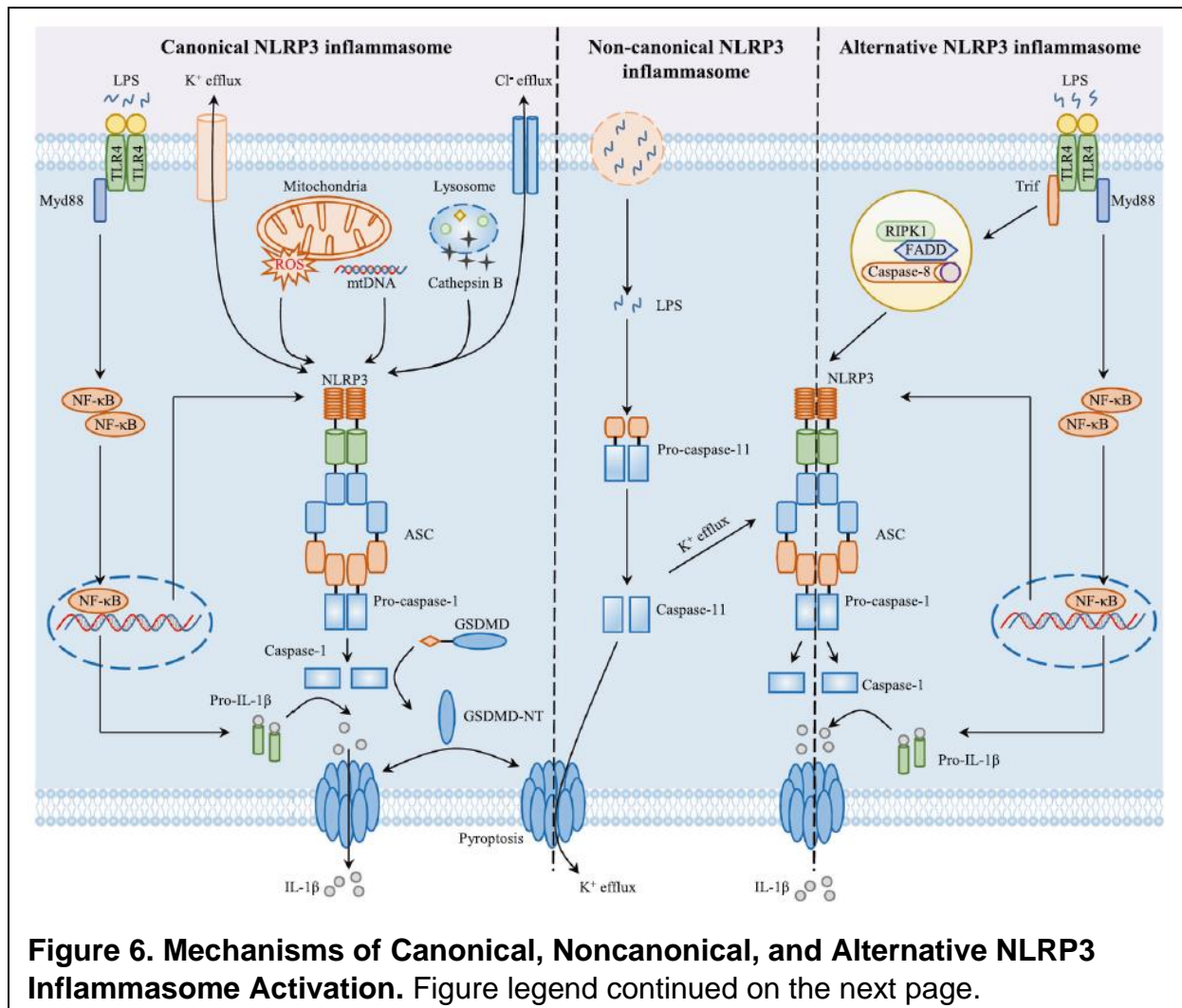


Figure 6. Mechanisms of Canonical, Noncanonical, and Alternative NLRP3 Inflammasome Activation. (Left) Canonical NLRP3 inflammasome activation requires two signals: the priming signal and the activation signal. During the priming step, TLRs, NLRs, and cytokine receptors induce activation of NF- κ B to upregulate the expression of proIL-1 β and NLRP3. During the activation step, a variety of PAMPs and DAMPs induce K⁺ efflux, Cl⁻ efflux, mitochondrial dysfunction, ROS release, mtDNA production, and lysosomal disruption to assemble and activate the NLRP3 inflammasome. Pro-caspase-1 then self-cleaves into its active form. It then cleaves proIL-1 β and proIL-18 into their mature forms allowing them to be released from the cell, and it cleaves GSDMD. The N-terminal domain of GSDMD forms pores in the PM to mediate the release of proinflammatory cytokines and induce an inflammatory form of cell death termed pyroptosis. (Middle) Cytosolic LPS is sensed by caspase-11 (in mice) and caspase-4/-5 (in humans) to initiate noncanonical NLRP3 inflammasome activation. Caspase-11 is activated by autoproteolysis. Active caspase-11 opens the pannexin-1 channel to induce K⁺ efflux to activate the canonical NLRP3 inflammasome. At the same time, caspase-11 cleaves GSDMD to induce membrane pore formation and pyroptosis. (Right) Alternative NLRP3 inflammasome activation only requires one signal. TLR ligands alone can activate the NLRP3 inflammasome in human and porcine monocytes via the TLR4-TRIF-RIPK1-FADD-CASP8 signaling axis which does not induce K⁺ efflux, ASC speck formation, or pyroptosis but does induce the release of IL-1 β through a noncanonical secretion pathway. Modified from [8].

The complex containing NLRP3, ASC, and caspase-1 is known as the NLRP3 inflammasome [116]. After the inflammasome is activated, procaspase-1 self-cleaves into its active form leading to the cleavage and maturation of the proinflammatory cytokines, IL-1 β and interleukin 18 (IL-18). Caspase-1 also cleaves gasdermin D (GSDMD), the N-terminal domain of which forms pores in the PM leading to the release of the proinflammatory cytokines, IL-1 β and IL-18, and induction of a type of inflammatory cell death known as pyroptosis [117-119].

The primary focus of this work is on the canonical inflammasome pathway, but it also has been recently identified that there are mechanisms of noncanonical and

alternative NLRP3 inflammasome activation (Fig. 6) (middle) (right). Briefly, in noncanonical inflammasome activation, cytosolic LPS is sensed by caspase-4/-5 in humans. Once activated by autoproteolysis, caspase-4/-5 opens the pannexin-1 channel to induce K^+ efflux and activate the NLRP3 inflammasome. Caspase-4/-5 can also then cleave GSDMD to form membrane pores and induce pyroptosis. In alternative inflammasome activation, only one signal is required in human monocytes. TLR ligands alone can activate the TLR4-TRIF-RIPK1-FADD-CASP8 signaling axis to induce the release of IL-1 β through a nonconventional secretion mechanism [8].

Gal-3 and Unconventional Protein Secretion.

In addition to the proinflammatory cytokines already mentioned, gal-3 is an inflammatory β -galactoside-binding lectin that also is secreted from activated macrophages. Galectins are a family of proteins that positively contribute to immunity and development but can negatively influence cancer and inflammation [120-123]. Gal-3 is a unique member of the galectin family in that it has an approximately 120 amino acid N-terminal domain of tandem repeats (proline, glycine, and tyrosine), a region that is susceptible to cleavage by metalloproteinases that is connected to a C-terminal CRD domain that can bind β -galactosides as well as the NWGR anti-death motif which is highly conserved within the Bcl-2 protein family [122, 124-126]. Gal-3 is post-translationally modified at Ser6 and Ser12 located in the N terminal domain which can modulate its ability to bind to carbohydrate domains and signal for its nuclear localization and oligomerization [125-127]. Purified gal-3 can associate in monomers, dimers, or oligomers in the absence of ligand binding and the protein can self-

oligomerize through the N-terminal domain [128, 129]. Following interaction with its ligand, there is cooperativity in the N-terminal domain of gal-3 that facilitates the recruitment of other gal-3 polypeptides [128, 130]. Gal-3 can be released from cells through several different mechanisms. Since gal-3 lacks a conventional leader signal sequence for secretion, it is thought that the N-terminal domain directs its localization to secretory vesicles [131, 132]. Gal-3 has been found localized in microdomains in the PM and can directly pass through the lipid bilayer through interactions with cholesterol and phospholipids [133]. Our data presented here and other previous work suggested that under inflammatory conditions, gal-3 is released through GSDMD pores [134].

Characterizing how gal-3 is released from cells is important for understanding its role in inflammatory responses and disease. Gal-3 is known to be upregulated in several neurodegenerative disease models [135-140]. Only a subset of galectins including gal-3 are known to be expressed in the brain, but their function is not yet well-understood [141, 142]. In microglia, there is minimal gal-3 expression at basal levels, but it can be upregulated by inflammatory signals [135]. Gal-3 has been found to contribute to both pro- and anti-inflammatory phenotypes primarily in microglia and oligodendrocytes in the brain, yet the underlying mechanisms of these functions are still ambiguous. It seems to depend on the type of injury, stage of disease/trauma, and timing of intervention [140, 141, 143-145]. Notably, in patients suffering from Huntington's disease, a neurodegenerative disease, plasma levels of gal-3 correlated with disease severity. Gal-3 expression levels also have been found to be elevated in brain sections from AD patients [141, 146, 147]. In this disease model, all gal-3 puncta

were detected in Iba-1 positive cells suggesting localization to microglia and not other cell types [141]. Prior work has found that LPS-treated microglial cells release gal-3 which can then promote inflammatory responses by signaling through TLR4 expressed by neighboring cells [135]. In contrast, another study found that gal-3 released from macrophages can negatively regulate LPS-induced inflammation by binding to LPS which prevents LPS from activating TLR4 [148]. When reviewing the literature, gal-3 has both pro- and anti-inflammatory effects in the brain that will warrant additional research. Understanding how gal-3 is released from microglia in the brain under various inflammatory conditions may allow for gal-3 to be targeted therapeutically to perhaps minimize the propagation of inflammatory responses that contribute to neurological disease development and progression.

Regulation of Inflammatory Signaling.

Inflammatory responses while beneficial when controlling infection need to be tightly regulated to prevent unnecessary damage to the host. Identifying novel regulators of inflammatory signaling is crucial to be able to fine-tune these responses during disease and mitigate unwanted responses under sterile or autoimmune conditions. Several autoinflammatory diseases are caused by the dysregulation of inflammasome activation resulting in high levels of secreted IL-1 β and/or IL-18, and we hypothesize that cells expressing decreased levels of VMP1 will exhibit dysregulated inflammatory responses [149]. In the following sections, mechanisms that regulate inflammatory signaling will be reviewed with particular emphasis on those mechanisms that are likely influenced by VMP1. VMP1 likely regulates inflammatory responses due

to its ability to regulate membrane contacts, calcium signaling, and mitochondrial function [5, 150].

Regulation of Toll-like Receptor Signaling.

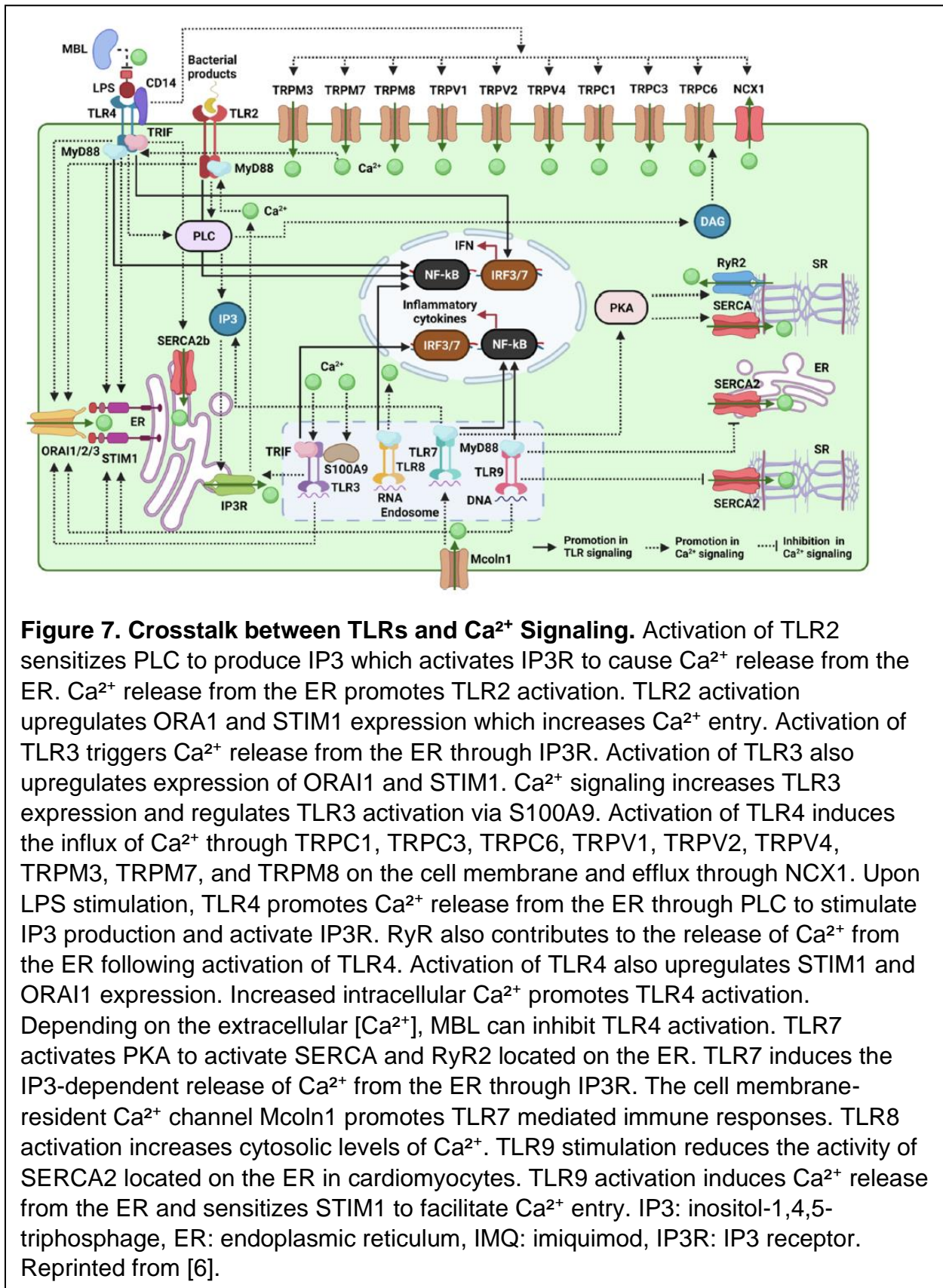
TLRs respond to a variety of structurally conserved molecules derived from microbes and as such these responses are regulated by several mechanisms. Several TLRs recognize nucleic acids including TLR3 which recognizes dsRNA; TLR7, TLR8, and TLR13 recognize fragments of single-stranded RNA with distinct sequence preferences; and TLR9 recognizes single-stranded DNA containing unmethylated CpG motifs. Collectively, these nucleic acid-sensing (NA-sensing) TLRs are particularly important for the response to viral infections but come with the risk of potentially sensing self-nucleic acids [151]. Improper activation of NA-sensing TLRs by self-nucleic acids has been associated with autoimmune and autoinflammatory diseases, including systemic lupus erythematosus and psoriasis [152-158]. Each TLR has a threshold that must be met for activation with each likely having distinct mechanisms of regulation. For these TLRs, the primary mechanisms of regulation include intracellular compartmentalization, ligand availability, receptor expression, and signal transduction. Compartmentalization of these TLRs to the endosome physically separates them from self-nucleic acids although it has been shown that these receptors can be activated if the ligands are specifically delivered to the endosomes [157, 159]. In contrast, the cGAS-STING pathway also recognizes DNA, but these sensors are localized in the cytoplasm where they can also sense self-nucleic acids [160]. Currently, there is a lack of information regarding how TLR expression is regulated, yet several studies have

identified increased expression of TLR3 and TLR4 to be associated with disease [161-164]. TLR activation can also be regulated at the level of signal transduction which will be outlined in the next section.

TLR Activation and Calcium Signaling.

Ca^{2+} is a second messenger molecule in several cellular processes. Changes in $[\text{Ca}^{2+}]$ also controls signal transduction downstream of TLRs (Fig. 7) [6]. The cytosolic levels of Ca^{2+} are regulated by the activity of several organelles with the ER and mitochondria being of particular interest here. The Ca^{2+} -ATPase, SERCA, transports Ca^{2+} from the cytoplasm to the ER. VMP1 regulates the activity of SERCA which by extension suggests that VMP1 can regulate Ca^{2+} fluxes under inflammatory conditions as described in this work. In opposition, Ca^{2+} is released from the ER via inositol 1,4,5-trisphosphate receptor channels (IP3Rs) and ryanodine receptors (RyRs). Mitochondria take up Ca^{2+} through the mitochondrial Ca^{2+} uniporter (MCU) complex and the voltage-dependent anion channels (VDACs). Mitochondria extrude Ca^{2+} into the cytoplasm through the mitochondrial NCX (mNCX) and the mitochondrial permeability transition pore (mPTP) [165-167]. The activity of these various channels helps to regulate cytoplasmic $[\text{Ca}^{2+}]$ which tend to be very low which creates an environment that is sensitive to changes in calcium.

Transient receptor potential (TRP) channels are a family of ion channels that mediate the movement of different cations, especially Ca^{2+} , across the plasma membrane and into the cell.



At least nine different members of this family of ion channels have been reported to be involved in increases in cytosolic Ca^{2+} levels induced by LPS activation of TLR4 [168-174]. Work using bone marrow-derived macrophages (BMDMs) demonstrated that the transient receptor potential melastatin-like 7 (TRPM7), a non-selective but Ca^{2+} -conducting ion channel, mediated the cytosolic Ca^{2+} elevations essential for LPS-induced macrophage activation [174]. Data suggested that TRPM7-dependent Ca^{2+} elevations were essential for the nuclear translocation of NF- κ B and that TRPM7-deficient macrophages were not able to produce IL-1 β and other proinflammatory cytokines [174]. Also, the ligands for TLR3, TLR4, and TLR9 induce calcium fluxes and activate calcium/calmodulin-dependent protein kinase II (CaMKII) in macrophages [175]. CaMKII- α can activate the mitogen-activated protein kinase (MAPK) and NF- κ B pathways. Selective inhibition or RNA interference of CaMKII suppressed the production of IL-6, TNF- α , and IFN α/β in macrophages. This study demonstrated that the cross-talk between intracellular calcium fluxes and the CaMKII pathway were needed for activation of TLR signaling in macrophages [175]. Overall, these data demonstrated that calcium fluxes were essential to produce proinflammatory cytokines downstream of TLR signaling.

The Role of Ca^{2+} Signaling on NF- κ B Activation.

NF- κ B is a transcription factor that is activated downstream of PRRs. Typically, in the resting state, the inhibitory I κ B proteins interact with NF- κ B p50/p65 dimers in the cytoplasm, forming an inactivation complex. Upon activation of this signaling pathway,

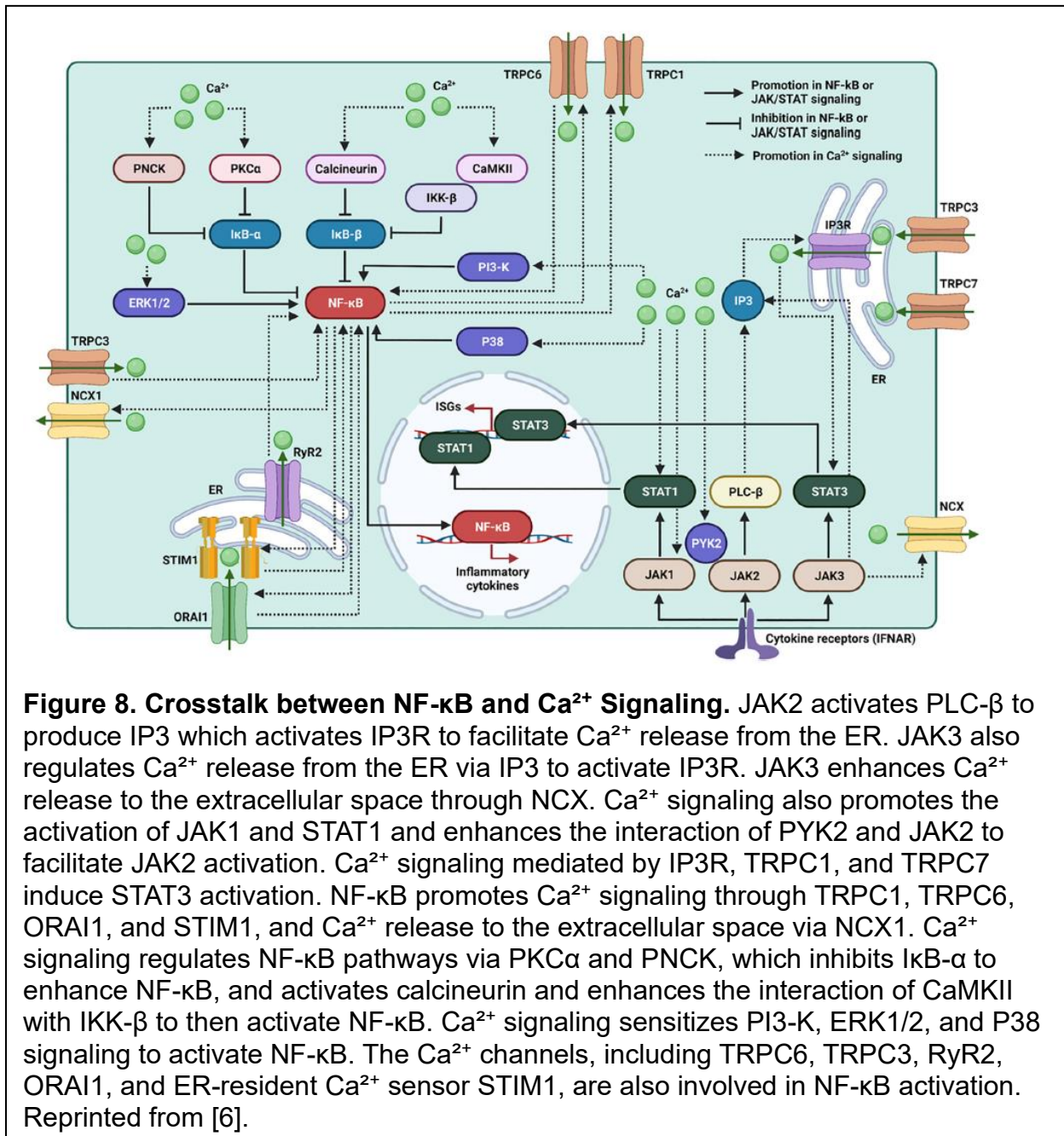
the inhibitory I κ B proteins can be phosphorylated and degraded in a ubiquitin-proteasome manner to allow the NF- κ B p65/p50 dimers to translocate to the nucleus and promote proinflammatory cytokine transcription [176].

Several studies support a critical role for Ca²⁺ signaling in regulating NF- κ B activation to promote gene transcription, cytokine secretion, inflammatory responses, and tumor microenvironment remodeling in various cell and animal models (Fig. 8) [177-180]. In most cases, an increase in Ca²⁺ activates NF- κ B through several different mediators. Ca²⁺ signaling can activate PKC- α to inhibit I κ B- α to increase NF- κ B activity and activate calcineurin to inhibit I κ B- β to activate NF- κ B [181]. Ca²⁺ can also activate CaMKII which can directly interact with IKK- β to modulate NF- κ B signaling [182]. The Ca²⁺/calmodulin-dependent kinase PNCK can phosphorylate the inhibitor I κ B- α to activate NF- κ B. In addition, several signaling pathways including ERK1/2, PI-3K, and P38, are sensitive to changes in Ca²⁺ and result in activation of NF- κ B [178, 183, 184]. Several other Ca²⁺ channels and sensors also have been identified for regulating Ca²⁺ signaling in a way that affects NF- κ B activation including TRPC3, TRPC6, RyR2, ORAI1, and STIM1 [179, 185-187]. Even though these Ca²⁺ channels and sensors have been identified for these regulatory roles, the detailed mechanisms for how changes in Ca²⁺ signaling result in NF- κ B activation have yet to be elucidated.

Calcium Flux and Inflammasome Activation.

Ca²⁺ flux or mobilization are considered an important upstream signal in NLRP3 inflammasome activation [188, 189]. Given that the cytoplasmic concentration of Ca²⁺ is

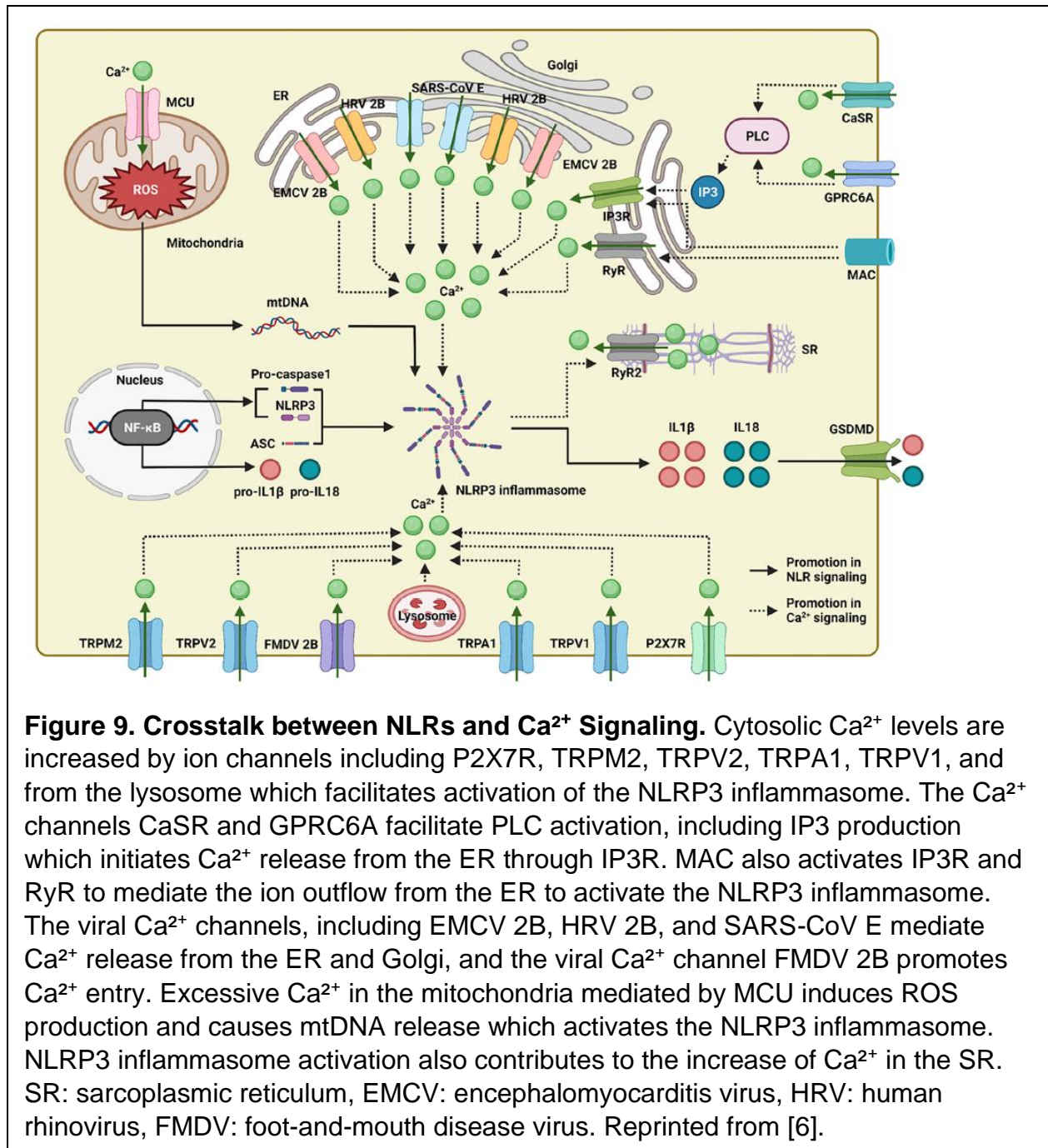
low, the two primary sources that cause Ca^{2+} mobilization come from the opening of plasma membrane channels and the release of intracellular ER-linked Ca^{2+} stores to create Ca^{2+} flux in the cytoplasm.



Since these pathways are linked, when one of these stores is released, the other one typically follows. An increase in cytosolic Ca^{2+} can be caused by an influx of extracellular Ca^{2+} through different Ca^{2+} channels including P2X7R, TRPM2, TRPV2, TRPA1, and TRPV1 which facilitate activation of the NLRP3 inflammasome [190-193]. RyR and IP3R are ion channels that are localized to the ER that facilitate the release of Ca^{2+} from the ER which can also sensitize the NLRP3 inflammasome [194]. Several G-protein coupled receptors (GPCR) can activate phospholipase C to produce IP3, a ligand of IP3R that has been found to promote NLRP3 inflammasome activation [195-198]. Two mechanisms have been proposed for how Ca^{2+} fluxes may induce inflammasome activation (Fig. 9). The first possibility is that Ca^{2+} promotes the interaction between NLRP3 and its adaptor ASC to activate the NLRP3 inflammasome, yet if this is the case the potential mechanisms are not well-characterized [188, 199]. Alternatively, excessive intracellular Ca^{2+} may lead to Ca^{2+} accumulation in the mitochondrial matrix through MCU. This Ca^{2+} overload leads to mitochondrial dysfunction accompanied by ROS production and release of mtDNA to the outer membrane. Ultimately, this exposed mtDNA promotes activation of the NLRP3 inflammasome [199, 200].

Complicating our understanding for a specific role of Ca^{2+} mobilization in NLRP3 inflammasome activation is the fact that K^{+} efflux can act as the counter ion at the plasma membrane to regulate Ca^{2+} flux. Data for several stimuli that activate this inflammasome suggested that Ca^{2+} flux and K^{+} efflux were coordinated in NLRP3

activation. For example, a classical second signal, ATP, binds to the P2X7 receptor to induce weak Ca^{2+} influx that is coupled with K^{+} efflux [201].



Further demonstrating how these ion fluxes are linked, K^+ efflux promotes the release of ER Ca^{2+} stores that is then followed by the opening of plasma membrane Ca^{2+} channels. Other activators of the NLRP3 inflammasome including nigericin, alum, monosodium urate crystals, and the membrane-attack complex induce Ca^{2+} flux as well as K^+ efflux [189, 194]. In contradiction of these findings, one study showed that for some stimuli, the Ca^{2+} flux actually occurred downstream of NLRP3 and caspase-1 activation suggesting it was not critical for NLRP3 inflammasome activation [202]. Overall, the exact role of Ca^{2+} flux in NLRP3 inflammasome activation is still debated. Another source of danger signals that activate the NLRP3 inflammasome are derived from mitochondria and will be described in the following sections.

Mitochondrial Homeostasis.

Mitochondria are dynamic organelles that are necessary for energy production through oxidative phosphorylation (OXPHOS), regulation of apoptosis, integration of various metabolic pathways, and maintenance of calcium homeostasis [203]. To carry out these processes, it is critical to preserve mitochondrial integrity and homeostasis which occurs through regular fission and fusion. A mitochondrion has several structural characteristics including an outer membrane, intermembrane space, inner membrane, and matrix. Of particular interest here is the mitochondrial matrix which contains the mitochondrial genome which consists of a 16.5 kb double-stranded closed circular DNA [204]. The mitochondrial genome contains 37 genes that encode 13 OXPHOS proteins, 2 ribosomal RNAs, and 22 transfer RNAs, yet most mitochondrial genes are encoded in

the nucleus and are transported to the mitochondria following synthesis in the cytoplasm.

Mitochondrial Fission and Fusion.

Mitochondrial dynamics are mediated by fission and fusion which results in a constant change in the number and morphology of mitochondria. These processes ensure that there is a sizable group of mitochondria that have optimal OXPHOS activity by moving and distributing mitochondrial content [205]. Mitochondrial fusion uses three membrane GTPases, mitofusin 1 (MFN1), mitofusin 2 (MFN2), and optic atrophy protein 1 (OPA1), to join two mitochondria at the outer and inner membrane interfaces. Conditions that promote fusion include inhibition of the mammalian target of rapamycin (mTOR)-induced autophagy, protein synthesis, and starvation [206-208]. Thus, mitochondrial fusion is necessary to promote optimal mitochondrial function because it allows for the exchange of gene products and metabolites.

MFN1 and MFN2 are located on the outer mitochondrial membrane and promote fusion. Interestingly, MFN2 is also located on the ER membrane where it connects the ER to mitochondria which allows for calcium uptake by the mitochondria [209]. Perhaps some similarities exist in the state of the cell between MFN2 KO and VMP1 KO [5]. MFN1 and MFN2 facilitate docking of the mitochondria at the outer membranes and their subsequent fusion. Under conditions of cellular stress, JNK phosphorylates MFN2 which recruits an E3 ubiquitin ligase to ubiquitinate MFN2 for proteasomal degradation. Degradation of MFN2 causes mitochondrial fragmentation and enhanced apoptotic death [210]. Another mechanism that regulates mitochondrial turnover is mediated by

MFN2 which recruits Parkin to damaged mitochondria and ultimately results in their degradation by mitophagy [211].

The other quality control mechanism for mitochondria is fission which is the process by which a mitochondrion divides into two mitochondria. Some of the reasons for fission include inheritance and partitioning of organelles during cell division, cytochrome C release during apoptosis, and to ensure the proper distribution of mitochondria [212-214]. Fission also promotes the removal of damaged mitochondria by mitophagy. When fission is not functioning properly, there is unbalanced fusion that results in an increase in the number of elongated mitochondria [205]. Alternatively, disruption in fusion leads to more fragmented mitochondria [215]. Fission is primarily coordinated by a large dynamin-like GTPase, known as dynamin-related protein 1 (DRP1). Mitochondrial division occurs where the ER interacts with the mitochondria. At this interaction point, the mitochondria are constricted then DRP1 is recruited. The average diameter decreases from around 300-500 nm to around 150 nm [205]. Ca^{2+} plays a role here where constriction of the inner mitochondrial membrane (IMM) at the mitochondria-ER contact site is Ca^{2+} -dependent [216]. There are many post-translational modifications of DRP1 that regulate the activation of fission [204]. Fission and fusion are two cellular processes that aim to maintain mitochondrial homeostasis and proper function in the cell.

Mitochondria-derived Danger Signals and Inflammasome Activation.

Another key upstream event of NLRP3 activation is mitochondrial dysfunction and the release of mitochondrial ROS (mtROS) and mtDNA into the cytosol (Fig. 10).

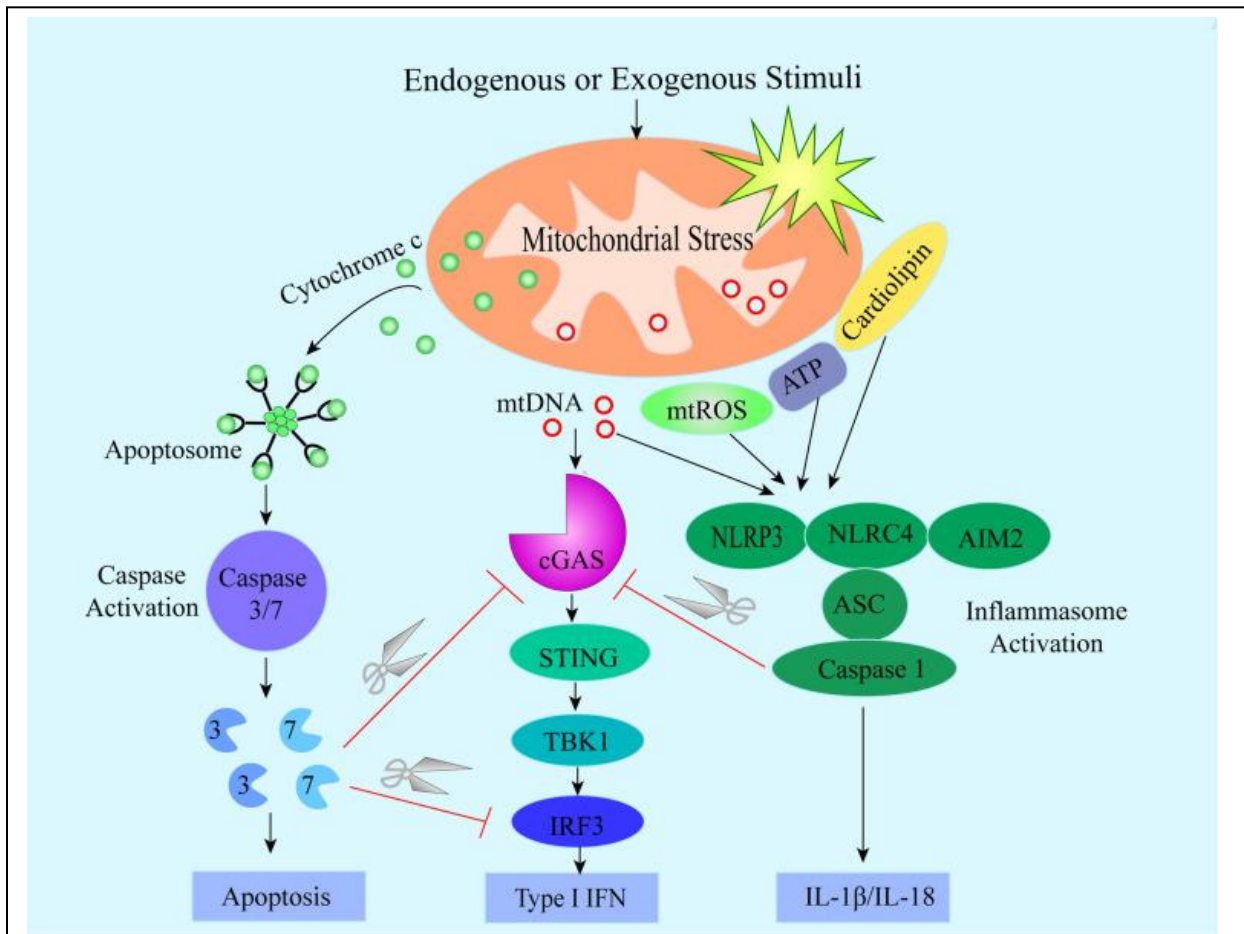


Figure 10. Mitochondrial Stress Can Trigger Innate Immune Responses.

Endogenous or exogenous stimuli induce cell stress that either directly or indirectly cause mitochondrial stress. Mitochondrial stress results in the release of mtROS, mtDNA, and ATP into the cytosol and extracellularly, cardiolipin externalization and cytochrome c release into the cytosol. Cytosolic mtDNA activates the cGAS-STING pathway to produce type I interferon. Signals including mtROS, mtDNA, cardiolipin, and ATP engage in the activation of several inflammasomes that leads to IL-1 β and IL-18 processing and secretion. Cytosolic cytochrome c triggers activation of apoptotic caspase-3/-7 which inhibits type I IFN production via cleaving cGAS and IRF3. Similarly, caspase-1 can cleave cGAS to prevent type I IFN expression. Reprinted from [4].

Under normal conditions, mitochondria produce reactive oxygen species (ROS) as a by-product of oxidative phosphorylation, but when the cell is under stress, mtROS levels significantly increase. Thus, an important regulator of NLRP3 activation is mitophagy, a

cellular process that removes damaged and dysfunctional mitochondria and reduces mtROS production [217]. A previous study showed that a novel pathway involving DRP1-Parkin1-VMP1 is needed for the selective degradation of damaged mitochondria through mitophagy in acute pancreatitis [150]. When mitophagy is impaired as is the case in VMP1 KO cells, there may be decreased negative regulation of the NLRP3 inflammasome and an accumulation of damaged mitochondria.

Another important signal in NLRP3 activation is circulating mtDNA released from damaged cells which acts as a DAMP [218]. mtDNA release from the cell has been found to be dependent on GSDMD pores in BMDMs activated by LPS and nigericin [219]. Endogenous newly synthesized mtDNA also has been considered a critical component of the NLRP3 signaling pathway [220-222]. Under conditions of oxidative stress, mtROS and Ca^{2+} together open the mPTP resulting in the release of mtDNA into the cytoplasm [222, 223]. Several activators of the NLRP3 inflammasome induce the rapid release of oxidized mtDNA into the cytoplasm [221]. Data showed that oxidized mtDNA activates the NLRP3 inflammasome, and non-oxidized mtDNA preferentially activates the AIM2 inflammasome [221]. In contradiction to previous findings, one study utilized a genetic deletion approach and found that there was no role for mPTP or mitophagy in NLRP3 activation [224]. Again, like with Ca^{2+} flux, there is conflicting data about the role for mitochondria in NLRP3 activation, and further studies are needed to elucidate the essential signals for NLRP3 inflammasome activation.

In addition to the role of mitochondria in NLRP3 activation, it is becoming increasingly evident that mitochondria are the docking sites for inflammasome

assembly. Typically, NLRP3 is a cytoplasmic protein that associates with the ER in unstimulated cells, but upon activation, NLRP3 becomes associated with mitochondria and the mitochondria-associated membrane (MAM) [217, 225]. While several mitochondrial proteins have been connected to inflammasome activation, the most relevant one in the context of this study is cardiolipin. Cardiolipin, a mitochondrial phospholipid of the inner membrane, is exposed on the outer membrane upon mitochondrial stress where it acts as the binding site for proteins associated with autophagy and apoptosis [226]. Cardiolipin has been shown to be necessary for inflammasome activation and binds NLRP3 and full-length caspase-1 independently [227, 228]. NLRP3 stimuli have been found to promote trans-Golgi network disassembly into vesicles which recruits NLRP3 and promotes NLRP3 aggregation needed for downstream ASC oligomerization and caspase-1 activation [229]. It is thought that perhaps then K^+ efflux dependent and mitochondria dependent NLRP3 activation may be separate pathways that converge on trans-Golgi disassembly, yet a unifying model for the various signals that activate the NLRP3 inflammasome has remained elusive.

cGAS-STING and Inflammasome Activation.

There are multiple cytosolic DNA sensors including cyclic GMP-AMP synthase (cGAS) which are involved in DNA-dependent immune responses. After cGAS recognizes cytosolic DNA, cyclic guanosine monophosphate-adenosine monophosphate (cGAMP) is produced. Next, cGAMP binds to the stimulator of interferon genes (STING) which is localized on the ER. Once activated, STING translocates to the Golgi apparatus, where it interacts with TBK1 to then trigger IRF3

activation and translocation to the nucleus to induce transcription of interferon genes. Additionally, STING recruits I κ B kinase (IKK) to phosphorylate I κ B α which results in activation of NF- κ B and induction of proinflammatory cytokine gene expression [230]. Previously, it had been thought that sensing of cytosolic DNA resulted in activation of the cGAS-STING pathway to trigger an antiviral response by inducing type I interferons [231, 232], whereas sensing of cytosolic DNA by AIM2 induced a proinflammatory response specifically through inflammasome activation [233, 234]. Yet the work of Gaidt et al. supported the idea that in human myeloid cells, AIM2 was not required for inflammasome activation. Instead, in human cells, activation of the cGAS-STING pathway led to NLRP3 inflammasome activation [235]. Furthermore, a recent study identified that mtDNA was released through the mPTP to activate the cGAS/STING pathway in amyotrophic lateral sclerosis [236]. Overall, it appears that mtDNA released from dysfunctional mitochondria can be sensed by the cGAS/STING pathway to activate the NLRP3 inflammasome.

Autophagy.

Macroautophagy or autophagy as it will be referred to hereafter is a cellular process that facilitates the degradation of unnecessary or dysfunctional cellular components (Fig. 2). The first step of autophagosome formation starts with the initiation and nucleation of a crescent-shaped IM that ultimately expands and seals [28]. Autophagosome formation occurs at the ER [237, 238]. When autophagy is induced, autophagosome formation occurs at PI(3)P-enriched ER subdomains called

omegasomes [237]. ER-mitochondrion contact sites, regions called the mitochondria-associated ER membrane are also involved in autophagosomal biogenesis [238, 239]. Three-dimensional (3D) electron tomography showed that the IM was located between ER cisternae during expansion of the autophagosome [240, 241]. It was thought that these contacts were important for the transport of lipids from the ER to allow for expansion of the IM although other sources were thought to also contribute lipids [29, 242]. When the IM closes, the outer surface of the autophagosome dissociates from the ER [240]. The autophagosome fused with endosomes to undergo a maturation process that ultimately resulted in it fusing with lysosomes [242]. As mentioned before, autophagy is impaired in VMP1 KO cells at the stage of autophagosome biogenesis and at the stage of autophagosome/lysosome fusion.

Ca²⁺ Modulation of IM Association with the ER.

IM association with the ER can be modulated by changes in Ca²⁺ levels. Interestingly, treatment with thapsigargin, a specific inhibitor of SERCA, which perturbs intracellular calcium ion homeostasis and induces ER stress, prevents detachment of IM/autophagosomes from the ER [243, 244]. SERCA helps to maintain the cytosolic [Ca²⁺] at low resting levels by transporting Ca²⁺ from the cytosol into the ER lumen [245]. In cells treated with thapsigargin, the IMs expanded into spherical-shaped structures that do not completely seal and remain associated with the ER [244]. Yet use of a low concentration of thapsigargin (100 nM) that does not elicit sustained or detectable changes in cytosolic Ca²⁺ levels was still able to block autophagy [244]. Collectively, these data suggested that VMP1 KO cells have persistent contact between

the ER and various organelles due to the ability of VMP1 to regulate SERCA activity and local $[Ca^{2+}]$ [5, 244].

Ca²⁺ Homeostasis and Mitochondrial Membrane Potential.

Calcium crosstalk occurs in the region between the ER and mitochondria known as the mitochondria-associated membrane to control cellular homeostasis [246].

Cellular Ca^{2+} levels are maintained through Ca^{2+} influx through cation channels located on the plasma membrane and the release of Ca^{2+} from intracellular stores. The main intracellular source of Ca^{2+} is the ER. Mitochondria are the main sources of ATP production in the cell, and there is an important link between mitochondrial levels of calcium and mitochondrial dynamics and function. Mitochondria can regulate the amplitude and timing of intracellular Ca^{2+} signals through mitochondrial calcium buffering capacity and mitochondrial functional interactions with other channels or organelles. Mitochondria can buffer Ca^{2+} levels between 50 and 500 nM in several cell types [247-249]. Mitochondria are particularly important in buffering severe Ca^{2+} overloads which tend to be associated with pathological conditions [249]. Close contact between mitochondria and cellular Ca^{2+} gates located in the ER and the cell membrane creates microdomains where an increase of $[Ca^{2+}]_{mito}$ parallels cytosolic Ca^{2+} signals [250]. Contacts between mitochondria and the ER increases $[Ca^{2+}]_{mito}$ through the opening of the IP_3 -gated channels in the ER. At the sites of these contacts, the mitochondrial surface is exposed to higher concentrations of Ca^{2+} than at other sites exposed to the bulk cytosol [251, 252]. Mitochondrial Ca^{2+} overload results in mitochondrial fragmentation [253].

When the cell is undergoing increased activity, transient cytoplasmic Ca^{2+} increases are sequestered by mitochondria through the mitochondrial Ca^{2+} uniporter which results in increased matrix Ca^{2+} levels [254-258]. Ca^{2+} enters mitochondria through the electrochemical gradient created by the mitochondrial membrane potential, and it exits the mitochondria via the Na^+ - Ca^{2+} and the H^+ - Ca^{2+} exchangers (NCX and HCX) in non-excitabile cells [259]. In the mid-20th century, it was observed that high levels of Ca^{2+} result in mitochondrial swelling and dysfunction [260, 261]. These findings resulted in the proposal of the existence of the mitochondrial permeability transition pore (mPTP). The mPTP is a non-specific channel located in the inner mitochondrial membrane. mPTP is engaged for prolonged periods of time in response to elevated intracellular Ca^{2+} levels and/or oxidative stress ultimately resulting in mitochondrial rupture. Opening of MPTP acutely results in the loss of mitochondrial inner membrane potential and release of molecules up to 1500 Da but long-term opening results in organelle swelling and rupture that leads to mitochondrial dysfunction and cell death [262, 263]. Typically, mitophagy is a specialized process that removes dysfunctional mitochondria. Upon mitochondrial depolarization, phosphatase and tensin homolog deleted on chromosome 10-induced kinase 1 (PINK1) and beclin 1 (BECN1) relocate to the surface of damaged mitochondria at the MAM site. These proteins then recruit others to result in autophagosome formation and mitophagy of damaged mitochondria [264]. Therefore, elevated Ca^{2+} levels can cause mitochondria to lose their membrane potential. In cells with dysregulated autophagic processes, there will be an accumulation of damaged mitochondria such as is the case in VMP1 KO cells.

VMP1 and Mitophagy.

The presence of mitochondrial stress can activate several innate immune pathways including NLRP3 inflammasome activation and apoptosis [4]. To control mitochondrial stress responses, a mitochondrial quality control mechanism that is a selective type of autophagy termed mitophagy exists to selectively degrade damaged mitochondria [4]. When mitophagy is active, mitochondria are engulfed in double-membrane vesicles that then fuse with lysosomes for degradation. When mitochondria lose their membrane potential, a sign of mitochondrial dysfunction, PTEN-induced kinase 1 (PINK1) accumulates in the mitochondrial outer membrane. Parkin1 then ubiquitinates these damaged mitochondria for autophagic degradation [265-267]. Prior work has suggested that VMP1 was required for mitophagy. In an acute pancreatitis model, mitochondria were a direct target of damage [150]. Data showed that VMP1 was involved and required for mitophagy during acute pancreatitis and in the case of decreased expression of VMP1 there was reduced mitochondrial degradation [150]. In the pancreatitis model, there is a redistribution of VMP1 around rounded mitochondria [150]. Overall, these data suggested that in models with decreased expression of VMP1 there would be an accumulation of damaged mitochondria resulting from decreased mitophagy.

Secretory Autophagy.

Secretory autophagy is a cellular process that facilitates the unconventional secretion of cytosolic cargo. The most often thought of cargo are leaderless cytosolic proteins which lack the N-terminal signal that normally allows for conventional protein

secretion through the endoplasmic reticulum and Golgi apparatus. Other types of cargo for unconventional secretion include cytosolic proteins with extracellular functions, aggregate forming proteins, cytoplasmic organellar material, and microbial release from cells for transmission. In the case of secretory autophagy, double membrane autophagosomes form and engulf cytoplasmic components except instead of fusing with lysosomes for degradation of their contents they fuse with the plasma membrane to expel their contents from the cell [268]. One important example of a cytosolic protein that undergoes unconventional secretion is IL-1 β [269-271]. A recent study found that in cells that have a defect in mitophagy as is the case with VMP1 KO cells, mitochondria can still be cleared from cells in a process independent of lysosomal degradation. Mitochondria can instead be cleared by extracellular release through a secretory autophagy pathway that was defined as Autophagic Secretion of Mitochondria (ASM). It was observed that when there was increased ASM, there was more activation of the cGAS/STING pathway in recipient cells [272]. Clearly, cells with impaired autophagic processes can utilize secretory autophagy to remove unwanted cellular contents that cannot be degraded through autophagy.

Another way that cargo can be released from cells is through extracellular vesicles (EVs). EVs are a heterogeneous population of membrane-enclosed cargoes that are released from cells to expel “waste” or to mediate intercellular signaling. Using proteomics approaches, several studies have found that various inflammasome activators including calcium oxalate, monosodium urate crystals, ATP, β -glucans, and viral RNA among others promote the release of EVs [273-278]. ATP activates the

NLRP3 inflammasome by binding to the P2X7R which allows for K⁺ efflux and the rapid release of EVs [273]. Several studies support the idea that gal-3 is released in EVs specifically through recruitment to multivesicular bodies by TSG101 [279-282]. Overall, under inflammatory conditions, cytoplasmic cargo can be released from cells through several different mechanisms including secretory autophagy and GSDMD pores.

Concluding Remarks.

Macrophages have intrinsic pathways to modulate inflammatory signaling to promote homeostasis. However, it is likely that in macrophages lacking VMP1 there is aberrant dysregulation to an extent that cannot be compensated for by these pathways. An overview for how Ca²⁺ flux and mitochondria-derived danger signals activate the NLRP3 inflammasome has been provided in the previous sections. Given what is known about the function of VMP1, it is feasible that VMP1 can regulate inflammatory responses by modulating SERCA activity and mitophagy. As mentioned before, VMP1 is localized to the ER where it interacts with SERCA, a Ca²⁺-ATPase, to modulate the local Ca²⁺ levels in the cytoplasm [5]. Previous work demonstrated that increased cytoplasmic [Ca²⁺] promoted the assembly of inflammasome components, but how exactly Ca²⁺ mediates this response is not well understood [188]. In activated cells or cells with dysregulation, there was an increase in the presence of DAMPs such as mtDNA which are known to activate the inflammasome [217, 220, 283]. Prior work demonstrated that VMP1 expression was required for mitophagy, the process that specifically degrades damaged mitochondria which are a source of DAMPs [150]. While it has been shown that VMP1 can modulate local [Ca²⁺] and mitochondrial homeostasis,

it had yet to be determined whether or how VMP1 might regulate inflammatory responses until now.

Previous studies have shown that VMP1 relocates to rounded, damaged mitochondria in pancreatitis [150]. When VMP1-localized autophagosomes were isolated, they contained damaged mitochondria suggesting that VMP1 has a role in maintaining mitochondrial homeostasis [150]. Additionally, in cells with downregulated VMP1 expression, there was reduced mitochondrial degradation [150], and in HeLa cells and Cos-7 cells with depleted VMP1, altered mitochondrial morphology, size and increased or absent cristae were observed [15]. Furthermore, our preliminary data and other work suggested that there was an accumulation of SQSTM1/p62 in VMP1 deficient cells which is typically evidence of impaired autophagy [284]. p62 is an autophagy substrate protein that acts as a receptor protein in signaling pathways that include NF κ B, Nrf2, and mTOR which are either directly part of inflammatory pathways or regulate inflammatory responses [285]. Therefore, we hypothesize that VMP1 may also regulate inflammatory responses by promoting mitochondrial homeostasis and that in KO cells potential accumulation of damaged mitochondria will prime cells to exacerbate their responses to additional inflammatory stimuli. The goal of this dissertation was to characterize a novel regulator of inflammatory responses, VMP1, such that we gain new insight into how dysregulated host cellular responses affect inflammatory responses to pathogen and damage associated signals.

CHAPTER TWO

MATERIALS AND METHODS

Cell Culture, Differentiation, and Treatments.

HEK293T and THP-1 cells were obtained from the American Type Culture Collection (ATCC). Cells were cultured with 5% CO₂ at 37°C in either DMEM or RPMI supplemented with 10% heat-inactivated fetal bovine serum (FBS) (Gibco), 10 µg/mL ciprofloxacin hydrochloride, 100 IU/mL penicillin, and 100 µg/mL streptomycin. THP-1s were differentiated by adding phorbol 12-myristate 13-acetate (PMA) (Sigma-Aldrich, P1585) at a concentration of 1 µg/mL for 48 h. The cells were then allowed to rest for 72 h prior to treatment. Unless otherwise noted, the cells were treated with 100 ng/mL lipopolysaccharide from *Escherichia coli* O55:B5 (Sigma-Aldrich, L4524) or were transfected with 50 µg/mL poly(I:C) (Sigma-Aldrich, P9582) using Lipofectamine 2000 (Fischer Scientific, 11-668-019) following the manufacturer's protocol for 4 h. The media was changed and then some wells were treated with 5 mM adenosine 5-triphosphate disodium salt hydrate (ATP) (Sigma-Aldrich, A2383) for 30 min. To measure the response to α-syn, α-syn fibrils were obtained as described previously, and 1 µM α-syn was added to differentiated THP-1s for 24 h [286]. To inhibit NLRP3 inflammasome activation, 10 µM MCC950 (Invivogen, inh-mcc) or DMSO control were added to the differentiated THP-1s in serum-free RPMI for 1 h prior to the addition of ATP. To test SERCA inhibition, 1 µM thapsigargin (Tocris, 1138) was added at the same time as any

inflammatory stimuli including when it served as a control. The supernatant or cells were then collected for analysis. To deplete extracellular Ca^{2+} , cells were pretreated with 2.2 mM EGTA (EMD Millipore Corp, 324626) for 30 min. To release Ca^{2+} stores, then either 1 μM thapsigargin, 1 μM ionomycin (Sigma-Aldrich, I9657) or 2.2 mM EGTA was added to cells for 4.5 h. The supernatant or cells were then collected for further analysis.

Cloning and Generation of Stable Cell Lines.

GSDMD knockout THP-1 cell lines were generated using a modified version of the LentiCRISPRv2 plasmid (Addgene plasmid number 52961, a gift from Feng Zhang) that has the puromycin resistance cassette replaced with a blasticidin resistance cassette to create LentiCRISPRv2-blasticidin [287]. The following oligonucleotide guide RNA sequence was annealed and cloned into LentiCRISPRv2-blasticidin: GSDMD guide RNA 5'-CCACGTACACGTTGTCCCCG-3' as described previously. Cells transduced with the LentiCRISPRv2-blasticidin backbone served as a control for selection. VMP1 knockout THP-1 cell lines were generated using a modified version of the LentiCRISPRv2 plasmid that has the puromycin resistance cassette replaced with a G418 resistance cassette to create LentiCRISPRv2-G418 [287]. The following oligonucleotide guide RNA sequence was annealed and cloned into LentiCRISPRv2-G418: VMP1 guide RNA 5'-CTTTTGTATGCCTACTGGAT-3' as described previously [12]. Cells transduced with the LentiCRISPRv2-G418 backbone served as a control for selection. To generate stable cell lines, lentivirus was prepared by transfecting equal amounts of VSV-G, psPAX2 (from Didier Trono, NIH AIDS Reagent program [catalog number 11348]) [288, 289], and LentiCRISPRv2-G418 (either the backbone or the clone

containing the guide RNA of interest) using polyethylenimine (PEI) into HEK293T cells. Retrovirus was prepared by transfecting equal amounts of VSV-G, pCigB, and pMSCVpuro-Mito-Pericam using PEI into HEK293T cells. Viral supernatant was harvested 48 h post-transfection and filtered through 0.45- μ m filters (Millipore). The concentrated supernatant was applied to THP-1 cells by spinoculation at 13°C for 2 h at 1,200 x *g*. Media was changed 24 h later. Forty-eight hours after transduction, geneticin (G418) (Gibco) was added to the cells at a concentration of 0.5 mg/mL. Following 3-4 weeks of selection, lymphocyte separation media was used to remove dead cells, and healthy cells were collected to validate the knockout by western blot.

To measure caspase-1 activation, THP-1s were transduced with lentiviral vector prepared as described above with a caspase-1 biosensor containing the IQAD amino acid target sequence as described previously [290].

Sandwich ELISAs.

Cell culture supernatants were analyzed using the following kits: Human IL-1 beta/IL-1F2 DuoSet ELISA (R&D Systems, DY201-05) for IL-1 β , Human IL-6 DuoSet ELISA (R&D Systems, DY206-05) for IL-6, and Human Galectin-3 DuoSet ELISA for gal-3 (R&D Systems, DY1154). The manufacturers' protocols were followed.

Alternatively, gal-3 protein levels were also measured using an in-house sandwich ELISA described previously [291]. Briefly, mouse anti-LGALS3 B2C10 (Santa Cruz Biotechnology, SC-32790) was diluted in pH 9.6 carbonate buffer to a final concentration of 1 μ g/mL to coat a 96-well Maxisorp ELISA plate (Nunc, 44-2402-22) at 4°C overnight on an orbital shaker. Between each step the wells were washed 3x-5x

with PBS containing Tween-20. The wells were blocked 1:1 with RPMI supplemented with 10% characterized FBS and PBS for 2 h at RT. The culture supernatant was then added to the wells. The standard curve was generated by serially diluting recombinant gal-3 (Abcam, ab89487). Biotin conjugated rat anti-LGALS3 (M3/38; Millipore Sigma, 125402) was diluted to a final concentration of 500 ng/mL in PBS with 1% bovine serum albumin (BSA) (Sigma-Aldrich, A7906) and added to the wells for 2 h on a rocker at RT. Then streptavidin HRP (ImmunoReagents, Ba-103-HRPX) was diluted to 1 µg/mL and incubated for 30 min at RT on a rocker. The HRP signal was detected with the addition of 1 x 3,3',5,5-tetramethylbenzidine (Invitrogen, 00-4201-56) and then the reaction was quenched with 2 N sulfuric acid. The absorbance was read at 450 nm on a PowerWave XS plate reader (BioTek Instruments) with Gen5 software. The standard curve was fit with a 4-Parameter Logistic (4PL) curve.

Quantitative Real-Time PCR.

Cells were treated as described above and RT-PCR was used to measure changes in gene expression. Total RNA was purified from cell lysates following treatment using the NucleoSpin RNA Plus extraction kit (Macherey-Nagel, 740984.250). cDNA was synthesized using the GoScript Reverse Transcriptase System (Promega, A5004). Quantitative PCR was performed using gene specific primers and Itaq™ Universal SYBR (Bio-Rad, 1725124). The following primer sets were used in this study: VMP1 fwd, 5'-GTGGCTTTCATTGGTGCTGTCC-3'; VMP1 rev, 5'-GAGTTCAACCGCTGCTGGATTC-3'; proIL-1β fwd, 5'-AATCTGTACCTGTCCTGCGTGTT-3'; proIL-1β rev, 5'-

TGGGTAATTTTTGGGATCTACACTCT-3'; IL-6 fwd, 5'-GGAGACTTGCCTGGTGAAAA-3'; IL-6 rev, 5'-ATCTGAGGTGCCCATGCTAC-3'; Igals3 fwd, 5'-GCCAACGAGCGGAAAATGG-3'; Igals3 rev, 5'-TCCTTGAGGGTTTGGGTTTCC-3'; GAPDH fwd, 5'-GCACCGTCAAGGCTGAGAAC-3'; GAPDH rev, 5'-GCCTTCTCCATGGTGGTGAA-3'. GAPDH was utilized as a housekeeping gene for normalization.

RNA-Sequencing and Pathway Analysis.

Control or VMP1 KO differentiated THP-1s were left untreated or treated with 100 ng/mL LPS (4 h) then 5 mM ATP (30 min). Supernatant was collected and analyzed by gal-3 ELISA as described above to ensure that the sample phenotype was consistent with previous experiments. RNA was isolated using the NucleoSpin RNA Plus extraction kit. Part of the RNA was saved for qPCR to assess proIL-1 β , IL-6, and gal-3 gene expression as described above. RNA samples were submitted to the University of Chicago Genomics Facility to assess the concentration and quality of the RNA. Samples that passed the check were then used for library preparation and whole genome sequencing using Illumina NovaSeq. Pathway analysis was performed following a previously published protocol [292]. Heatmaps were generated using the pheatmap function (RRID:SCR_016418) in R.

Western Blotting.

Protein was isolated by lysing pelleted cells using lysis buffer containing 100 mM Tris, pH 8.0, 1% NP-40 (Thermo Fischer Scientific, 85124), 150 mM sodium chloride and Pierce protease inhibitor cocktail (Thermo Fischer Scientific, 32953) on ice for 30

min. The lysates were centrifuged at 4°C for 10 min at 10,000 x *g* and then the supernatant was collected and transferred to a new tube. Protein from the supernatant was concentrated using ethanol precipitation. Prior to collecting supernatant samples, for the media change before the addition of ATP for 30 min, the media was replaced with serum free media. One volume of protein solution was combined with 9 volumes of 100% cold ethanol. The samples were vortexed and stored at -20°C overnight. The samples were then centrifuged for 10 min at 15,000 x *g*. The supernatant was removed, and the pellet was washed with cold ethanol. The sample was vortexed and repelleted for 10 min at 15,000 x *g*. The ethanol was aspirated off. The samples were dried to eliminate ethanol residue, and then the samples were resuspended in 6x SDS. The protein concentrations were determined by Pierce 660 nm protein assay (Thermo Fischer Scientific, 22660). In brief, 2x SDS was added to the lysed sample and boiled at 95°C for 5 min. An equal amount of protein was loaded into a 12% polyacrylamide gel or a precast 4-20% gradient polyacrylamide gel (Mini-PROTEAN TGX Precast Polyacrylamide Gels, Bio-Rad, 4561096) for SDS-PAGE. After separation, the proteins were transferred to a nitrocellulose membrane (Bio-Rad, 162-0115) and probed overnight at 4°C unless otherwise indicated with the primary antibody diluted in powdered milk block solution at 2.5 g/50 mL of Tris-buffered saline, 0.1% Tween 20 (Sigma-Aldrich, P7949-500ML). The primary antibodies were rabbit anti-GSDMDC1 (1:1000; Novus Biologicals, NBP2-33422), mouse anti-galectin-3 clone Gal397 (1:1000; BioLegend, 126701), rabbit anti-VMP1 (1:1000; StressMarq Biosciences, SPC-680D), mouse anti- β -actin (1:1000 at RT for 1 hr; Proteintech, 66009-1-Ig), rabbit anti-caspase-

3 (1:1000; Cell Signaling, 9662S), rabbit anti-cleaved caspase-3 (Asp175) (1:1000; Cell Signaling, 9661S), rabbit anti-LC3B (1:1000; Sigma-Aldrich, L7543), and rabbit anti-p62 (1:500; Cell Signaling, 7695S).

The nitrocellulose membrane was washed in Tri-buffered saline, 0.1% Tween 20 and probed with horseradish peroxidase (HRP)-conjugated goat anti-mouse (Thermo Fischer Scientific, 12-349) or HRP-conjugated anti-rabbit secondary antibody (Thermo Fisher Scientific, 12-348) diluted in milk block solution at 1:10000 for 30 min. HRP was detected with the addition of SuperSignal West Femto Chemiluminescent Substrate (Thermo Fischer Scientific, PI34096). Chemiluminescence levels were measured using the FluorchemE Imaging System (Protein Simple).

Caspase-1 Activation Assays.

For the FAM-FLICA caspase-1 activation assay, following treatment, the cells were incubated with FAM-FLICA caspase-1 (YVAD) substrate following the manufacturer's protocol (Immunochemistry Technologies, 97). Briefly, the FLICA substrate that was resuspended in DMSO was diluted in PBS 1:5. The diluted substrate was added to the wells at a final concentration of 1:30. The plate was incubated at 37°C for 1 h. The cells were washed with apoptosis buffer from the kit and were allowed to sit for 10 min in the incubator. Hoechst dye was added at a dilution of 0.5% to apoptosis buffer. The cells were incubated with the dye for 15 min then the cells were washed once with 1x apoptosis buffer then fresh buffer was added prior to imaging. A 20x lens was used to take 10 images per well. Data were collected by z-stack imaging and were analyzed as maximum intensity projections (MIPs). Cells were imaged using z-stacks

with 1 μm between each stack and a total of 5 z-stacks. A surface algorithm was built in Imaris around each individual cell, and the data were displayed as the intensity max of each individual cell for a given treatment.

To measure caspase-1 activation using the biosensor, following treatment, cells were lysed with 1x passive lysis buffer (Promega, E1941). Lysates were transferred to a white 96 well plate in duplicate or triplicate. Firefly luciferase substrate was added, and luminescence (relative light units) was quantified.

Lactate Dehydrogenase Assay.

Lactate dehydrogenase (LDH) release was measured using a previously published protocol [291, 293]. To measure LDH release, supernatant was collected 3 h after signal 2. The samples were plated in duplicate in a clear 96-well plate. Signal was measured by reading the absorbance at $\lambda = 490 \text{ nm}$ on a Synergy HTX Multi-Mode plate reader (BioTek Instruments) with Gen5 software.

Purification of Extracellular Vesicles.

Either control or GSDMD KO THP-1s were differentiated as described above in 10 cm dishes at a density of 10,000,000 cells per dish. Cells were treated as described above. Then the supernatant was collected to purify the EVs. EVs were isolated in a 15 mL conical which was centrifuged in a tabletop centrifuge at $300 \times g$ for 20 min at 4°C . The supernatant was collected and added to Beckman Coulter polycarbonate centrifuge tubes (#344059). The samples were spun at $10,000 \times g$ with the SW41 TI Beckman rotor in an Optima L-90K ultracentrifuge at 4°C for 30 min. The supernatant was then transferred to a new centrifuge tube and spun at $100,000 \times g$ for 90 min at 4°C . The

supernatant was discarded, and the centrifuge tube was filled with PBS prior to a second spin at 100,000 x *g* for 90 min at 4°C. The pellet was then resuspended in 100 µL PBS.

Extracellular Vesicle Immunofluorescence Staining and Imaging.

To adhere EVs to coverslips, 30 µL of resuspended EVs were added to 470 µL PBS then was added into a 24-well plate containing a glass coverslip (Fischerbrand Cover Glasses, 12-545-J, 22 x 60-1). The plate was spinoculated by centrifugation at 13°C for 2 h at 1200 x *g* onto the coverslips. The EVs were then fixed in a solution of 0.1 M PIPES containing 3.7% formaldehyde, methanol free (Polysciences, 04018-1) for 10 min and washed 3x with PBS. The EVs were permeabilized with a 0.1% solution of saponin in block solution composed of 500 µL PBS supplemented with 10% normal donkey serum and 0.01% NaN₃ for 5 min. After washing the coverslips 3x in PBS, the coverslips were incubated with the primary antibodies, rat M3/38 anti-galectin-3 antibody (1:500; Biolegend, 125402), mouse anti-CD63 (1:2000; BD Pharminogen, 556019), mouse anti-CD9 (1:2000; BD Pharminogen, 555370), and mouse anti-CD81 (1:2000; BD Pharminogen, 9149590) for 1 h at RT. The coverslips were washed 3x in PBS. The coverslips were then incubated with the secondary antibodies including 488 conjugated donkey anti-mouse (1:300; Jackson ImmunoResearch Laboratories, 715-545-150) and 647 conjugated donkey anti-rat (1:300; Jackson ImmunoResearch Laboratories, 712-605-150) in block solution for 20 min at RT. The coverslips were then washed 3x with PBS. The coverslips were fixed and mounted (Electron Microscopy

Sciences, Fluoro-gel with Tris buffer, #17985-11) onto slides (Globe Scientific Inc., Diamond White Glass 25 x 75 x 1 mm, 0.5 gloss, #1380-30).

EVs were imaged on a DeltaVision wide-field fluorescence microscope (Applied Precision, Inc.). It has a digital camera (CoolSNAP HQ2; Photometrics). An oil immersion Olympus Plan Apo 60x objective lens (N.A.=1.42) was coated with 1.518 refraction index low autofluorescence immersion oil, Olympus Type F (Fischer Scientific, NC0297589). For each coverslip, 20 images were acquired with 40 z-stacks per image at 0.2 μm per z-stack for 8 μm total. For image analysis, the spots algorithm in Imaris was used. The algorithm was built around the 488 tetraspanin channel. The estimated XY diameter was 0.5 μm and the estimated Z diameter was 1 μm .

Calcium Live Cell Imaging.

To measure $[\text{Ca}^{2+}]_{\text{cyt}}$, cells were incubated at RT with the high affinity Ca^{2+} indicator Fluo-4/AM (ThermoFisher Scientific, F14201) for 15 min in Tyrode solution (NaCl 135 mM; KCl 4 mM; CaCl_2 3 mM; MgCl_2 1 mM; glucose 10 mM; HEPES 10 mM; pH 7.4). Fluo-4 was measured at an excitation/emission of 488/>515 nm. Cells were perfused with Tyrode solution for 2 min for a baseline recording. Then cells were perfused with 5 mM ATP in Tyrode solution for 1 min or 5 μM thapsigargin (Tocris, 1138) in Tyrode solution without CaCl_2 for 2 min. Once the recording returned to baseline, 2 μM ionomycin (Sigma-Aldrich) in Tyrode solution was added to reach F_{max} . A laser scanning confocal microscope (Radiance 2000 MP, Bio-Rad, UK) equipped with a 40x oil-immersion objective lens (N.A.=1.3) was used to record changes in cytosolic $[\text{Ca}^{2+}]_{\text{cyt}}$. Fluo-4 recordings were acquired in line-scan mode (3 ms per scan; pixel size

0.12 μm). All images were analyzed using ImageJ software (NIH, USA). The $[\text{Ca}^{2+}]_{\text{cyt}}$ was calculated by the following formula: $[\text{Ca}^{2+}]_{\text{cyt}} = (F_0 - F_{\text{min}})/(F_{\text{max}} - F_{\text{min}})$, where F_0 was the Fluo-4 fluorescence; F_{max} and F_{min} were the fluorescence levels at 3 mM Ca^{2+} /ionomycin and at the lowest baseline recording, respectively. The calcium-induced calcium release was calculated as the summation of the area under the curve for 150 seconds for ATP and 900 seconds for thapsigargin reported in arbitrary units.

To measure $[\text{Ca}^{2+}]_{\text{mito}}$, either control or VMP1 KO THP-1s were transduced with retroviral vector containing a pMSCVpuro-Mito-Pericam construct as described above [294]. pMSCVpuro-Mito-Pericam was a gift from Björn Stork (Addgene plasmid #87381, <http://n2t.net/addgene:87381>; RRID:Addgene_87381). THP-1s were differentiated in delta T dishes (Bioprotechs, 04200417B). Prior to imaging, the media was replaced by Tyrode solution (NaCl 135 mM; KCl 4 mM; CaCl_2 3 mM; MgCl_2 1 mM; glucose 10 mM; HEPES 10 mM; pH 7.4). Images were acquired using the 60x lens with the EMCCD camera. Cells were excited at 380 nm (DAPI excitation) or 495 nm (FITC excitation) and emission was recorded at 510 nm [295]. Baseline recordings were taken for approximately 30 sec prior to the addition of 5 mM ATP. Five points were taken per dish, and recordings were taken every 8 sec for about 5 min. All images were analyzed using ImageJ software (NIH, USA). The influx rate was quantified for each cell by using the slope of the linear fit of the fluorescence change during 15 sec following the addition of ATP. The efflux rate was quantified for each cell using the slope of the linear fit of a 50 sec period after calcium levels started to decline.

MitoTracker Live Cell Imaging.

To assess mitochondrial mass and mitochondrial membrane potential, THP-1s were differentiated in delta T dishes (Bioprotechs, 04200417B) and treated as described above. Following treatment, cells were incubated with a final concentration of 100 nM MitoTracker Red CMXRos (Invitrogen, M7512), 50 nM MitoTracker Green FM (Cell Signaling Technology, 9074S), and 67 ng/mL Hoechst 33342 (ImmunoChemistry Technologies, 639) in serum free RPMI media for 20 min in the incubator. The cells were washed once with FluoroBrite™ DMEM (Gibco, A1896701) supplemented with 10% FBS and 4 mM L-glutamine (Thermo Fisher Scientific, 25030081). Prior to imaging, the heat chamber was set to 37°C and supplemented with 5% CO₂. The exposure conditions were determined based on the treatment conditions where it was expected for there to be the lowest intensity of MitoTracker Red. For each dish, 20 images were acquired with 20 z-stacks per image at 0.5 μm per z-stack for 10 μm total.

Immunofluorescence Imaging.

THP-1s were differentiated onto glass coverslips (Fisherbrand Cover Glasses, 12-545-J, 22 x 60-1) and treated as described above. To visualize mtDNA in the cytoplasm, following treatment, cells were incubated with a final concentration of 100 nM MitoTracker Red CMXRos (Invitrogen, M7512) in serum free RPMI media for 30 min in the incubator. Cells were then washed once with serum free RPMI media then were fixed with 3.7% formaldehyde, methanol free (Polysciences, 04018-1) in 0.1 M piperazine-*N-N*'bis[2-ethanesulfonic acid] (PIPES) buffer for 10 min. Cells were then washed 3x with PBS. The cells were permeabilized with 0.1% saponin in PBS block

solution supplemented with 10% NDS and 0.01% sodium azide and incubated with mouse anti-DNA clone AC-30-10 (1:25, Millipore Sigma; CBL186) for 1 h at RT. Cells were then washed 3x with PBS. Cells were then incubated with 100 ng/mL Hoechst 33342, 488 conjugated donkey anti-mouse (1:300; Jackson ImmunoResearch Laboratories, 715-545-150), and phalloidin-iFluor 647 reagent (1:1000, Abcam; ab176759) for 20 min at RT. Cells were then washed 3x with PBS and were mounted onto coverslips. For each coverslip, 15 images were acquired with 20 z-stacks per image at 0.5 μm per z-stack for 10 μm total.

To visualize LC3/LAMP1, cells were fixed with 3.7% formaldehyde, methanol free in 0.1 M PIPES buffer for 10 min. Cells were then washed 3x with PBS. The cells were permeabilized with 0.1% saponin in PBS block solution supplemented with 10% NDS and 0.01% sodium azide and incubated with rabbit anti-LAMP1 (1:1000, Abcam; ab24170) and mouse anti-LC3B (E5Q2K) (1:300, Cell Signaling; 83506) for 1 h at RT. Cells were then washed 3x with PBS. Cells were then incubated with 100 ng/mL Hoechst 33342, 488 conjugated donkey anti-mouse (1:300), 647 conjugated donkey anti-rabbit (1:300, Jackson ImmunoResearch Laboratories; 711-605-152) for 20 min at RT. Cells were then washed 3x with PBS and were mounted on coverslips. For each coverslip, 15 images were acquired with 20 z-stacks per image at 0.5 μm per z-stack for 10 μm total.

Wide-field Fluorescence Deconvolution Microscopy.

Cells were imaged on a DeltaVision wide-field fluorescence microscope (Applied Precision, Inc.). It has a digital camera (CoolSNAP HQ2; Photometrics) that was used

for fixed cell imaging, and the gain was set to 4.00. For live cell imaging experiments, an EMCCD camera (Photometrics) was used, and the gain was set to 700. An oil immersion Olympus Plan Apo 60x objective lens (N.A.=1.42), Olympus UplanSApo 100x objective lens (N.A. = 1.40), or Olympus LUCPlanFLN 20x objective lens (N.A. = 0.45) were coated with 1.518 refraction index low autofluorescence immersion oil, Olympus Type F (Fischer Scientific, NC0297589). A 250 watt Xenon Arc lamp was used to direct excitation lighting from the back of the microscope and focused from below onto the coverslip held on an Olympus IX-71 stage. Dichroic filter set used the Alexa setting: FITC excitation: 475/28 Emission: 523/36; A594 excitation: 575/25 emission: 632/30; CY5 excitation: 632/20 emission: 67634; DAPI excitation: 390/18 emission: 435/38. Exposure times varied depending on the type of experiment and staining conditions.

Image Analysis.

The collected z-stack images were used as reconstructed 3-dimensional MIPs for analysis with Imaris software (version 7.6.4, Bitplane) specifically the 3-dimensional masking algorithm function. The same masking algorithm was applied to all images and conditions of a single experiment to allow for consistent group comparisons using the Batch Coordinator tool (Imaris, Bitplane). For the MitoTracker live cell assay, the spots algorithm was built around the MitoTracker Green signal with an estimated diameter of 0.750 μm . For the mtDNA immunofluorescence imaging, a surfaces algorithm was built around the 647 phalloidin channel with the diameter equal to 20 μm and volume above 78.5 μm^3 to create two new channels one for inside of the cell and one for outside of the

cell. A spots algorithm was then built around the 488 DNA signal with an estimated diameter of $0.400\ \mu\text{m}$ and volume between $0.500\ \mu\text{m}^3$ and $2.000\ \mu\text{m}^3$. For the LC3/LAMP1 immunofluorescence imaging, a spots algorithm was built around the 488 LAMP1 signal with an estimated diameter of $0.400\ \mu\text{m}$ and area above $0.100\ \mu\text{m}^2$. Another spots algorithm was built around the 647 LC3 signal with an estimated diameter of $0.500\ \mu\text{m}$ and area above $0.500\ \mu\text{m}^2$.

Quantification of Cellular and Cell-free mtDNA using qPCR.

Quantitative PCR was performed to measure both cellular and cell-free mtDNA as described in a published protocol [296]. Briefly, cells were treated as described above then the supernatant and cell pellets were collected. The supernatant was spun down at 1500 rpm for 10 min at 4°C to remove cell debris. The cell pellets were resuspended in $200\ \mu\text{L}$ PBS. DNA was isolated following the manufacturer's protocol from the QIAamp DNA Mini Kit (Qiagen, 51304) except the samples were lysed with buffer AL, mixed by pulse-vortexing, and were incubated at 56°C for 10 min. The DNA was then placed in a bath sonicator for 5 min for supernatant or 10 min for cell lysate. After sonication, the concentration of DNA in each sample was determined and was adjusted to the same concentration. The standard curves were generated as described. The quantity of mtDNA in the supernatant was reported as the absolute copy number per μL . The quantity of mtDNA in the cell lysate was reported as the fold difference using the formula $2^{(-\Delta\Delta C_t)}$.

Lysosome Dysfunction Assay.

THP-1s were differentiated as described above in a clear bottom, black 96-well plate (Thermo Fisher Scientific, 07-200-565). Cells were treated as described previously including 0.1 μ M bafilomycin (Cayman Chemicals, 11038) for 4 h. Following treatment, cells were loaded with Magic Red cathepsin B dye (ImmunoChemistry Technologies, 937) for 30 min based on the manufacturers' protocol. Cells were washed 3x with FluoroBrite™ DMEM (Gibco, A1896701) supplemented with 10% FBS and 4 mM L-glutamine (Thermo Fisher Scientific, 25030081). The fluorescence signal was measured using a 528 nm excitation wavelength and 628 nm emission wavelength on a Synergy HTX Multi-Mode plate reader (BioTek Instruments) with Gen5 software. The background signal of a well containing cells without dye was subtracted from each experimental well. Graphed data were normalized to untreated control cells.

Statistical Analysis.

Data were analyzed using GraphPad Prism 5.0. Unless otherwise stated, graphs were presented as the mean \pm SEM of at least three independent experiments. Statistical differences were calculated using one-way or two-way ANOVA with Bonferroni post-test, repeated measures ANOVA with Bonferroni post-test, repeated measures ANOVA with Dunnett's multiple comparison test, or two-tailed unpaired t-test as indicated in the figure legends. P-values < 0.05 were considered significant and were designated by: * $p < 0.05$, ** $p < 0.01$, *** $p < 0.001$.

CHAPTER THREE

RESULTS

SECTION ONE: THE UNCONVENTIONAL SECRETION OF GAL-3 FOLLOWING INFLAMMATORY STIMULATION

Rationale.

Galectins, a family of proteins that recognize β -galactosides, have diverse functions that notably contribute to cell activation, proliferation, and apoptosis [297-299]. Interestingly, several galectins modulate processes of disease pathology and progression such as inflammation [135, 300-302]. Of interest here, gal-3 is widely expressed in inflammatory cells and contributes to numerous inflammatory conditions [141, 146, 303-305]. Gal-3 can be released from macrophages and microglial cells, resident macrophages in the CNS, to propagate inflammatory responses in Alzheimer's disease and others [135, 146, 306]. Depending on the cellular environment, galectins can be found both inside and outside of the cell with their localization relating to their function [131]. These proteins lack a classical leader signal resulting in unconventional secretion from cells, yet the underlying mechanisms directing gal-3 release from cells are poorly characterized [131]. Understanding how gal-3 is released and how its structure is involved will be instrumental in developing targeted therapeutics which can promote gal-3 function that is neuroprotective of which there are currently no candidates in trial.

Several studies have aimed to understand the unconventional secretion of other leaderless proteins such as IL-1 β and high motility group box 1 (HMGB1). These proteins can be released by secretory autophagy via EVs or they can directly translocate across the PM with some evidence suggesting that gal-3 can also be secreted through these mechanisms. The secretory pathway utilized by gal-3 may depend on the initiating signal [270, 307, 308]. We and others have previously shown that gal-3 localizes to damaged lysosomes and endosomes suggesting release in EVs upon cellular stress [304, 309-312]. Other potential signals include inflammatory responses driven by activation of TLRs and inflammasomes [97]. Conflicting data show that macrophages classically activated by TLR agonists can release either more or less gal-3 [135, 148, 308, 313]. Other inflammatory stimuli may also determine gal-3 release as inflammasome activation has been found to promote fusion of a secretory lysosome with the PM to release the inflammatory mediators, caspase-1 and IL-1 β [314, 315]. However, TLR and inflammasome activation have also been found to induce autophagy which in some cases resulted in reduced IL-1 β release suggesting at least one mechanism that may influence gal-3 release [316-319]. These conflicting observations may be explained by posttranslational modifications or differences in the localization of gal-3 in the cell upon activation by different inflammatory stimuli, but these hypotheses have yet to be rigorously tested [308].

Some data suggest that gal-3 is predominately secreted outside of EVs by directly crossing the plasma membrane [133, 311]. One possible mechanism for direct

translocation is through GSDMD pores which form following inflammasome activation as part of pyroptosis, a type of inflammatory programmed cell death [118, 119, 134, 320]. Some data suggests that autophagy can protect infected cells from pyroptosis which may negatively regulate gal-3 release, but this idea has not yet been tested [321]. Additionally, the protease, caspase-1, is activated by the inflammasome, and several studies have shown that even proteins such as HMGB1 and IL-1 α that are not substrates of caspase-1 are dependent on the active enzyme for their release, yet why there is this dependence is not understood [307, 322-324]. Proteomics studies have found that gal-3 can bind to caspase-1, but whether caspase-1 influences gal-3 release has not yet been determined [307]. Thus, the underlying mechanisms that delineate how gal-3 is secreted following activation by various inflammatory stimuli need to be well-characterized. The central hypothesis of this section is that inflammatory signals selectively induce gal-3 release through either secretory autophagy or direct translocation across the PM through GSDMD pores in human macrophage-like cells.

Results.

Gal-3 is Predominantly Released through GSDMD Pores under Inflammatory Conditions.

To determine whether GSDMD is required for the release of gal-3 under inflammatory conditions, we utilized CRISPR-Cas9 to knockout GSDMD in THP-1 cells, a human macrophage-like cell line. The knockout was verified by western blot (Fig. 11A). To induce inflammatory responses in these cells, differentiated THP-1s were treated with LPS which activates TLR4 and upregulates proinflammatory genes then the

cells were treated with ATP which activates the inflammasome resulting in formation of GSDMD pores.

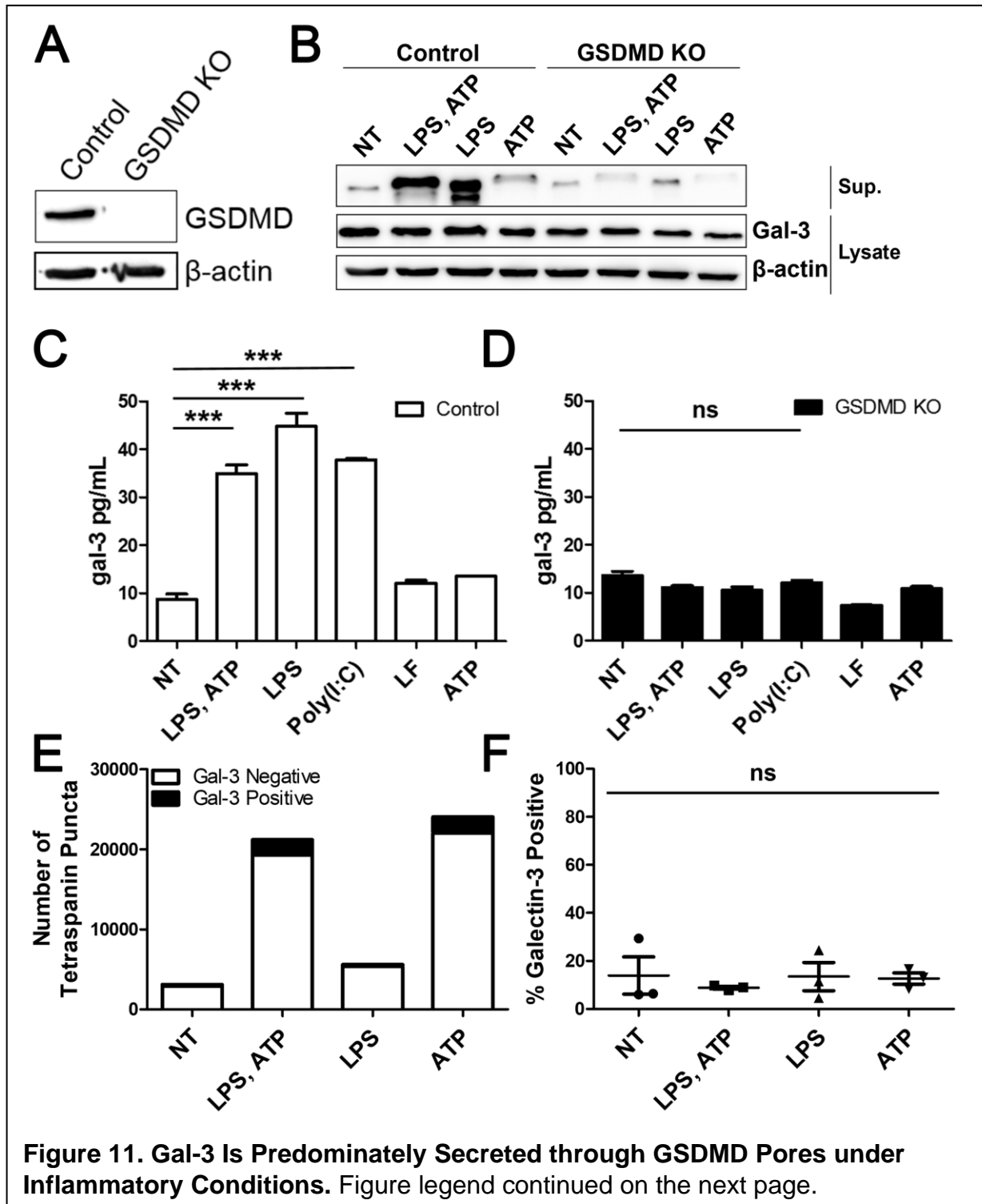


Figure 11. Gal-3 Is Predominately Secreted through GSDMD Pores under Inflammatory Conditions. THP-1 cells were depleted of GSDMD by using CRISPR-Cas9 genome editing. A) Protein expression in the depleted cells was confirmed by western blotting. B) Differentiated control or GSDMD KO THP-1s were treated with 100 ng/mL LPS for 4 h ± 5 mM ATP for 30 min or 5 mM ATP alone for 30 min. Supernatant and lysates were collected and probed for gal-3 protein levels. C-D) Differentiated control or GSDMD KO THP-1s were treated with 100 ng/mL LPS for 4 h ± 5 mM ATP for 30 min, 50 µg/mL poly(I:C) for 4 h, Lipofectamine2000 as a transfection control, or 5 mM ATP for 30 min. Supernatant was collected at the same time for all treatments, and gal-3 released into the supernatant was measured by ELISA. Data are displayed for C) control cells and D) GSDMD KO cells. E) Immunofluorescence microscopy was performed to visualize EVs released into the supernatant from untreated or LPS and ATP treated control or GSDMD KO cells. The EVs were stained with a tetraspanin cocktail and gal-3. The number of tetraspanin puncta that were either positive or negative for gal-3 are displayed. F) Quantification of the percentage of tetraspanin puncta that were positive for gal-3. Data are shown as mean ± SEM and are either representative of or the average of at least three independent experiments. Statistical differences were calculated with two-way ANOVA followed by Bonferroni post-test. For all statistical tests, *, **, ***, $p < 0.05, 0.01, \text{ and } 0.001$, respectively.

LPS alone can also noncanonically activate the inflammasome to form GSDMD pores [8]. To measure gal-3 release in the supernatant from GSDMD KO THP-1s, cells were treated with inflammatory stimuli then the supernatant was collected. Treatment of THP-1s with LPS and ATP or LPS alone resulted in detection of gal-3 in the supernatant by western blot, but in treated GSDMD KO THP-1s, there was a decrease in the release of gal-3 from these cells (Fig. 11B). The amount of gal-3 in the lysates was comparable between the control and GSDMD KO cells and did not change with the addition of inflammatory stimuli. In addition, the release of gal-3 from control or GSDMD KO THP-1s was quantified by ELISA. In this experiment, cells also were treated with poly(I:C) which can induce NLRP3 inflammasome activation and formation of GSDMD pores [325]. There was an increase in the release of gal-3 from control THP-

1s treated with LPS and ATP, LPS alone, and poly(I:C) (Fig. 11C). The release of gal-3 from treated GSDMD KO THP-1s was reduced to levels comparable to the no treatment control suggesting that the release of gal-3 under these inflammatory conditions was dependent on GSDMD pores (Fig. 11D).

Given our previous reports, we hypothesized that gal-3 also can be released in EVs under inflammatory conditions [291]. To determine whether gal-3 is released in EVs, we utilized an immunofluorescence-based assay previously developed in our lab named EV multiplex analysis of colocalization (EV-MAC) [326]. Here EVs were stained with anti-CD9, anti-CD63, and anti-CD81 which all recognize tetraspanins which are transmembrane proteins that are considered a marker of EVs [327]. It is thought that CD9, CD63, and CD81 are unevenly distributed amongst EVs which is why here a tetraspanin cocktail of all three was utilized. A spots algorithm was built around the tetraspanins which allowed us to quantify the number of EVs released under different conditions and ask what percentage of tetraspanin puncta were also positive for gal-3. There was a large increase in the number of tetraspanin puncta that were released from LPS and ATP or ATP only treated THP-1s (Fig. 11E). These results were consistent with a previous study that found that stimulation of the P2X7R by ATP resulted in an increase in the shedding of EVs [328]. To determine whether gal-3 is released in EVs under inflammatory conditions, we quantified the percentage of tetraspanin puncta that were positive for gal-3. The data showed that there was no difference in the relative percentage of EVs containing gal-3 under inflammatory conditions (Fig. 11F). On average, about 10-15% of EVs contain gal-3. Even though there was a large increase in

the number of EVs released under certain inflammatory conditions, the relative amount containing gal-3 was the same under different conditions. Collectively, these data suggested that gal-3 can be released in EVs although it was predominantly released through GSDMD pores under these inflammatory conditions.

Discussion.

In this chapter, we elucidate the mechanism for how gal-3 is released following activation of the cells with inflammatory stimuli. Initially, we hypothesized that gal-3 was likely released in EVs because there was evidence that this was a predominant mechanism of release in our work and others [279, 291]. Rupture of vesicular membranes exposes intraluminal glycans which are recognized by galectins. Autophagic proteins are recruited and galectins are introduced to the autophagic-lysosomal pathway which ultimately results in unconventional secretion [291]. Alternatively, recent work demonstrated that gal-3 can be released through GSDMD pores formed as a result of inflammasome activation in BMDMs [134]. Numerous examples in the literature indicate that there are differences in the inflammatory responses of human and murine derived macrophages [329-331]. Our data in differentiated THP-1s, a human model macrophage-like cell line, demonstrated that gal-3 can be released both in EVs as well as through GSDMD pores. Even though the number of EVs released under inflammatory conditions increased greatly with ATP activation the relative percentage of EVs containing gal-3 was comparable between cells treated with inflammatory stimuli compared to control. The predominant mechanism for gal-3 release following activation by LPS and ATP, LPS alone, and

poly(I:C) alone was through GSDMD pores. It may be interesting in the future to leverage the EV-MAC assay to analyze the contents of the EVs released from macrophages treated with inflammatory stimuli since the number of EVs increased greatly with ATP activation [326]. The advantage of the EV-MAC approach is that it allows for the contents of individual EVs to be determined in contrast to the previous approaches that use western blotting to identify the bulk contents of EVs. Overall, these data suggested that gal-3 was predominantly released through GSDMD pores in response to canonical inflammatory stimuli.

In the next section, we will assess the potential regulatory role of VMP1 in inflammatory responses. Now that we have demonstrated that gal-3 was released through GSDMD pores downstream of inflammasome activation, we can compare patterns of gal-3 and IL-1 β secretion from VMP1 KO cells. It can help us to determine whether the response in VMP1 KO cells is due to changes in inflammasome activation or potentially other mechanisms.

SECTION TWO: VMP1 RESTRICTS INFLAMMASOME ACTIVATION THROUGH ITS MODULATION OF SERCA ACTIVITY AND AUTOPHAGY

Rationale.

VMP1 was first characterized in acute pancreatitis models, an inflammatory disease that results in significant cell death [10]. More recently, it has been identified that VMP1 expression is associated with the severity of cancer and inflammatory bowel disease [332, 333]. With connections to inflammatory disease, we aimed to understand how VMP1 may regulate inflammatory signaling. In the canonical inflammatory pathway,

two signals are required: the first signal induces upregulation of proinflammatory gene expression, and the second signal activates a multiprotein complex specifically the NLRP3 inflammasome. Activation of these pathways ultimately results in the release of inflammatory mediators such as IL-6, IL-1 β , and gal-3. Interestingly, both pathways are activated at least in part by changes in intracellular calcium levels which are known to be influenced by VMP1 [188, 334, 335], yet a regulatory role for VMP1 in these responses has not yet been identified. Intriguingly, while there are many known activators of inflammasomes, questions persist about which specific signals are required for inflammasome activation particularly when more than one signal is present in the same cell. Thus, identifying and characterizing a novel regulator of these pathways will be instrumental in being able to specifically target and successfully modulate inflammatory responses in disease.

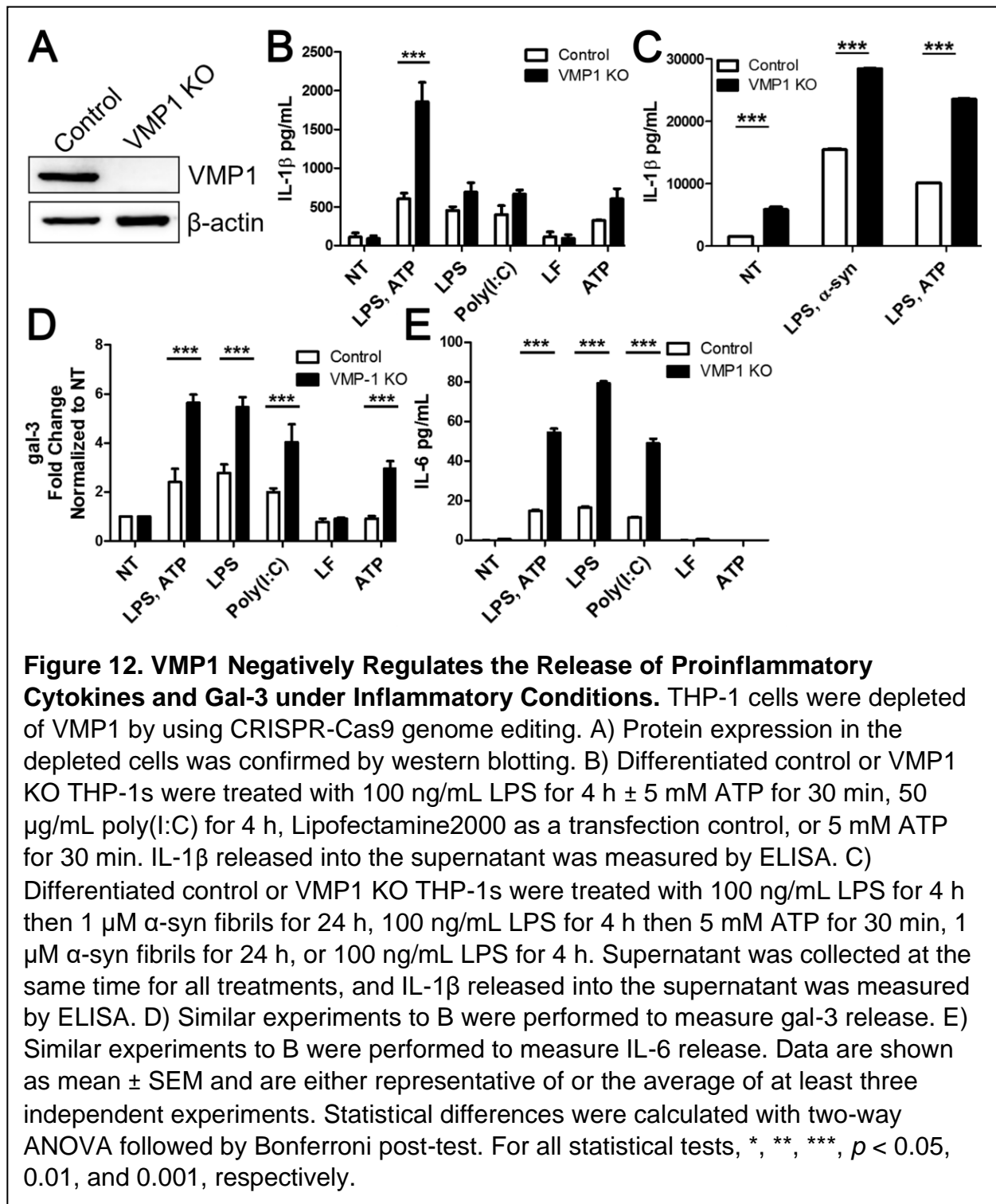
Surprisingly, better characterized VMP1 orthologs have pleiotropic phenotypes suggesting that VMP1 likely regulates several cellular processes including protein secretion [16-18]. Of interest here was characterizing how VMP1 may affect the release of proinflammatory cytokines and gal-3 following inflammatory activation of macrophages. Existing data suggested that both damaged mitochondria and calcium fluxes can activate inflammatory pathways, but how VMP1 modulation of these signals may impact cellular inflammatory responses was not yet understood. Perhaps given its known functions, VMP1 may regulate these responses by degrading damaged mitochondria and buffering cytoplasmic Ca²⁺ concentrations [5, 150]. Thus, the underlying mechanisms that delineate how VMP1 regulates inflammatory signaling

pathways need to be well-characterized. The central hypothesis of this section is that VMP1 modulates cytoplasmic Ca²⁺ concentrations and mediates the degradation of damaged mitochondria to negatively regulate inflammasome activation and the release of proinflammatory cytokines and gal-3.

Results.

VMP1 Negatively Regulates the Release of Proinflammatory Molecules.

To determine whether VMP1 affects the secretion of proinflammatory molecules, we utilized CRISPR-Cas9 to knockout VMP1 in THP-1s, a human model macrophage like cell line [12, 336]. The knockout was verified by western blot (Fig. 12A). To induce canonical inflammatory signaling, differentiated THP-1s were treated with LPS to activate TLR4 and induce the upregulation of inflammatory cytokine gene expression and then ATP to activate the inflammasome. To induce noncanonical activation of the inflammasome, LPS alone was used [337]. Transfected poly(I:C), representative of cytosolic dsRNA produced during viral infection, was also used to activate the NLRP3 inflammasome [325]. VMP1 expression does not change even when cells are treated with inflammatory stimuli (Fig. 13A). To initially assess whether there are differences in inflammatory responses in VMP1KO cells, IL-1 β release was measured. Treatment of VMP1 KO THP-1s with LPS and ATP resulted in increased secretion of IL-1 β compared to treated control cells suggesting that there may be increased inflammasome activation in VMP1 KO cells (Fig. 12B). Since it was recently observed that PD patients have reduced expression of VMP1 in PBMCs, we wanted to ask whether primed VMP1 KO macrophages treated with α -syn release more IL-1 β .

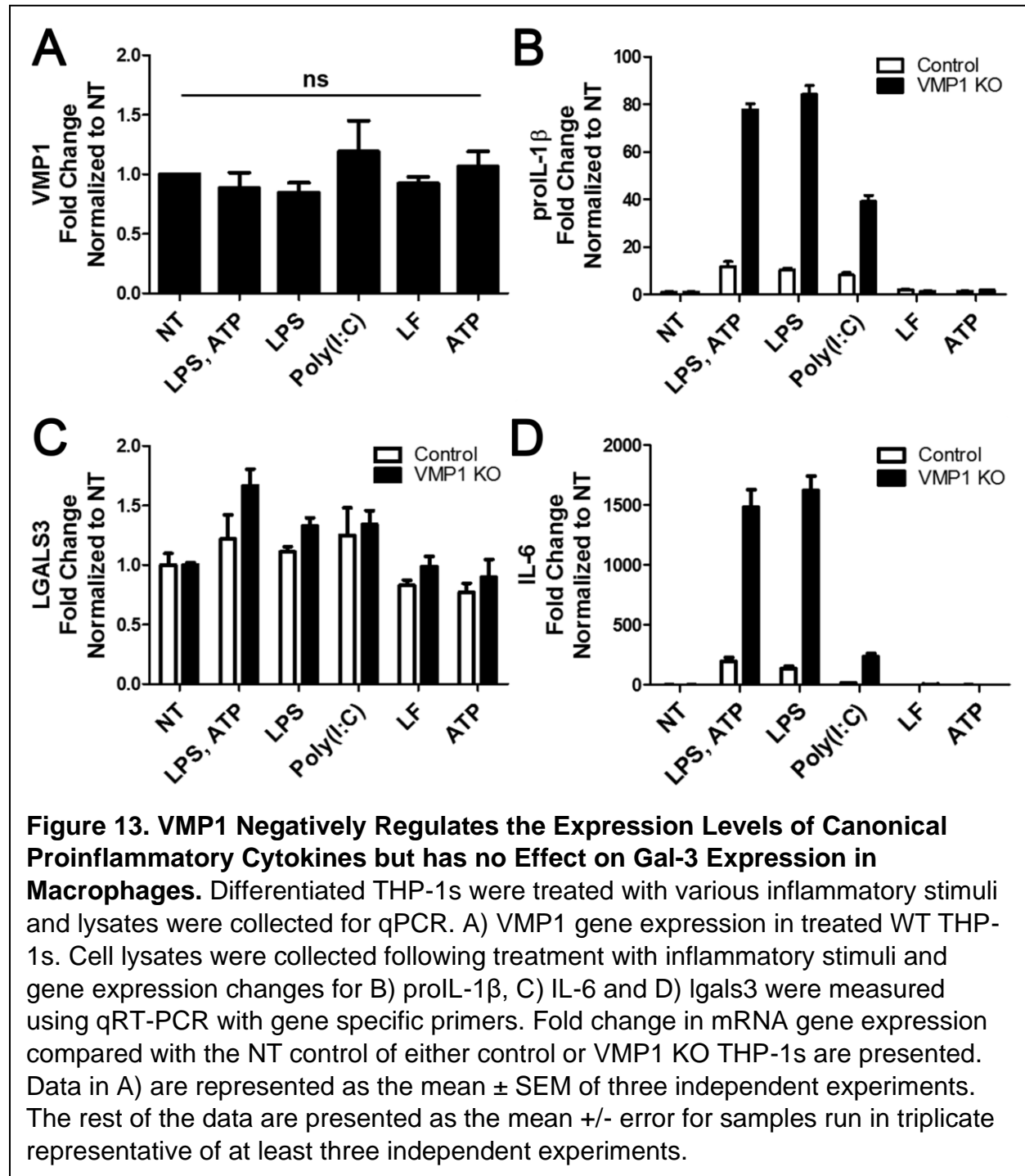


Under these conditions, supernatant was collected after 24 hrs. There was elevated basal IL-1β release from VMP1 KO cells compared to control cells suggesting that

VMP1 KO cells were already more proinflammatory without the addition of inflammatory stimuli (Fig. 12C). Primed VMP1 KO cells treated with α -syn released more IL-1 β than control cells (Fig. 12C). These data suggested that PD patients with decreased VMP1 expression may have an increased basal level of inflammation as well as exacerbated inflammatory responses to protein aggregates characteristic of the disease.

Previous reports and our data above suggested that gal-3 was released through GSDMD pores under inflammatory conditions. As expected VMP1 KO cells treated with LPS and ATP, LPS alone, and poly(I:C) alone had increased release of gal-3 which was consistent with the results for IL-1 β release (Fig. 12D). Additionally, VMP1 KO cells treated with ATP alone had increased gal-3 release compared to treated control cells (Fig. 12D). Given that the autophagosome-lysosome pathway (ALP) was impaired in VMP1 KO cells and that there was an increase in EV release with ATP treatment (Fig. 11E), perhaps that is why there was increased gal-3 release from ATP treated VMP1 KO cells although this would need to be tested directly [5, 31]. Interestingly, VMP1 KO cells had increased IL-6 release from cells treated with LPS and ATP, LPS alone, and poly(I:C) alone (Fig. 12E). IL-6 gene expression is upregulated following TLR activation, yet its release occurs independently of inflammasome activation. VMP1 negatively regulated the expression of proinflammatory cytokines, proIL-1 β and IL-6, but had no effect on the expression of gal-3 (Fig. 13B, 13C, and 13D). Perhaps increased expression of IL-6 in VMP1 KO cells was sufficient to result in its increased release, but that would need to be tested. Overall, increased release of IL-6 when cells were treated

with LPS and ATP, LPS alone and poly(I:C) alone suggested that VMP1 may promote hypersensitive TLR signaling (Fig. 12E).



Second, increased IL-1 β release from LPS and ATP treated VMP1 KO macrophages suggested that dysregulation in VMP1 KO cells may induce increased inflammasome activation (Fig. 12B). Therefore, these data suggested that VMP1 is a novel regulator of inflammatory signaling and that it may have this effect either by 1) creating a state that allows for hyperactivation of TLR signaling and/or 2) promoting dysregulation such that conditions promote increased inflammasome activation. Collectively, these data suggested that VMP1 negatively yet differentially regulated the release of IL-1 β , IL-6, and gal-3 depending on the inflammatory stimuli and that VMP1 KO cells have elevated basal inflammatory responses.

VMP1 KO Cells have Increased Caspase-1 and Caspase-3 Activation Depending on the Stimuli.

To determine whether VMP1 KO cells have increased inflammasome activation, we employed a fluorochrome-labeled inhibitors of caspases assay (FLICA) to measure active caspase-1. Treatment of VMP1 KO cells with LPS and ATP and ATP alone resulted in an increase in FLICA signal compared to control cells suggesting that when cells were treated with these inflammatory stimuli there was an increase in caspase-1 activation (Fig. 14A). To assess changes in inflammasome activation over time, we measured biosensor activation where upon inflammasome activation, a caspase-1 consensus sequence is cleaved resulting in active firefly luciferase [290]. We observed that in VMP1 KO cells treated with LPS and ATP there was increased biosensor activation at 4 h which is right before the addition of ATP and at 7.5 h which is several hours after the addition of ATP (Fig. 14B). Similar trends were observed for cells treated with LPS alone (Fig. 14C). There was no difference in biosensor activation between

VMP1 KO and control cells treated with poly(I:C) which was consistent with the FLICA data (Fig. 14D). Since there was no difference in inflammasome activation in poly(I:C) treated cells, there might be an inflammasome independent reason for why there was increased release of gal-3 in VMP1 KO cells compared to control cells. Interestingly, there was increased inflammasome activation in VMP1 KO cells treated with ATP alone even at time points prior to the addition of the DAMP supporting the idea that there were elevated basal inflammatory responses in VMP1 KO cells compared to control cells (Fig. 14E). Collectively, these data suggested that there was increased caspase-1 activation in VMP1 KO cells treated with LPS and ATP.

To determine whether this increase in inflammasome activation was specific to the NLRP3 inflammasome, we pretreated cells with MCC950, a specific inhibitor of the NLRP3 inflammasome, prior to the addition of ATP then measured caspase-1 biosensor activation [338]. When either LPS and ATP treated VMP1 KO or control cells were pretreated with MCC950, there was a decrease in caspase-1 activation comparable to the no treatment control (Fig. 14F). These data suggested that it was specifically the NLRP3 inflammasome that was being activated in VMP1 KO cells. To assess whether there was increased cell death in treated VMP1 KO cells compared to control, we probed for cleaved caspase-3, a marker of apoptotic cell death, by western blot. An increase in cleaved caspase-3 was detected in VMP1 KO cells treated with LPS and ATP and poly(I:C) as well as a slight increase with LPS treatment alone indicating that there was induction of cell death (Fig. 14G). Additionally, LDH release was quantified as an indicator of pyroptosis [339].

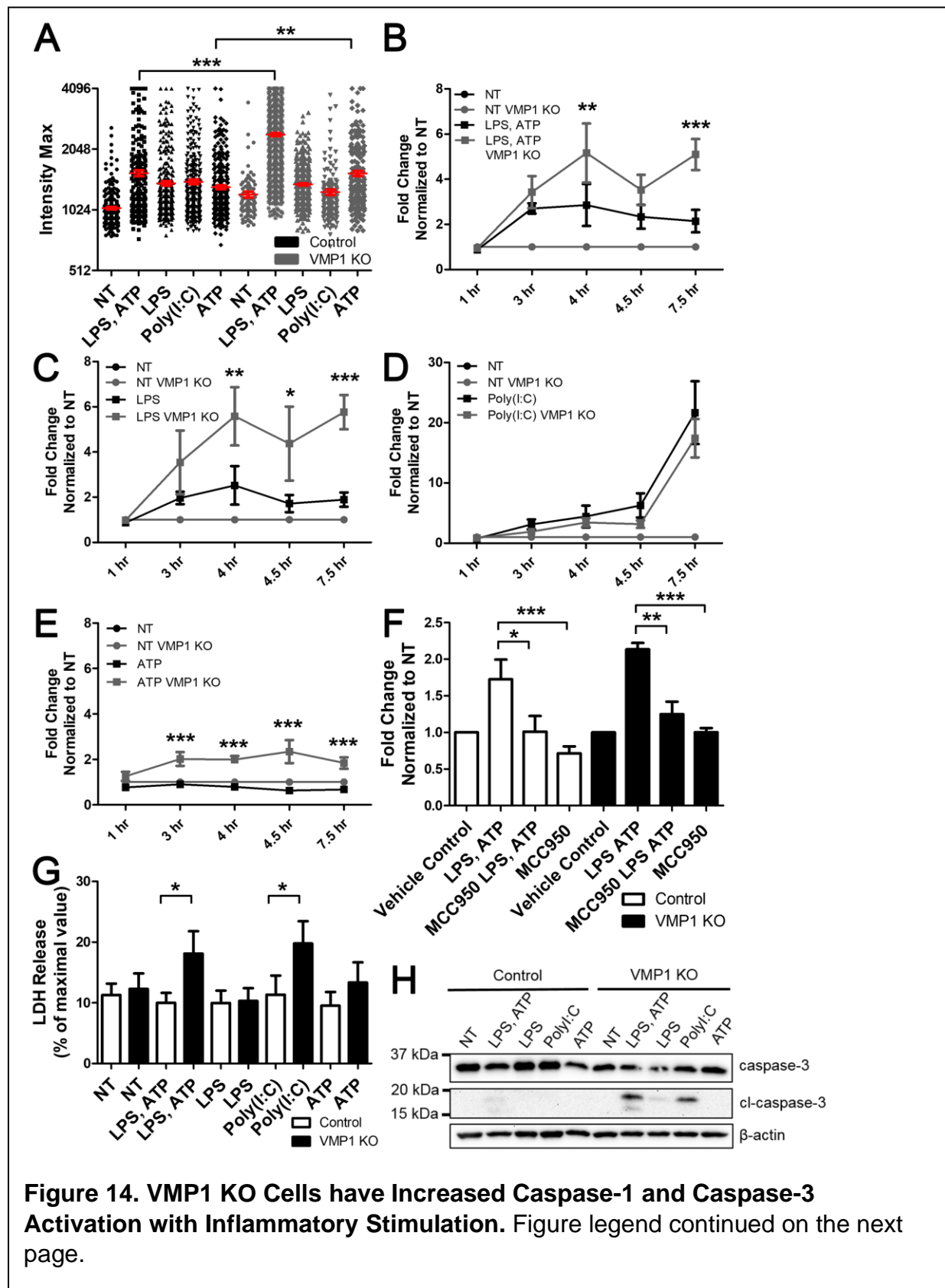


Figure 14. VMP1 KO Cells have Increased Caspase-1 and Caspase-3 Activation with Inflammatory Stimulation. Figure legend continued on the next page.

Figure 14. VMP1 KO Cells have Increased Caspase-1 and Caspase-3 Activation with Inflammatory Stimulation. Differentiated control or VMP1 KO cells were treated with LPS and ATP, LPS, poly(I:C), and ATP. A) Caspase-1 activation was assessed by confocal microscopy using a FLICA assay. Data are represented as the intensity max per cell from 10 images per treatment. B-E) Control or VMP1 KO THP-1s transduced with the C7 biosensor were activated with B) LPS and ATP, C) LPS, D) poly(I:C), and E) ATP and luminescence was measured at 1 h, 3 h, 4 h, 4.5 h, and 7.5 h following treatment. F) THP-1s were treated with an NLRP3 inflammasome inhibitor, MCC950, then caspase-1 activation was measured with the C7 biosensor. G) Caspase-3 and cleaved caspase-3 were measured by western blotting. H) THP-1s were treated with inflammatory stimuli then cell death was measured by LDH assay. Data are shown as mean \pm SEM and are either representative of or the average of at least three independent experiments. Statistical differences were calculated with two-way ANOVA followed by Bonferroni post-test or repeated measures ANOVA followed by Bonferroni post-test. For all statistical tests, *, **, ***, $p < 0.05$, 0.01, and 0.001, respectively.

An increase in LDH release was measured from VMP1 KO cells treated with LPS and ATP and poly(I:C) which corresponded with the amount of cleaved caspase-3 (Fig. 14H). Collectively, these data suggested that in VMP1 KO cells there was increased caspase-1 activation specifically through the NLRP3 inflammasome along with increased cell death corresponding to treatment with specific inflammatory stimuli.

VMP1 KO Cells have Depleted ER Ca²⁺ Stores but Elevated Intracellular [Ca²⁺] with ATP Activation.

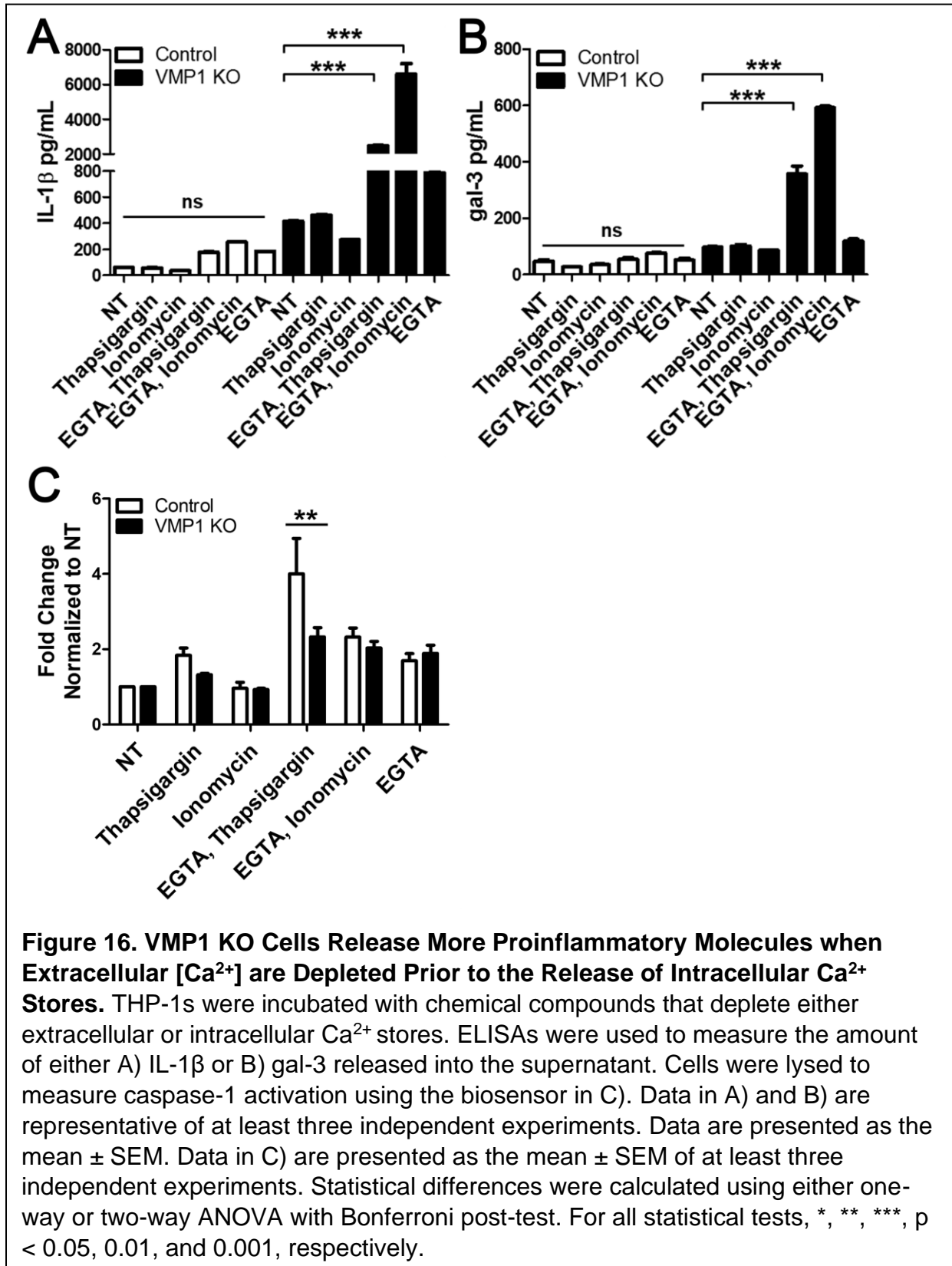
Previous work in the literature suggests VMP1 can regulate the activity of the ER calcium channel SERCA by stabilizing it in its active form and directly preventing interaction with its inhibitory binding partners [5]. This study primarily focused on characterizing how this function of VMP1 influenced membrane contacts at the ER, but it did not address how this interaction influenced other calcium sensitive pathways in the cell [5]. In particular, when cells are activated with ATP, there is K⁺ efflux through the P2X7 receptor that is accompanied by an influx of Ca²⁺ which may be perturbed in

VMP1 KO cells that have diminished SERCA activity [340]. To measure changes in intracellular $[Ca^{2+}]$, a high-affinity Ca^{2+} indicator, Fluo-4 AM, was used with live cell imaging. To assess whether there were changes in $[Ca^{2+}]_{cyt}$ when cells were activated with ATP, differentiated VMP1 KO or control cells were perfused with a solution of ATP in Tyrode solution containing 3 mM Ca^{2+} . There was a longer response to ATP treatment in VMP1 KO cells compared to control (Fig. 15A). The average calcium induced calcium release (CICR) area was calculated for several cells. The CICR area describes a general mechanism whereby Ca^{2+} triggers the release of further Ca^{2+} from intracellular stores. The CICR area for ATP-treated VMP1 KO was greater than control cells (Fig. 15B). Previous studies have demonstrated that VMP1 can regulate the activity of SERCA, a Ca^{2+} -ATPase [5]. To measure the relative amount of Ca^{2+} stored in the ER of VMP1 KO versus control cells, differentiated THP-1s were perfused with a solution containing thapsigargin, a non-competitive inhibitor of the sarco/endoplasmic reticulum Ca^{2+} -ATPase, in Tyrode solution without Ca^{2+} . These data showed that there was a small amount of Ca^{2+} in the VMP1 KO cells that was rapidly released upon the addition of thapsigargin compared to control cells that comparatively have a sustained release of Ca^{2+} (Fig. 15C-D). To test whether the VMP1 regulation of SERCA contributed to inflammasome activation, cells were treated with inflammatory stimuli in the presence of thapsigargin or thapsigargin alone. The data showed that there was increased caspase-1 activation in control THP-1s when cells were treated with LPS and ATP or ATP alone in the presence of thapsigargin suggesting that inhibition of SERCA was contributing to the exacerbated inflammatory phenotype observed in VMP1 KO

Figure 15. VMP1 KO Cells have Depleted ER Ca²⁺ Stores, but Increased Intracellular [Ca²⁺] with ATP Treatment. Either control or VMP1 KO THP-1s were perfused with Tyrode solution containing 3 mM Ca²⁺ for 1 min then were either perfused with A-B) ATP or C-D) thapsigargin prior to adding F_{max} consisting of Tyrode solution with 3 mM Ca²⁺ and ionomycin. A,C) Representative traces of the normalized fluorescence intensity of individual cells. B,D) Average calcium-induced calcium release (CICR) area under the curve of individual cells for either B) 150 sec or D) 900 sec. E) Caspase-1 activation assessed using confocal microscopy and a FLICA assay. Data are represented as the intensity max of individual cells for a given treatment. Statistical differences were calculated with two-tailed unpaired t-tests or one-way ANOVA followed by Bonferroni post-test. For all statistical tests, *, **, ***, *p* < 0.05, 0.01, and 0.001, respectively.

When VMP1 KO cells were treated with LPS and ATP in the presence of thapsigargin, there was a decrease in caspase-1 activation which might be explained by the depleted ER store of Ca²⁺ prior to the addition of ATP. Previous studies have shown that Ca²⁺ mobilization can contribute to inflammasome activation [189]. To determine whether Ca²⁺ fluxes alone influence inflammasome activation, cells were treated with thapsigargin. The results showed a slight increase in FLICA signal in either control or VMP1 KO cells treated with thapsigargin suggesting that Ca²⁺ release from the ER has a modest effect on inflammasome activation (Fig. 15E).

To further determine whether Ca²⁺ mobilization affects inflammasome activation and cytokine release, differentiated THP-1s were incubated with chemical compounds that deplete extracellular Ca²⁺ or inhibit release of Ca²⁺ from inside of the cell. There was an increase in the release of IL-1 β and gal-3 when VMP1 KO cells were incubated with EGTA and thapsigargin or EGTA and ionomycin (Fig. 16A-B). This increase was likely due to the dysregulated response to changes in Ca²⁺ in VMP1 KO cells that then induced K⁺ efflux which is a known activator of the inflammasome [341].



Caspase-1 activation measured by the biosensor corresponded with these data where there was a modest increase in caspase-1 activation with thapsigargin treatment, but there was a larger increase in this activation when extracellular Ca^{2+} was depleted with EGTA (Fig. 16C). Taken together, these data suggested that when VMP1 was not present to regulate SERCA, there were elevated levels of intracellular Ca^{2+} following inflammatory stimulation. In WT cells, treatment with thapsigargin increased caspase-1 activation suggesting that at least in part there was increased inflammasome activation due to inhibition of the SERCA pump. Yet there were likely other changes associated with VMP1 function that also increased inflammasome activation.

VMP1 KO Cells have an Increased Rate of Ca^{2+} Influx into Mitochondria upon ATP Stimulation.

To quantify the effect of VMP1 on mitochondrial buffering of Ca^{2+} , a stable THP-1 cell line expressing the Ca^{2+} -sensitive ratiometric fluorescent protein mito-pericam were generated [294]. This construct consists of a fluorescent [Ca^{2+}] probe that contains a modified permutated EYFP where the C- and N- terminal domains were exchanged and connected by a Gly-rich linker as well as the introduction of the following mutations: F46L, Q69K, H148D, V163A, S175G, and Y203F. This sequence is flanked by calmodulin (CaM) at the C-terminus and by an M13 peptide (the CaM binding site (K566-L591) of human MYLK2) at the N-terminus. This construct has a localization signal for mitochondria and can be excited at different wavelengths depending on how much calcium is present (Fig. 17A and 17B). An increase in [Ca^{2+}] leads to binding of CaM to M13 peptide which results in a conformational change. This structural change results in a shift of excitation from ~410 nm to ~495 nm with the emission peak

remaining the same at ~515 nm. The fluorescence intensity ratio of Ex495/Ex410 increases up to tenfold with elevated $[Ca^{2+}]$. Live cell imaging was performed with recordings of the basal level of fluorescence in the DAPI and FITC channels then for a period after the addition of inflammatory stimuli.

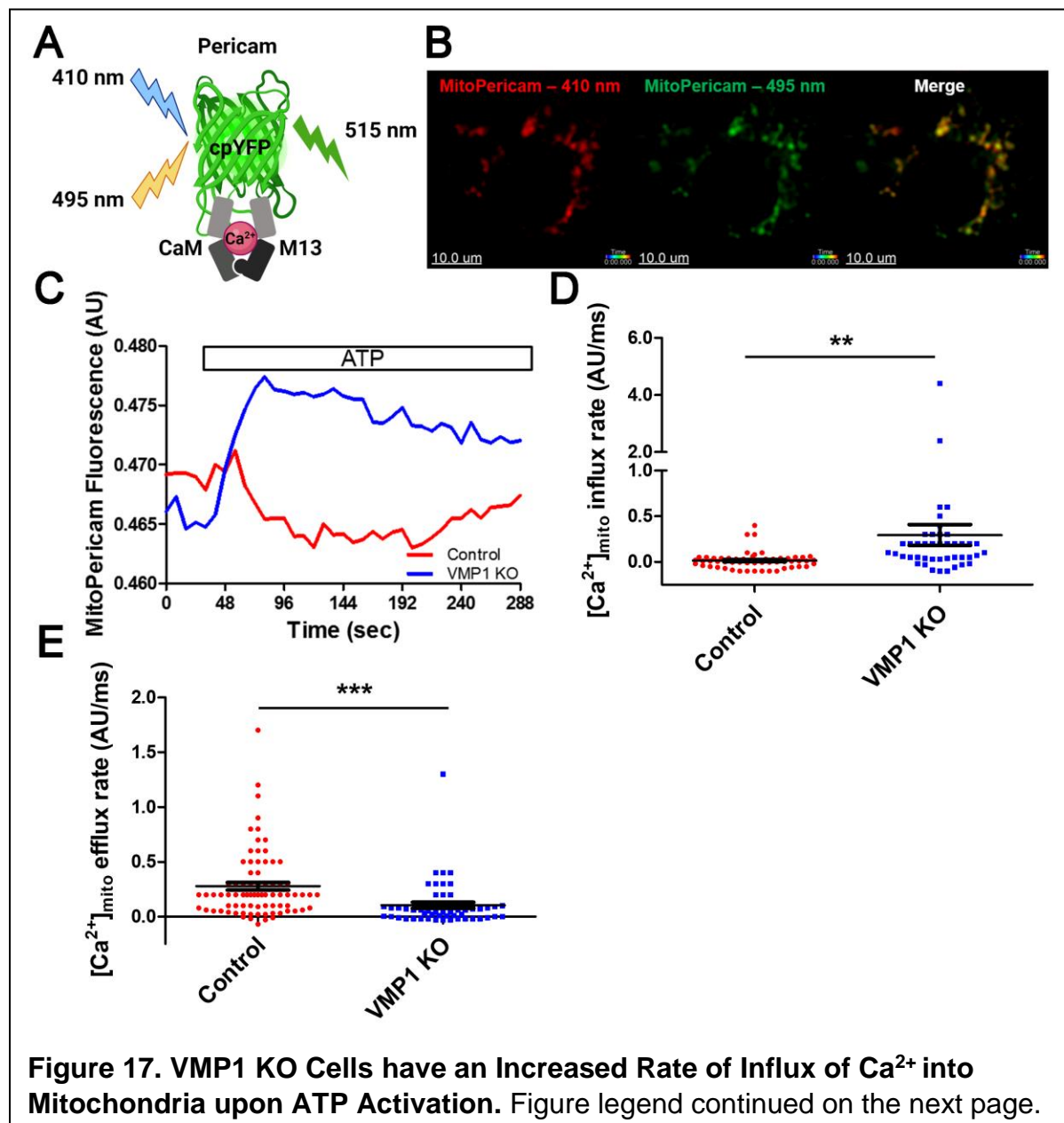


Figure 17. VMP1 KO cells have an Increased Rate of Influx of Ca²⁺ into Mitochondria upon ATP Activation. Differentiated control or VMP1 KO THP-1s were transduced with a pMSCVpuro-Mito-Pericam construct. Cells were excited at 410 nm and 495 nm first to collect baseline recordings then cells were activated with ATP. A) Schematic illustrating how the pMSCVpuro-Mito-Pericam construct works. The ratiometric pericam is a fluorescent [Ca²⁺] probe that contains a modified permuted EYFP flanked by calmodulin and an M13 peptide which contains the CaM binding site. At low [Ca²⁺], the construct is excited at 410 nm, but an increase in [Ca²⁺] facilitates the binding of CaM to the M13 peptide resulting in structural changes that cause a shift of the excitation maximum from ~410 nm to ~495 nm. B) Representative images of cells expressing the mito-pericam construct. C) Representative traces of the ratio of fluorescence intensity at 495 nm/410 nm of individual cells. D) Average [Ca²⁺]_{mito} influx rate of individual cells over 15 sec. E) Average [Ca²⁺]_{mito} efflux rate of individual cells over 50 sec. Data are either representative of three independent experiments (C) or the average of individual cells from at least three independent experiments. Statistical differences were calculated with two-tailed unpaired t-tests. For all statistical tests, *, **, ***, *p* < 0.05, 0.01, and 0.001, respectively.

To assess changes in the [Ca²⁺]_{mito} of VMP1 KO versus control cells upon ATP stimulation, images were acquired by exciting the cells at 410 nm and 495 nm for baseline recordings then ATP was added. The mito-pericam fluorescence intensity was displayed as the ratio of 495 nm/410 nm. Representative traces of the fluorescence intensity of VMP1 KO or control cells demonstrated that upon ATP stimulation, there was an increase in the ratio of the fluorescence intensity for VMP1 KO cells compared to control cells (Fig. 17C). To determine the influx rate of Ca²⁺ into mitochondria, the slope of the line for the fluorescence intensity ratio was determined over a 15 sec interval following the addition of ATP. On average, the [Ca²⁺]_{mito} influx rate was faster in VMP1 KO cells compared to control cells (Fig. 17D). To determine the efflux rate of Ca²⁺ from mitochondria, the slope of the line for the fluorescence intensity ratio was determined over a 50 sec period after calcium levels started to decline. The efflux rate

of $[Ca^{2+}]_{mito}$ was faster for control cells treated with ATP suggesting that calcium was extruded faster from control cells than VMP1 KO cells (Fig. 17E). Collectively, these data suggested that mitochondrial calcium dynamics were altered in VMP1 KO cells such that there was increased uptake of Ca^{2+} following ATP stimulation as evidenced by an increased influx rate over the same period as control as well as a decreased extrusion rate of Ca^{2+} from the mitochondria following ATP stimulation.

VMP1 KO Cells have More and Smaller Mitochondria that Lose their Membrane Potential with LPS and ATP Treatment.

To characterize mitochondrial fitness, we developed an approach where live differentiated THP-1s were incubated with fluorescent mitochondrial dyes then confocal microscopy images were acquired. Differentiated THP-1s were incubated with MitoTracker Green (MTG) dye and MitoTracker Red CMXRos (CMXRos) dye. MTG is a fluorescent probe that assesses mitochondrial mass. It accumulates in mitochondria independently of the mitochondrial transmembrane potential meaning that it labels mitochondria in living cells. CMXRos is a fluorescent probe that stains mitochondria, but its accumulation is dependent upon the mitochondrial membrane potential. At steady state, macrophages have high mitochondrial polarization, but upon macrophage activation, it is typical to observe a loss in mitochondrial membrane potential. An algorithm was built around the MTG channel using Imaris to allow us to not only measure the membrane potential of individual mitochondria but also to quantify the number of mitochondria per cell and the average mitochondrial volume (Fig. 18A). To further assess the relative amounts of functional or dysfunctional mitochondria, the intensity max of the CMXRos was plotted on the y-axis and the intensity max of the

MTG was plotted on the x-axis. Gridlines were drawn where mitochondria that were CMXRos and MTG high were considered functional and mitochondria that were CMXRos low and MTG high were considered dysfunctional.

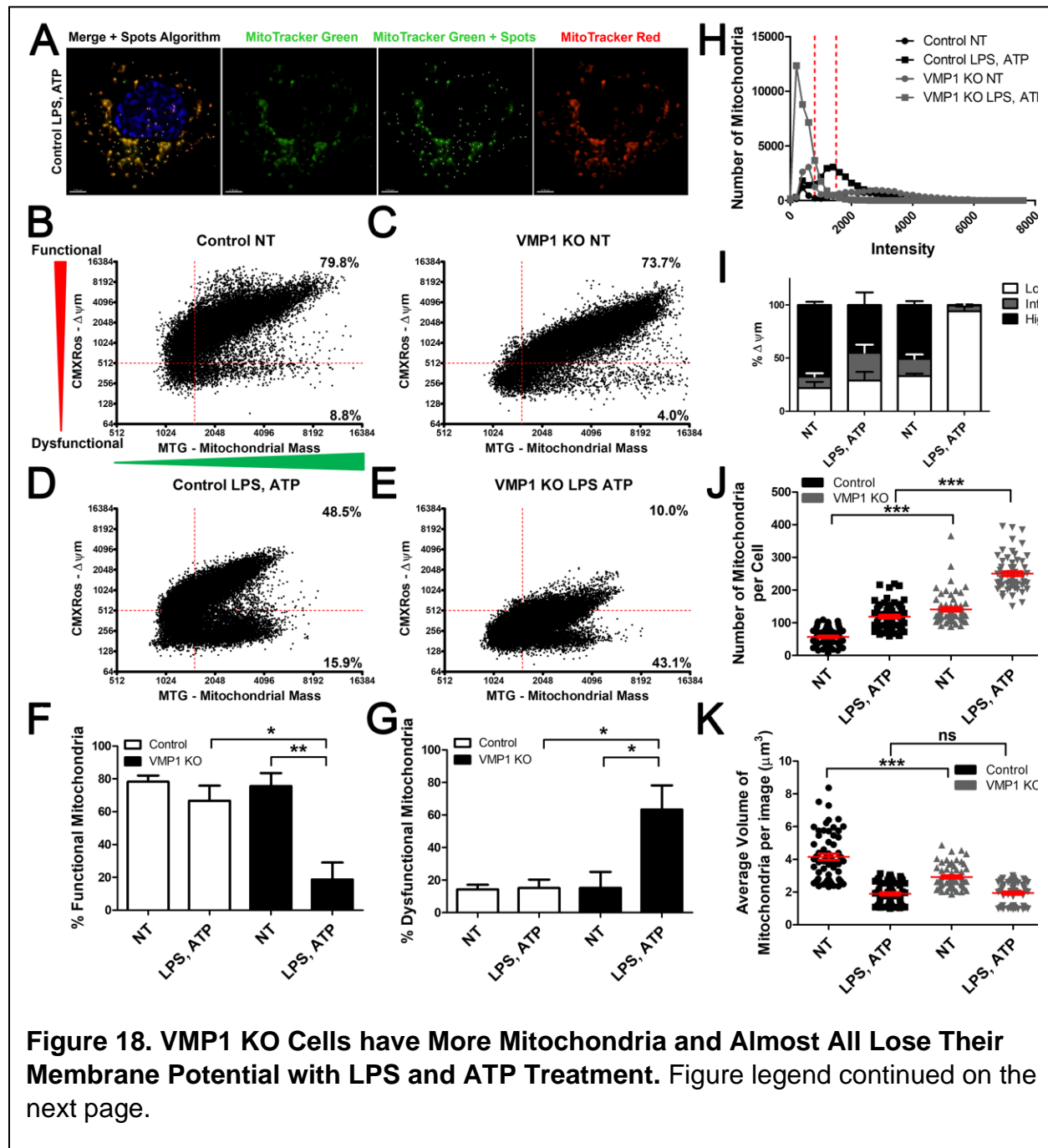


Figure 18. VMP1 KO Cells have More Mitochondria and Almost All Lose Their Membrane Potential with LPS and ATP Treatment. Control or VMP1 KO cells were left untreated or treated with LPS and ATP. Live cells were stained with CMXRos with its accumulation in the cell dependent on mitochondrial membrane potential and with MTG to assess mitochondrial mass. Imaris was then used to build a spots algorithm around the MTG channel. A) Representative image of treated control THP-1s that were incubated with CMXRos and MTG. B) Quantification of the average number of mitochondria per cell per image. C) Quantification of the average volume of individual mitochondria per image. D-G) Plots of the intensity max of CMXRos vs. MTG for individual mitochondria. Percentages in the upper right quadrant correspond to functional mitochondria and percentages in the lower right quadrant correspond to dysfunctional mitochondria. H) Percentages for CMXRos High/MTG High populations corresponding to functional mitochondria represented as the mean \pm SEM for three independent experiments. I) Percentages for CMXRos Low/MTG High populations corresponding to dysfunctional mitochondria represented as the mean \pm SEM for three independent experiments. J) Representative histogram depicting the number of mitochondria in each bin of intensity max for the CMXRos channel. K) Plot showing the percentage of mitochondria that have low, intermediate, and high mitochondrial membrane potential. Statistical differences were calculated with one-way ANOVA followed by Bonferroni post-test. For all statistical tests, *, **, ***, $p < 0.05$, 0.01 , and 0.001 , respectively.

Most mitochondria in untreated control cells were functional, and with treatment, the functional population decreased which corresponded to an increase in dysfunctional mitochondria (Fig. 18B, 18D). Interestingly, untreated VMP1 KO cells had similar populations of mitochondria to control cells although with LPS and ATP treatment, there was a drastic decrease in the percentage of functional mitochondrial and a large increase in the percentage of dysfunctional mitochondria (Fig. 18C, 18E). In LPS and ATP treated VMP1 KO cells, where instead of most mitochondria being functional, only about 20% of the mitochondria were functional (Fig. 18F). The inverse trend was observed for dysfunctional mitochondria where about 60% of the mitochondria were

dysfunctional in the LPS and ATP treated VMP1 KO cells compared to less than 20% in the other conditions (Fig. 18G).

Establishment of mitochondrial membrane potential is needed for normal cellular function, but under inflammatory conditions, it has been observed that there is a loss of membrane potential [217, 342]. To determine the relative membrane potential under these conditions, histograms of the max intensity of the CMXRos channel for each mitochondrion were generated (Fig. 18H). There was an increase in the percentage of mitochondria that have intermediate to low membrane potential in treated control cells. There was a dramatic loss in membrane potential in VMP1 KO cells treated with LPS and ATP such that at least 90% of the mitochondria have low membrane potential (Fig. 18I). Collectively, these data demonstrated that VMP1 KO cells have more and smaller mitochondria perhaps suggesting that there was more fission occurring. Additionally, treated VMP1 KO cells have a large population of dysfunctional mitochondria that corresponded to almost all the mitochondria having low membrane potential.

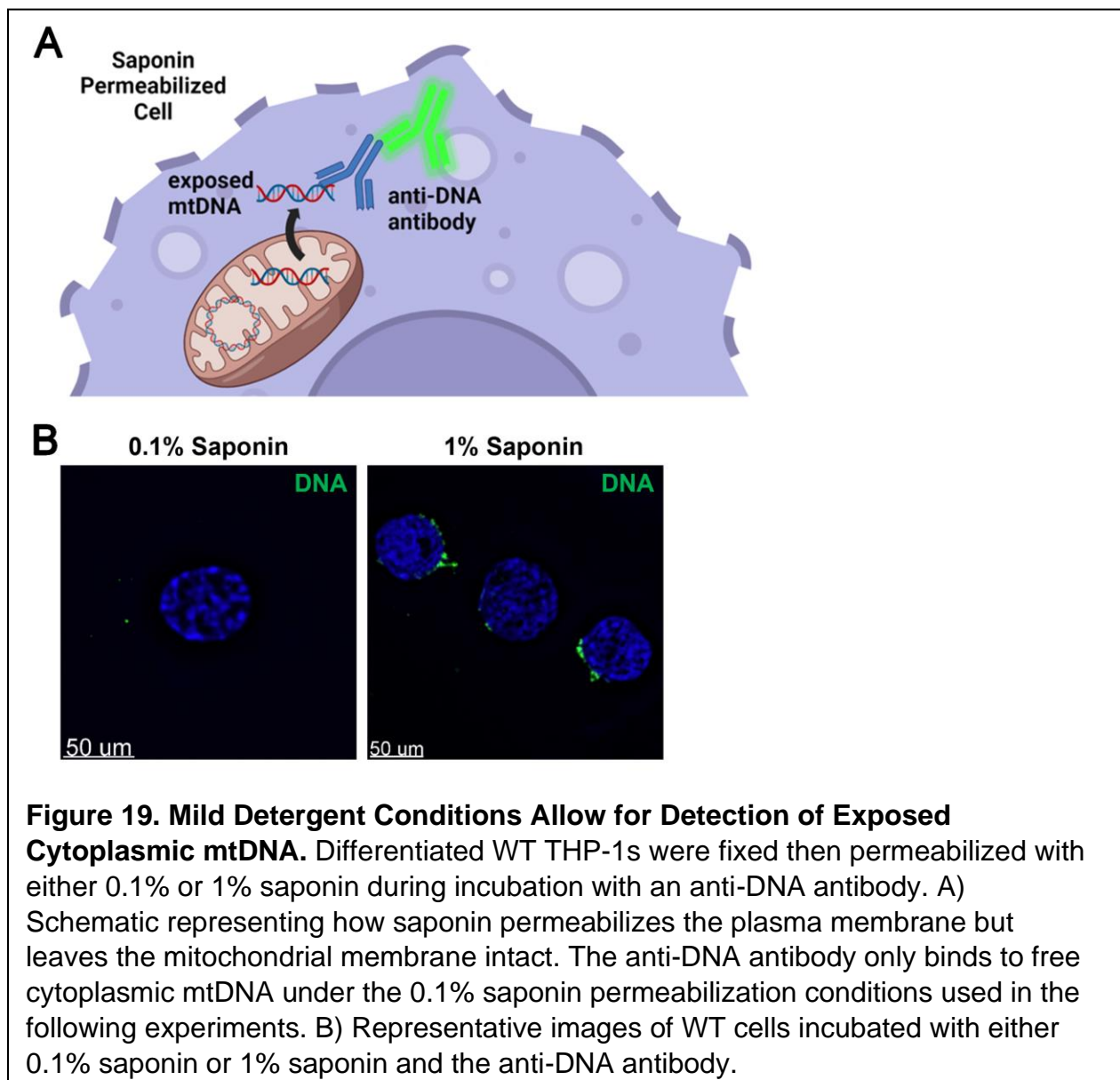
Treatment of control THP-1s with LPS and ATP resulted in an increase in the number of mitochondria that was comparable to VMP1 KO cells. The average number of mitochondria per cell was highest for VMP1 KO cells treated with LPS and ATP (Fig. 18J). These results were consistent with the average volume of mitochondria which showed that control THP-1s have the largest and most variability in volume. The other conditions had smaller average volumes (Fig. 18K). Previous work suggested that altered mitochondrial fusion can result in mitochondrial fragmentation and increased apoptotic cell death [210]. Our data supported that there may be a defect in

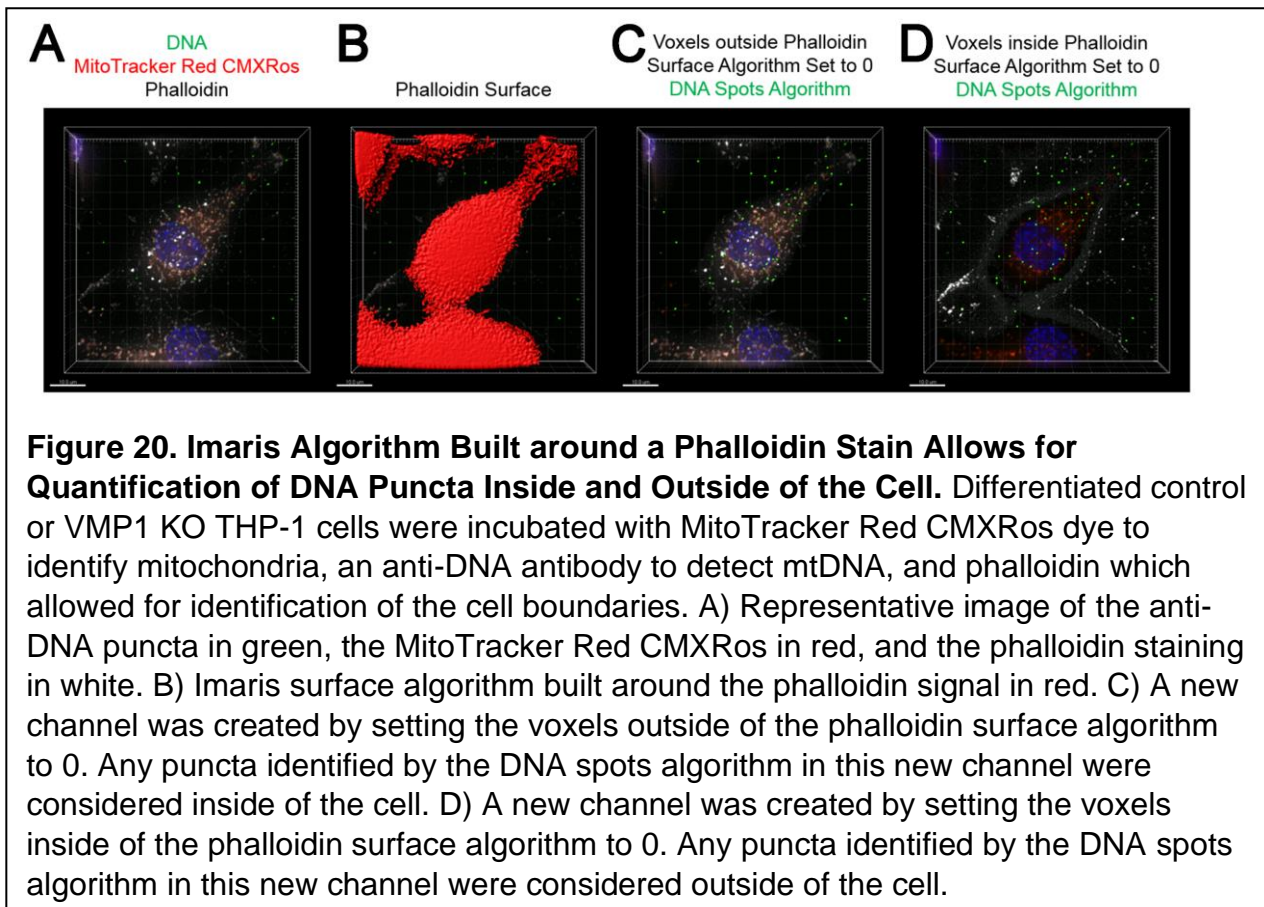
mitochondrial fusion in treated VMP1 KO cells given that there was an increase in the number of mitochondria as well as the presence of cleaved caspase-3 indicative of apoptotic cell death (Fig. 18J and 14G). Alternatively, it is known that when there is an accumulation of damage in mitochondria, fission separates damaged parts of the mitochondria for degradation [343]. Changes in mitochondrial fission and fusion under these conditions in VMP1 KO cells would need to be tested in future experiments.

VMP1 KO Cells have Increased Levels of Exposed Cytoplasmic mtDNA and Extracellular mtDNA.

Mitochondrial damage results in the release of mtDNA and mtROS [221, 222]. Since almost all the mitochondria in LPS and ATP treated VMP1 KO cells lost their membrane potential, it seems likely that there would be increased release of mtDNA from these cells. To determine whether there was increased exposed cytoplasmic mtDNA in VMP1 KO cells, differentiated THP-1s were treated then incubated with CMXRos and stained with anti-DNA antibodies (Fig. 19A and 19B). Only free cytoplasmic mtDNA is recognized by the anti-DNA antibody under the mild 0.1% saponin permeabilization conditions used in the following experiment. To quantify the number of DNA puncta inside and outside of the cell, cells were incubated with a fluorescent phalloidin probe to stain the actin filaments and identify the boundaries of the cell (Fig. 20A). In Imaris, an algorithm was built around the phalloidin stain (Fig. 20B). It was then possible to create two new channels: one that identified regions in an image that were inside of a cell and one that identified regions in an image that were outside of a cell. Voxels outside of the phalloidin surface algorithm were set to 0 to identify regions inside of the cell in a new channel (Fig. 20C). Voxels inside of the

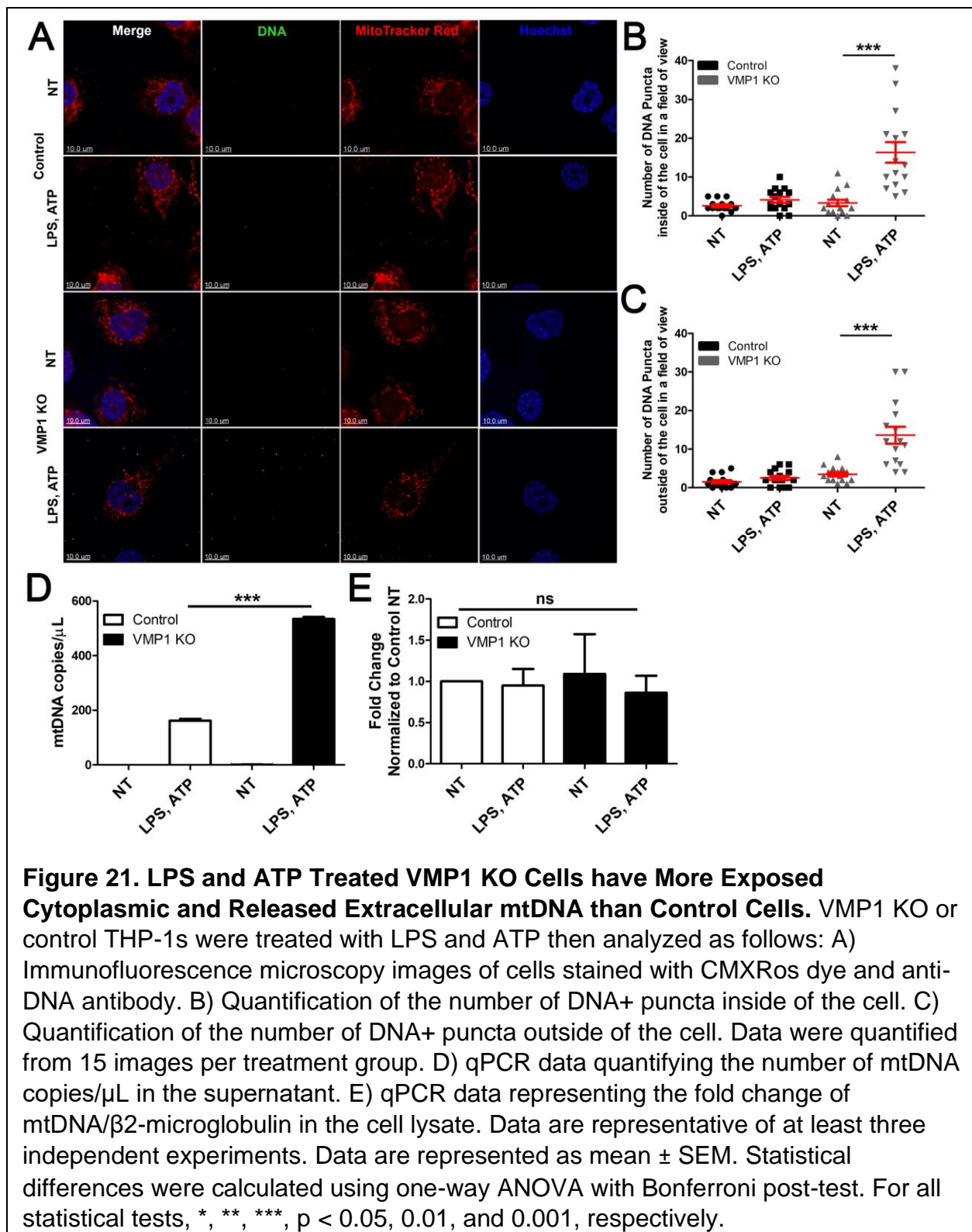
phalloidin surface algorithm were set to 0 to identify regions outside of the cell in a new channel (Fig. 20D). In Imaris, a spots algorithm was then built around the DNA puncta. If the DNA puncta were inside of the cell, then they will be counted in the new channel that set the voxels outside of the phalloidin surface algorithm to 0. If the DNA puncta were outside of the cell, then they will be counted in the new channel that set the voxels inside of the phalloidin surface algorithm to 0.





Representative images showed that only when VMP1 KO cells were treated with LPS and ATP was there an increase in DNA puncta (Fig. 21A). Imaris was utilized to build a surface around fluorescently labeled phalloidin which binds to actin in the cell. Then the number of DNA puncta inside and outside of the cell were quantified. The data demonstrated that there were relatively few DNA puncta inside of the control cells regardless of treatment, but there was a large increase in the number of DNA puncta inside of the cell in a field of view for LPS and ATP treated VMP1 KO cells (Fig. 21B). Interestingly, it was observed that there were DNA puncta on the coverslips outside of the cell in VMP1 KO cells treated with LPS and ATP (Fig. 21C). To quantify the cell-free mtDNA, qPCR was utilized where DNA was isolated from the supernatant and primers

specific to genes expressed in the small, circular mitochondrial genome were used.



Given that this is a sensitive assay, here mtDNA was detected in the supernatant of LPS and ATP treated control cells, but a larger number of mtDNA copies was detected in the supernatant from LPS and ATP treated VMP1 KO cells (Fig. 21D). These data were consistent with a recent study that quantified the release of mtDNA through GSDMD pores from BMDMs treated with LPS and nigericin, a pore-forming toxin that induces activation of the NLRP3 inflammasome [219]. Interestingly, there was no difference in the amount of mtDNA across conditions in the cell lysates even though there were more but smaller mitochondria in VMP1 KO cells suggesting that there was still the same amount of total mtDNA in these cells (Fig. 21E). Overall, these data suggested that VMP1 KO cells have more exposed cytoplasmic mtDNA that can be sensed and contribute to inflammatory responses as well as an increased release of mtDNA. Cell-free mitochondrial DNA (cfmtDNA) is increasingly being associated with pathogenic conditions including AD, PD, and MS [344].

VMP1 KO Cells have Disrupted Autophagic Flux and Increased Lysosomal Activity.

Since autophagy modulates inflammatory responses and previous reports suggested that VMP1 KO can impair autophagic flux, we wanted to assess autophagic processes in VMP1 KO macrophages under basal and inflammatory conditions [31, 222, 318]. To assess autophagosome/lysosome fusion, cells were stained for microtubule-associated protein 1A/1B-light chain 3 (LC3) and lysosome-associated membrane protein 1 (LAMP1). Double staining or colocalization of two structures suggested fusion of the autophagosome and lysosome (Fig. 22A). The number of LAMP1+ puncta were about the same between control and VMP1 KO cells with a slight

increase in control cells treated with LPS and ATP (Fig. 22B). The number of LC3+ puncta in VMP1 KO cells increased compared to control suggesting that there was an accumulation in VMP1 KO cells (Fig. 22C). Interestingly, the number of LC3+ puncta with LPS and ATP treatment for both control and VMP1 KO cells decreased, but in KO cells it was the same average number as untreated control (Fig. 22C). In untreated control cells, there was some colocalization between LC3 and LAMP1 suggesting fusion of the autophagosome and lysosome which was disrupted in treated control cells and untreated and treated VMP1 KO cells (Fig. 22D) which was consistent with previous reports [5, 31]. Immunoblotting results demonstrated an increase in LC3II levels in VMP1 KO cells and an accumulation of p62 compared to control suggesting that autophagic flux was disrupted (Fig. 22E). Furthermore, to assess lysosomal function, a Magic Red assay was used to measure cathepsin B activity, an enzyme involved in the routine turnover of proteins. Bafilomycin A1 was used as a control because it raises lysosomal pH resulting in the degradation of cathepsins. There was a slight increase in cathepsin B activity in LPS and ATP control cells as well as about a two-fold increase in untreated and treated VMP1 KO cells which was consistent with previous findings that cathepsin B is required for NLRP3 assembly and activation (Fig. 22F) [345]. Taken together, these data suggested that autophagy was disrupted in VMP1 KO cells and that there was increased lysosomal activity which likely contributed to increased NLRP3 inflammasome activation and release of mtDNA.

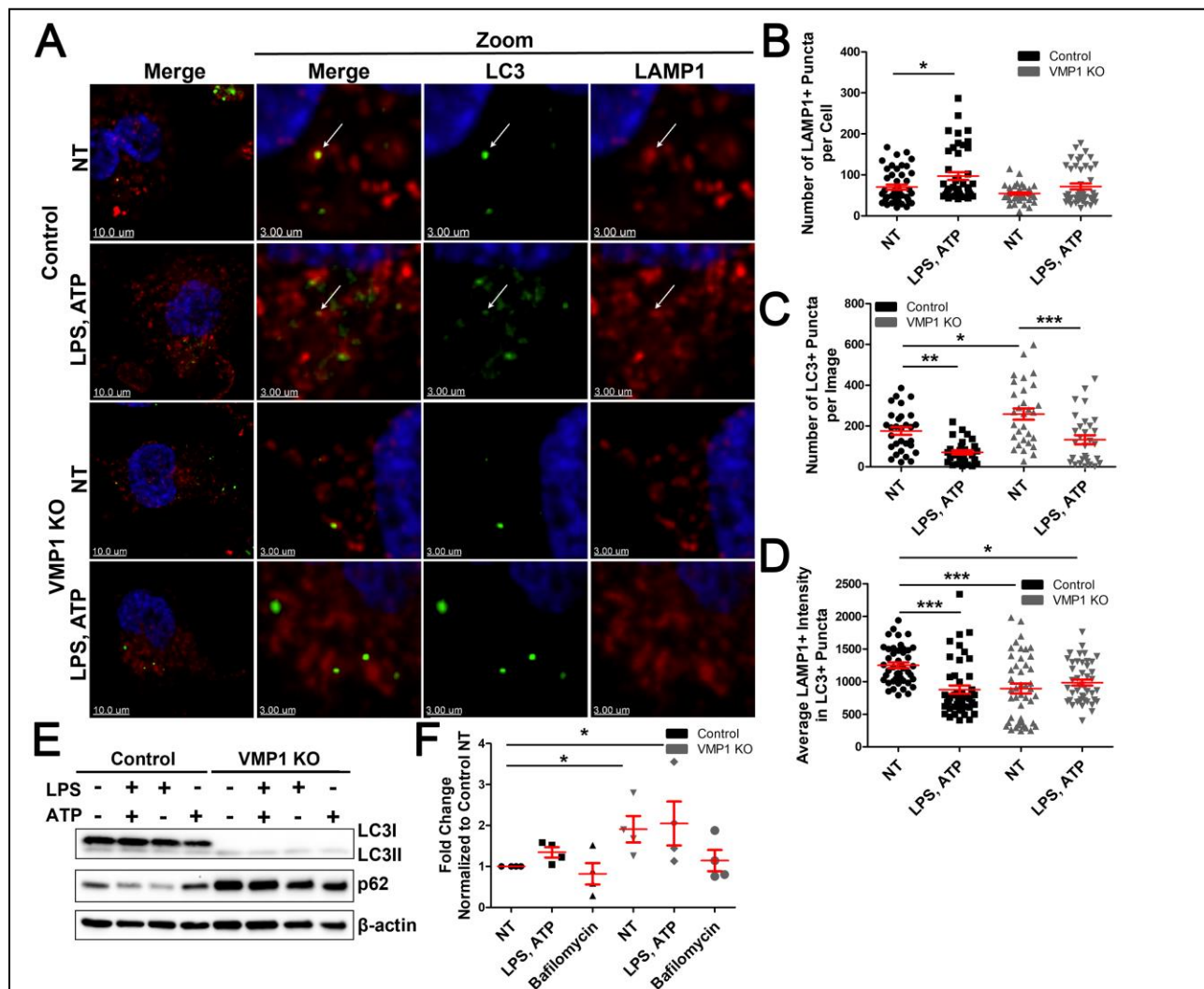
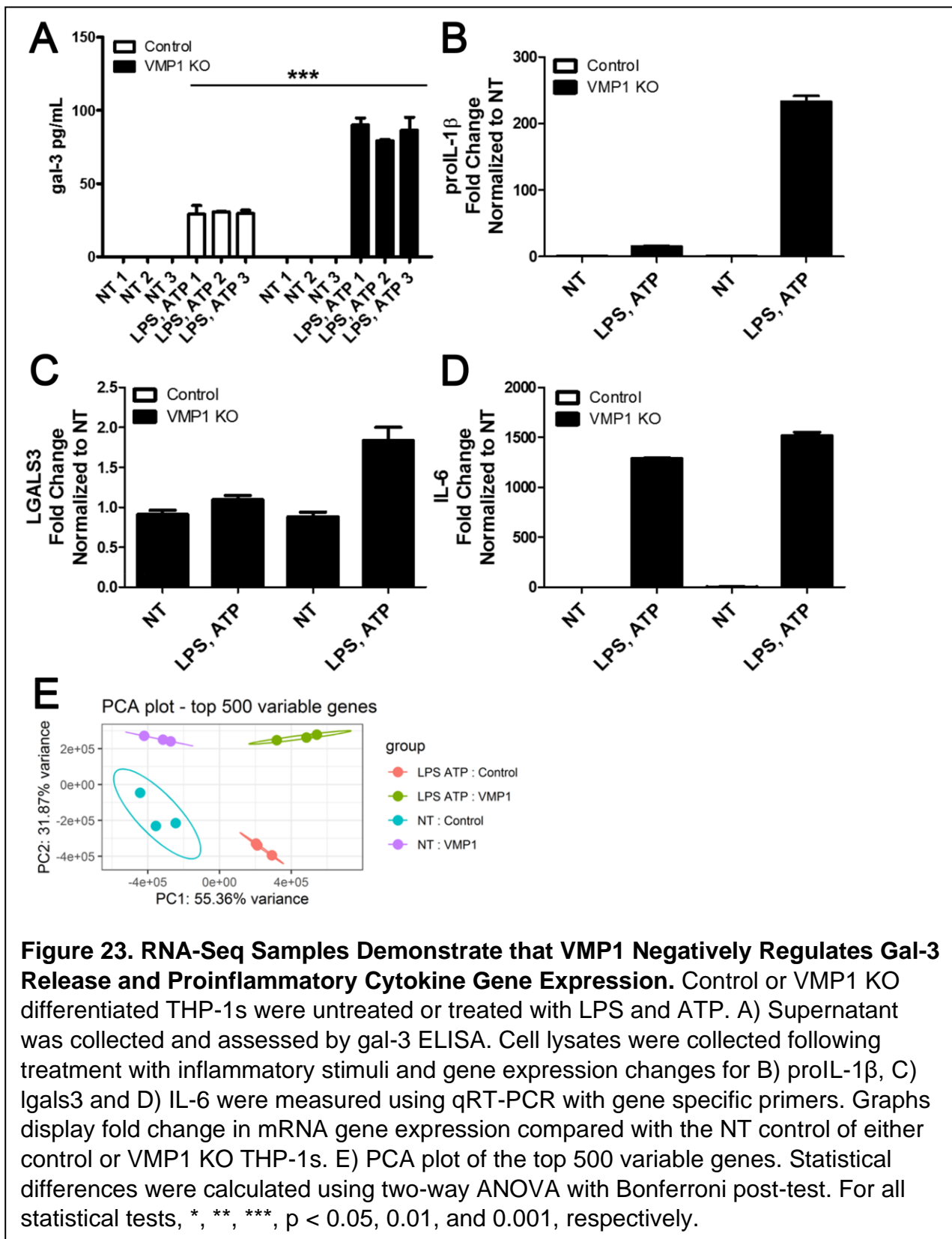


Figure 22. VMP1 KO Cells have Disrupted Autophagic Flux and Increased Cathepsin B Activity. A) Representative images from control or VMP1 KO cells untreated or treated with LPS and ATP then stained for LAMP1 and LC3. The white arrows point to colocalization of LAMP1 and LC3. B) Quantification of the number of LAMP1+ puncta per cell. C) Quantification of the number of LC3+ puncta per image. D) Quantification of the average LAMP1 intensity per image in LC3+ puncta. Data are from at least three independent experiments with at least 10 images per condition. E) LC3B and SQSTM1/p62 levels probed by western blot. F) Lysosomal dysfunction assay represented by the fold change in fluorescence of cells loaded with Magic Red dye indicative of cathepsin B activity. Statistical differences were calculated using one-way ANOVA with Bonferroni post-test or Dunnett's multiple comparison test. For all statistical tests, *, **, ***, $p < 0.05$, 0.01 , and 0.001 , respectively.

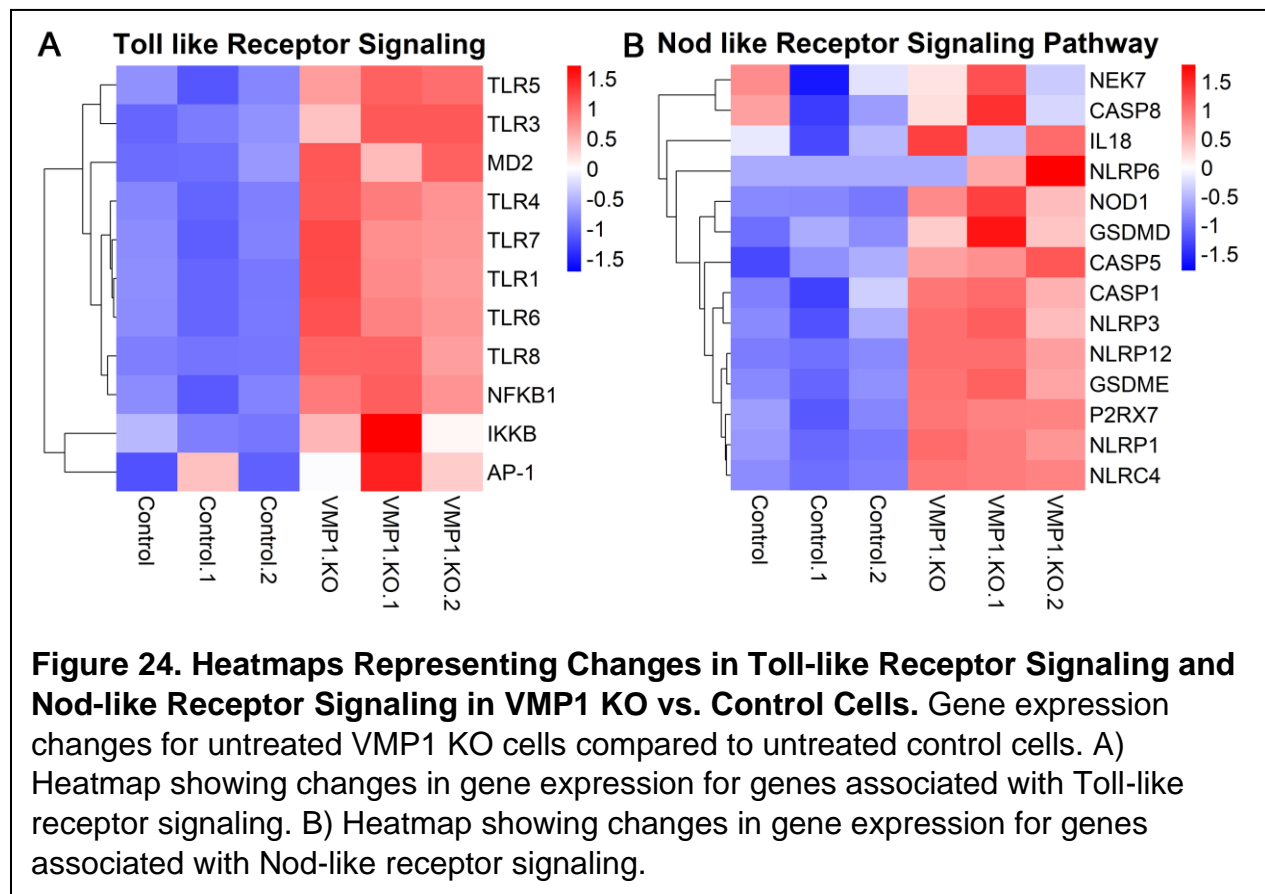
VMP1 KO Cells have Several Global Pathway Gene Expression Changes that Prime them for Proinflammatory Responses.

To determine global gene expression changes in VMP1 KO macrophages compared to CRISPR control cells, differentiated VMP1 KO or CRISPR control THP-1s were left untreated or treated with LPS and ATP. Each treatment condition was performed in triplicate. To confirm the phenotype of these samples, the supernatant was collected for a gal-3 ELISA (Fig. 23A). The data showed that there was an increase in the release of gal-3 from the VMP1 KO replicates treated with LPS and ATP compared to treated control cells. RNA was isolated and qPCR was performed to measure gene expression changes for proIL-1 β , IL-6, and Igals3. Again, these data were consistent with previous experiments where LPS and ATP treated VMP1 KO THP-1s had an increased fold change in gene expression for proIL-1 β and IL-6 compared to treated control cells (Fig. 23B and 23D). There was a slight increase in Igals3 gene expression in LPS and ATP treated VMP1 KO cells (Fig. 23C). These samples were then analyzed by RNA-Seq to identify global differential gene expression between conditions. A principle component analysis (PCA) plot was generated for the RNA-Seq data (Fig. 23E). Samples with similar expression profiles are clustered together. All three replicates of a given condition cluster together. Interestingly, there was no overlap between the different condition clusters. Principle component 1 reveals the most variation, and it separated the samples based on treatment vs. no treatment.



Principle component 2 reveals the second most variation, and it separated the samples based on VMP1 KO vs. control. The data were then analyzed following a workflow that displayed upregulated and downregulated genes in a KEGG pathway [292].

Pathway analysis revealed that VMP1 KO cells were primed to recognize proinflammatory stimuli. Most toll-like receptors were upregulated in untreated VMP1 KO cells compared to control cells (Fig. 24A). This upregulation suggested that VMP1 KO cells were primed to recognize both extracellular and intracellular PAMPs. Analysis of TLR signaling pathways also identified upregulation of the transcription factors, NF- κ B and AP-1, which are responsible for upregulating proinflammatory cytokine gene expression.

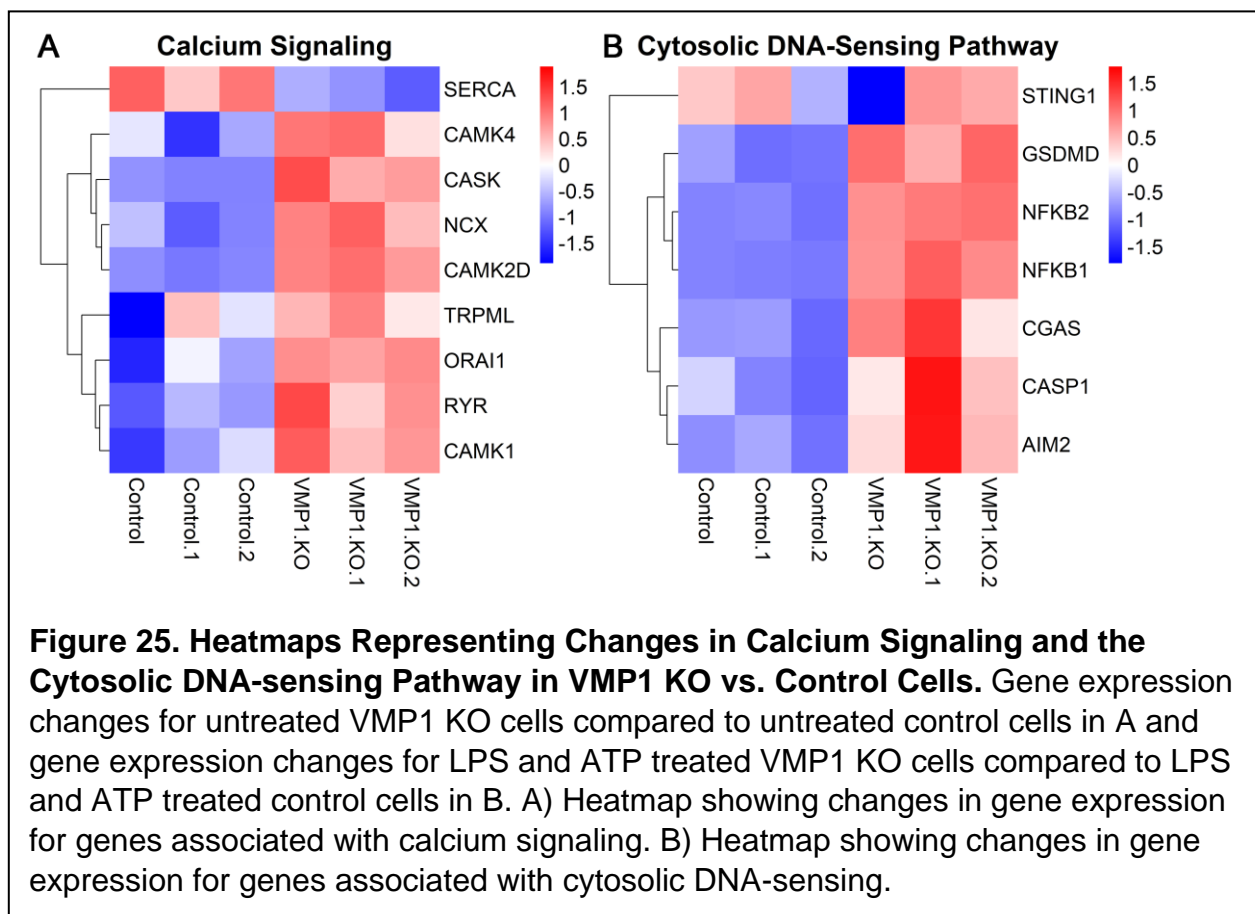


Additionally, expression of IKK β , one of the kinases responsible for phosphorylating I κ B subunits in the NF- κ B:I κ B complex triggering their ubiquitin-dependent degradation and activation of NF- κ B, was also upregulated. In the steady state, it appeared that VMP1 KO cells were in a state primed for activation by PAMPs.

Several members of the Nod-like receptor signaling pathway as well as genes involved in inflammasome activation also had increased expression in VMP1 KO cells compared to control (Fig. 24B). ATP binds to and activates P2X7R to promote K⁺ efflux and downstream inflammasome activation. Considering that P2X7R was upregulated in VMP1 KO cells, it suggested that KO cells were also primed to respond to DAMPs. Several sensors that ultimately oligomerize to form the inflammasome complex were also upregulated. These sensors included NLRP6, NOD1, NLRP3, NLRP12, NLRP1, and NLRC4 which are all activated by different stimuli. Although the focus of this study has been on the NLRP3 inflammasome activation, perhaps VMP1 KO cells may also experience exacerbated inflammatory responses when exposed to other inflammatory stimuli that activate some of these other sensors although this would need to be tested experimentally. Activation of the inflammasome results in activation of the protease, caspase-1 which was also upregulated in VMP1 KO cells compared to control. Upon activation, caspase-1 cleaves GSDMD and IL-18 which were both upregulated in untreated VMP1 KO cells. Collectively, analysis of genes involved in Toll-like receptor and Nod-like receptor signaling pathways suggested that VMP1 KO cells were primed to respond to inflammatory stimuli which corresponded to data from an earlier

experiment which showed an increased release of IL-1 β from untreated VMP1 KO cells compared to control cells at a 24 h time point (Fig. 12C).

Analysis of genes involved in calcium signaling demonstrated that several calcium channels localized to the PM and the ER were upregulated (Fig. 25A). Experimental data showed that the calcium responses in VMP1 KO cells were dysregulated (Figs. 15 and 17). Interestingly, live cell imaging experiments showed that the Ca²⁺ ER stores were depleted in VMP1 KO cells (Fig. 15), and a previous study demonstrated that one function of VMP1 was to regulate SERCA activity [5]. This RNA-Seq data showed decreased expression of SERCA in VMP1 KO cells which suggested that perhaps reduced SERCA activity was due not only to the absence of VMP1 expression but also reduced expression of SERCA. The Na⁺-Ca²⁺ exchanger (NCX) was upregulated in VMP1 KO cells. This channel is localized to the PM and the mitochondrial membrane. It typically transports Ca²⁺ out of mitochondria and outside of the cell while transporting Na⁺ in the opposite direction. ORAI1, TRMPL, and RYR are calcium channels that were also upregulated in VMP1 KO cells. They all move Ca²⁺ into the cytoplasm. Experimental data measuring the intracellular [Ca²⁺] and Ca²⁺ levels in the mitochondria suggested that VMP1 KO cells have dysregulated Ca²⁺ responses (Figs. 15 and 17), yet how changes in the expression of these calcium channels might contribute to the dysregulation responses would need to be tested experimentally. Furthermore, several calcium/calmodulin-dependent protein kinases were also upregulated in VMP1 KO cells. These kinases are key regulators of calcium signaling and, in some cases, have been shown to mediate inflammatory responses [346].

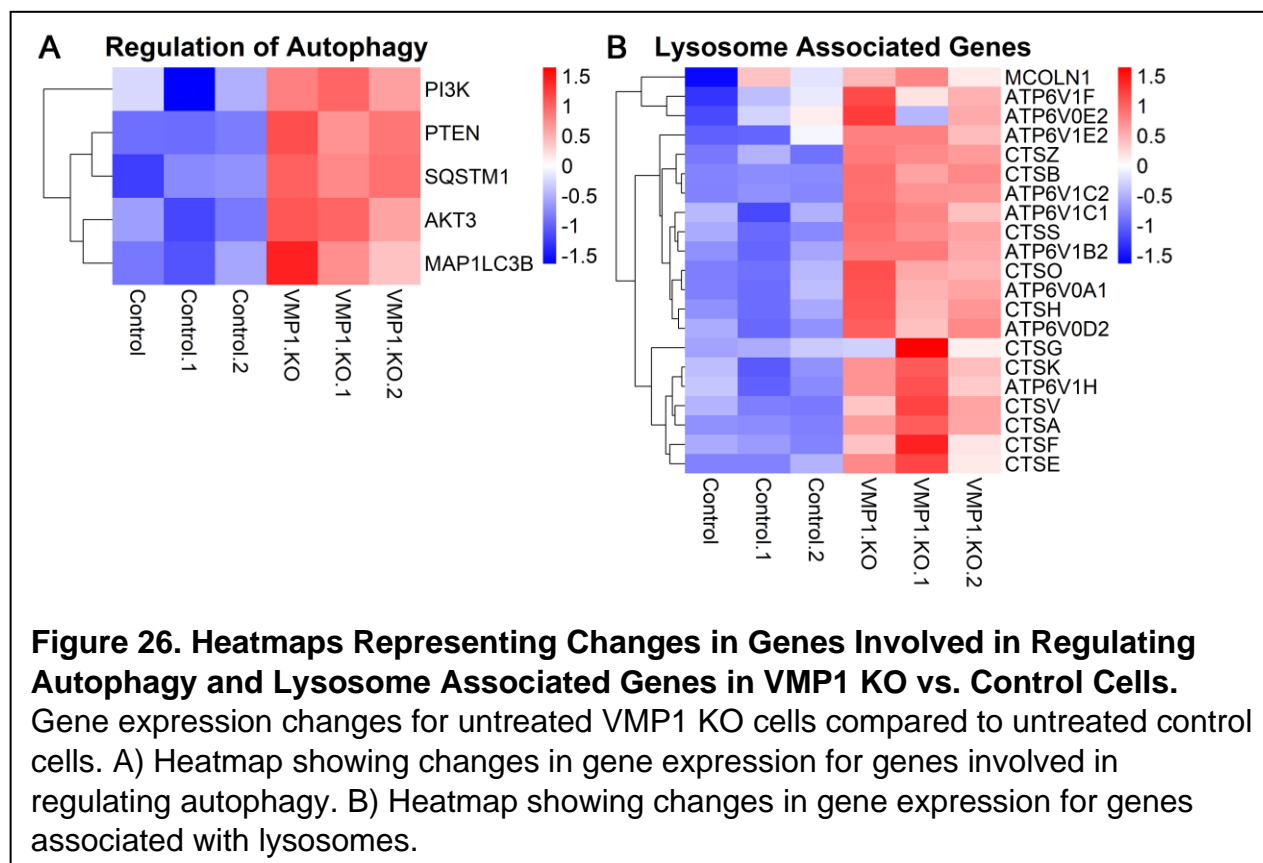


Overall, several Ca^{2+} channels were upregulated as well as other regulators of calcium signaling which was supportive of experimental data showing dysregulated calcium responses in VMP1 KO cells (Figs. 15 and 17). Additional experiments would need to be performed to determine whether changes in the expression of these calcium channels contribute to the responses observed in VMP1 KO cells.

VMP1 KO cells have increased exposed cytoplasmic levels of mtDNA which exacerbate inflammasome activation (Fig. 21). When comparing gene expression changes for the cytoplasmic DNA-sensing pathway for LPS and ATP treated VMP1 KO cells compared to treated control cells, the expression pattern suggested that VMP1 KO cells would respond more to exposed cytoplasmic mtDNA (Fig. 25B). Measurement of

inflammasome activation in VMP1 KO cells treated with the NLRP3 specific inhibitor, MCC950, showed that increased inflammasome activation in VMP1 KO cells was due to increased NLRP3 inflammasome activation (Fig. 14F). Several studies suggested the sensing of DNA by the cGAS/STING pathway resulted in NLRP3 inflammasome activation [235, 347]. In treated VMP1 KO cells, cGAS was upregulated with no change in STING expression which may increase sensing of exposed cytoplasmic DNA in these cells. Several other key inflammatory proteins were also upregulated in treated VMP1 KO cells versus treated control cells including NF- κ B, GSDMD, procaspase-1, and AIM2 which can also sense DNA in the cytoplasm and form another inflammasome complex. Taken together, these data support the hypothesis that in VMP1 KO cells exposed cytoplasmic mtDNA is being sensed by the cGAS/STING pathway resulting in increased NLRP3 inflammasome activation although it would need to be tested by knocking out cGAS to see whether that would ameliorate exacerbated inflammatory responses.

Prior studies as well as our work demonstrated that autophagic flux was impaired in VMP1 KO cells [5, 31] (Fig. 22). Several genes involved in regulating autophagy were upregulated in VMP1 KO cells including SQSTM1 (p62) which accumulated in VMP1 KO cells as shown by western blot (Fig. 22E and 26A). Furthermore, there was increased expression of MAP1LC3B in VMP1 KO cells as well increased levels of LC3II by western blot (Fig. 22E and 26A). RNA-Seq data showed that there was increased expression of Akt, PTEN, and PI3K in VMP1 KO cells (Fig. 26A). These genes promote cell survival and perhaps activation of this pathway may balance dysregulated responses in VMP1 KO cells although this hypothesis would need to be tested.



Furthermore, several genes associated with lysosomes were upregulated in VMP1 KO cells (Fig. 26B). MCOLN1 is a transmembrane protein that localizes to lysosomes and is involved in the late endosomal pathway and lysosomal exocytosis. Its activity is regulated by changes in $[Ca^{2+}]$ [348]. Perhaps upregulation of this gene is involved in the release of mtDNA from treated VMP1 KO cells although that would need to be tested. Several components of the V-ATPase were upregulated in VMP1 KO cells. V-ATPases are the proton pumps responsible for the acidification of lysosomes [349]. Further supporting increased lysosome activity in VMP1 KO cells was upregulation of a number of cathepsins which are lysosomal proteases that are involved in protein degradation, energy metabolism, and immune responses [350]. An assay using Magic Red which measures cathepsin B activity showed increased activity in untreated and

treated VMP1 KO cells compared to control cells (Fig. 22F). Several lysosome-associated genes were upregulated in VMP1 KO cells which along with the Magic Red data suggested that there was increased lysosomal activity in VMP1 KO cells. Collectively, the RNA-Seq data supported experimental data demonstrating that VMP1 negatively regulates inflammatory responses in macrophages and suggested several proteins that may be essential for the regulatory role of VMP1 in inflammatory responses that can be tested in future experiments.

CHAPTER FOUR

DISCUSSION

In this study, we investigated how the protein, VMP1 known for its ability to modulate SERCA activity and autophagy, may regulate inflammatory responses (Fig. 27). It is increasingly appreciated that disruption of autophagy results in dysregulated inflammatory responses that are often associated with disease [351]. We used CRISPR-Cas9 to genetically delete VMP1 to elucidate whether VMP1 regulates innate inflammatory responses [5]. This study is the first to characterize the role of VMP1 in innate immune responses and autophagic processes in macrophages. Initial experiments demonstrated that VMP1 negatively, yet differentially regulated the release of IL-1 β , IL-6, and gal-3 in response to multiple NLRP3 inflammasome agonists (Fig. 12). Perhaps this differential secretion depending on the agonist was due in part to different mechanisms of secretion for each of these proteins. For example, our work demonstrated that gal-3 can be released in EVs, but that it was predominantly released through GSDMD pores in response to inflammatory stimuli in differentiated THP-1s (Fig. 11). Similarly, IL-1 β typically is thought of for its secretion through GSDMD pores in response to inflammatory stimuli. Yet the literature demonstrates that this is not the only pathway of secretion for IL-1 β .

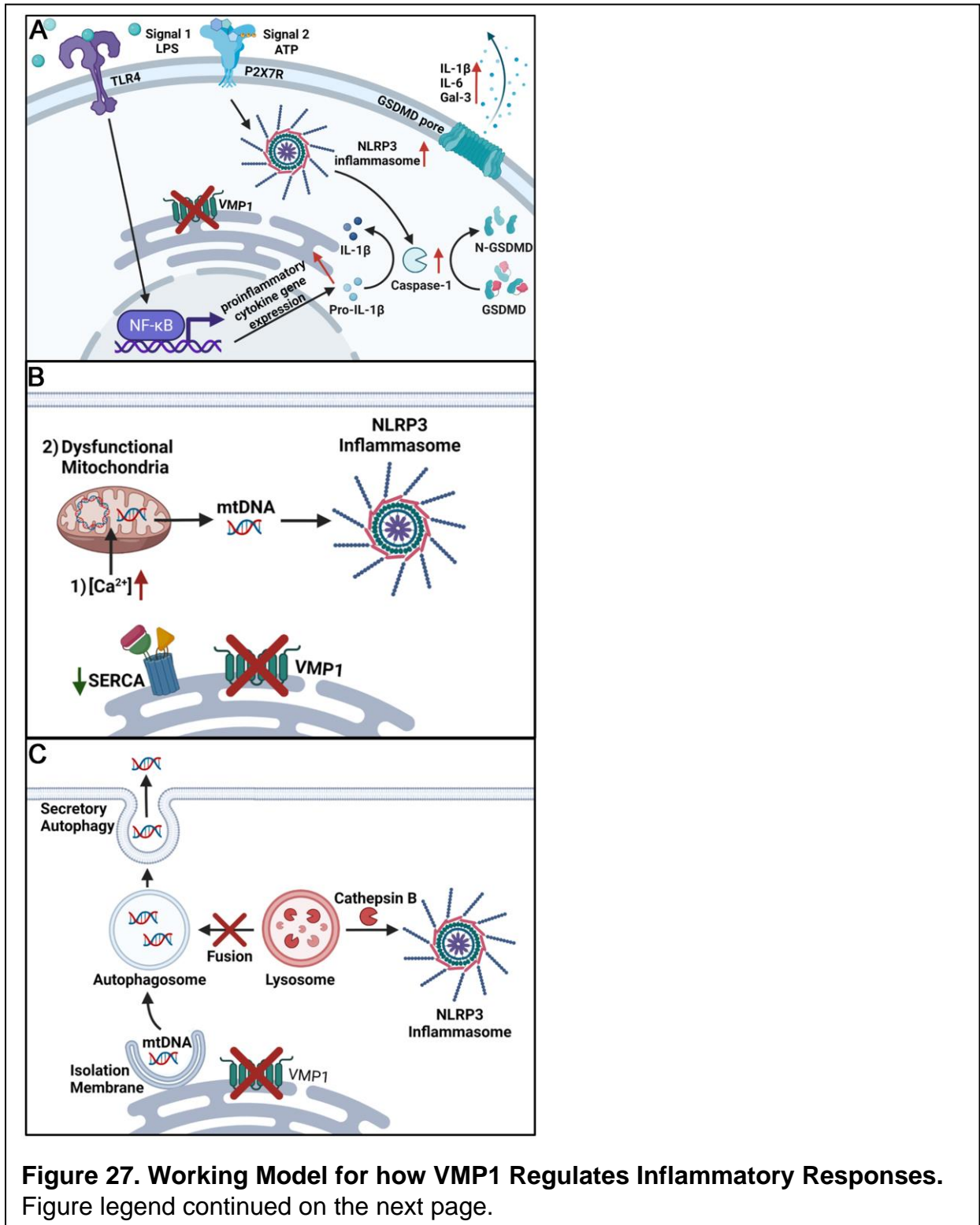


Figure 27. Working Model for how VMP1 Regulates Inflammatory Responses. A) Overview of how VMP1 regulates inflammatory pathways: In VMP1 KO cells treated with LPS and ATP, there was increased proinflammatory cytokine gene expression, NLRP3 inflammasome activation, caspase-1 activation, and release of IL-1 β , IL-6, and gal-3. These exacerbated inflammatory phenotypes in VMP1 KO cells were likely due to the two known functions of VMP1: regulation of SERCA activity and autophagy. **B) SERCA activity:** VMP1 KO cells have decreased expression of SERCA accompanied by decreased SERCA activity. Upon activation with ATP, VMP1 KO cells have elevated cytoplasmic [Ca²⁺]. Mitochondria in VMP1 KO cells have increased influx and decreased efflux of Ca²⁺ resulting in loss of membrane potential, mitochondrial dysfunction, and exposure of cytoplasmic mtDNA. mtDNA is then hypothesized to act as a DAMP to increase activation of the NLRP3 inflammasome in VMP1 KO cells. **C) Autophagy:** VMP1 KO cells exhibited impaired autophagic flux specifically at the stage of autophagosome/lysosome fusion. In VMP1 KO cells, there was tethering of the isolation membrane with the ER. However, some autophagosomes still formed and we hypothesize that the extracellular mtDNA we detect is being released through secretory autophagy. Additionally, VMP1 KO cells have increased cathepsin B activity which we hypothesize also contributes to increased NLRP3 inflammasome activation.

When IL-1 β is cleaved, it becomes positively charged which facilitates its movement the plasma membrane where its fast release is mediated through GSDMD pores [352] and its slow release is mediated through a GSDMD-independent pathway that has yet to be fully elucidated [353]. Additionally, IL-6 release occurs through the conventional ER-Golgi mechanism of secretion [354]. Evidence in the literature suggests that VMP1 can regulate protein secretion [16]. Thus, it would be interesting in future studies to elucidate which secretory pathways these proinflammatory molecules are utilizing in VMP1 KO cells because it seems feasible to hypothesize that there would be differences between cells in which VMP1 was knocked out compared to cells expressing normal levels of VMP1.

Increased release of IL-1 β in response to the canonical NLRP3 inflammasome activators, LPS and ATP, in VMP1 KO cells suggested this phenotype was due in part to increased inflammasome activation. Interestingly, even though LPS and poly(I:C) treatment alone upregulated proIL-1 β expression to the same extent as LPS and ATP treatment, there was no difference in IL-1 β release from VMP1 KO compared to control. Similar secretion patterns were observed for IL-6 and gal-3 in response to inflammatory stimuli in VMP1 KO compared to control which differed from the secretion patterns observed from cells depleted of other autophagy-associated proteins. [355, 356]. Given that there are multiple mechanisms for the secretion of IL-1 β , IL-6, and gal-3 with some overlap, it seems plausible that VMP1 regulates secretory pathways although this idea would need to be tested in future studies [134, 357-359].

VMP1 KO macrophages had increased caspase-1 activation in response to LPS and ATP (Fig. 14). Use of MCC950, a specific inhibitor of the NLRP3 inflammasome, indicated that this increase in caspase-1 activation was mediated specifically by the NLRP3 inflammasome. Many agonists can activate the NLRP3 inflammasome by inducing a variety of downstream signals, yet a consensus model for activation has not yet been identified [360]. Data acquired in VMP1 KO cells suggested that multiple signals associated with NLRP3 inflammasome activation were present when cells were activated by canonical inflammatory stimuli. These signals included Ca²⁺ mobilization, mitochondrial dysfunction, and release of mtDNA (Fig. 15, 17, 18, and 21). Although Ca²⁺ mobilization as a signal upstream of NLRP3 inflammasome activation is controversial, our data demonstrated that in control THP-1s treated with thapsigargin,

an inhibitor of the Ca^{2+} ATPase SERCA, alongside LPS and ATP, there was an increase in caspase-1 activation like what was observed in VMP1 KO cells that have diminished SERCA activity (Fig. 15) [5, 188, 189, 202]. Our data suggested that Ca^{2+} mobilization alone was not sufficient to induce inflammasome activation (Fig. 16), but impaired responses to changes in cytoplasmic $[\text{Ca}^{2+}]$ exacerbated responses to additional inflammatory stimuli. Measurement of changes in $[\text{Ca}^{2+}]$ in proximity to mitochondria in response to ATP showed that there was an increased rate of influx and a decreased rate of efflux in VMP1 KO cells compared to control (Fig. 17). Based on what is known in the literature, we believe that Ca^{2+} overload in the mitochondria resulted in the loss of mitochondrial membrane potential and release of mtDNA (Fig. 18 and 21). Extension of MAMs as is the case for VMP1 KO cells affects the transfer of Ca^{2+} from the ER to mitochondria and in our case resulted in a mitochondrial Ca^{2+} overload [5, 361]. Dysregulated opening of the mPTP triggers the release of matrix metabolites leading to the loss of mitochondrial membrane potential, inhibition of oxidative phosphorylation, and mitochondrial swelling [362-364]. Furthermore, in VMP1 KO cells we observed increased levels of cleaved caspase-3 when cells were treated with inflammatory stimuli, and previous work has shown that NLRP3 activators can trigger apoptosis leading to the loss of mitochondrial membrane potential and release of mtDNA into the cytosol which can then trigger NLRP3 inflammasome activation [221]. Overall, we hypothesize that in VMP1 KO cells treated with inflammatory stimuli, there is an increase in $[\text{Ca}^{2+}]$ that results in the loss of mitochondrial membrane potential and

release of mtDNA which we believe is being sensed by the cGAS/STING pathway to increase NLRP3 inflammasome activation.

This work introduces a novel approach to assess mitochondrial function in cells. Live cell confocal microscopy allowed us to visualize individual mitochondria in cells which was an improvement on the resolution of the previous assay. Analysis of these images using Imaris allowed for an unbiased approach where an algorithm was built around individual mitochondria that were identified by MitoTracker Green dye which accumulates in mitochondria based on their mass but independent of membrane potential. Using this approach, we can determine several parameters of the individual mitochondria including the number, size, and volume which can give a sense for how mitochondrial dynamics change in cells under different conditions which is information that is lost in the flow cytometry-based assay. Furthermore, it allowed for the mitochondrial membrane potential to be quantified in each mitochondrion. The data can be displayed in plots analogous to flow plots to allow for quantification of the relative percentages of mitochondria that can be considered functional or dysfunctional, yet there was improved resolution in our assay where we were able to determine the relative percentage of mitochondria that have low, intermediate, or high mitochondrial membrane potential. This work established a robust assay for characterizing the mitochondrial dynamics in untreated or treated cells.

Our work identified that VMP1 KO cells have an increased release of mtDNA that was quantified in the supernatant by qPCR using primers specific to mitochondrial genes, but we also utilized a microscopy-based approach to quantify the release of

mtDNA. We used mild saponin conditions that allowed for us to only detect exposed cytoplasmic mtDNA (Fig. 19), and we stained the cells with phalloidin to leverage Imaris to build an algorithm around the phalloidin stain such that we could identify mtDNA puncta that were located inside or outside of the cell (Fig. 20). Future studies can utilize this microscopy-based approach to determine how mtDNA is being released from VMP1 KO cells. We hypothesize that it is through secretory autophagy because of decreased autophagosome/lysosome fusion in VMP1 KO cells, but this would need to be tested directly. Furthermore, this imaging-based approach would address the question of whether dysfunctional mitochondria are also being released from the cell along with the mtDNA.

Previous studies have demonstrated that in VMP1 KO cells autophagy is impaired at autophagosome/lysosome fusion [5, 31]. Our data was consistent with these findings with our data showing that in VMP1 KO cells there was less colocalization between LC3 and LAMP1 and an accumulation of p62 (Fig. 22). We hypothesize that this defect in autophagy likely resulted in the persistence of dysfunctional mitochondria and increased NLRP3 inflammasome activation in VMP1 KO cells [217, 221, 222, 365]. Along these lines, previous work demonstrated that activation of the AIM2 and NLRP3 inflammasomes trigger caspase-1 dependent mitochondrial damage. This mitochondrial damage includes mtROS production, loss of mitochondrial membrane potential, and inhibition of mitophagy which likely amplifies inflammatory responses due to mitochondrial damage [366]. Interestingly and perhaps in contrast to this previous study, in our study we observed a modest increase in mitochondria that lost their membrane

potential with LPS and ATP activation in control cells compared to almost all mitochondria losing their membrane potential in VMP1 KO cells (Fig. 18). Perhaps because our experiments were performed 30 min after adding ATP, the phenotype we observed for VMP1 KO cells was more pronounced compared to control cells. Maybe we would observe more evidence of mitochondrial damage at later time points following caspase-1 activation in control cells. Overall, it seems likely that impaired autophagic flux in VMP1 KO cells would allow for damaged mitochondria to persist and augment inflammatory responses.

Typically, with NLRP3 activation, p62 is recruited to damaged mitochondria which are then ubiquitinated through a Parkin-mediated mechanism for degradation, but in VMP1 KO cells mitophagy is defective and there is an accumulation of damaged mitochondria [150, 342]. Additionally, upon inflammasome activation, p62 interacts with ASC targeting the inflammasome components to autophagosomes for degradation to control inflammatory responses which is another mechanism that is likely defective in VMP1 KO cells [318]. Aside from promoting inflammasome activation, autophagy inhibition can elevate IL-1 β release due to an increase in available proIL-1 β for cleavage in the cytosol similar to what we observed in VMP1 KO cells (Fig.12) [313]. Cathepsin B which is released from damaged lysosomes was more active in VMP1 KO cells and has been shown to be essential for NLRP3 inflammasome activation (Fig. 22) [345, 367]. Our work demonstrated that there was increased release of mtDNA from VMP1 KO cells in response to LPS and ATP compared to control cells (Fig. 21). Recent work suggested that mtDNA is primarily released from the cell due to membrane rupture, but

a fraction of the mtDNA can also be released through GSDMD/gasdermin E (GSDME) pores upon pyroptotic/apoptotic cell death [219]. We hypothesize that it is more likely that in VMP1 KO cells due to diminished autophagosome fusion with the lysosome, there would be increased fusion of the autophagosome with the plasma membrane to release mtDNA through secretory autophagy [368].

Even though this work primarily focused on addressing how two known functions of VMP1 particularly its modulation of SERCA activity and autophagic flux may be mediating exacerbated inflammatory responses, there are additional functions of VMP1 that may be contributing to this phenotype. For example, it is known that in VMP1 KO cells there is this sustained interaction between the ER membrane and several organelles that is mediated by the interaction between VMP1 and SERCA [5]. These sustained membrane contacts may also influence inflammasome activation, and it would be interesting to look at the localization of inflammasome components in VMP1 KO cells before and after treatment with inflammatory stimuli. In an unstimulated cell, NLRP3 localizes to the ER and cytosol, but upon stimulation, NLRP3 in the ER localizes adjacent to ASC in mitochondria [369, 370]. The NLRP3 inflammasome complex is assembled at highly specialized contact sites between the ER and mitochondria known as MAMs [369]. It is thought that this localization of NLRP3 to MAMs/mitochondria may contribute to the immediate recognition of and response to mitochondrial damage and mtDNA translocation [369]. Perhaps the increased presence of MAMs in VMP1 KO cells may be the reason for increased basal inflammatory responses compared to control cells. Maybe the proximity of NLRP3 and ASC in VMP1 KO cells may result in the

formation of an inflammasome complex under basal conditions that can then cleave proIL-1 β and allow for it to be released from the cell (Fig. 12C). Even though the priming signal typically results in the upregulation of inflammasome components and proinflammatory cytokine gene expression, the basal level of proIL-1 β is high in differentiated THP-1 cells suggesting that there may be sufficient levels for it to be cleaved in untreated VMP1 KO cells.

As mentioned previously, VMP1 is an integral membrane protein localized to the ER, but recently, it has been identified to also have phospholipid scramblase activity which is important for maintaining the normal distribution of phosphatidylserine and cholesterol [14, 371]. In the absence of VMP1, more cholesterol becomes accessible on the cytoplasmic leaflet of the PM as well as an increase in phosphatidylserine in the cytoplasmic leaflet of cellular membranes. It is thought that the role of VMP1 in maintaining cellular lipid distribution may explain how VMP1 can be involved in so many different cellular processes. Lipid composition in the ER can greatly impact the biogenesis of autophagosomes suggesting another way for how VMP1 can be influencing autophagy and inflammatory responses in macrophages independently of its ability to alter [Ca²⁺] [372, 373]. Furthermore, elevated levels of cholesterol can also increase inflammatory responses. For example, excess cholesterol can form cholesterol crystals which can directly activate the NLRP3 inflammasome [374]. Non-crystalline cholesterol at high concentrations also can trigger inflammasome activation by impairing mitochondrial function [375, 376]. Yet other studies suggest that cholesterol can have inhibitory effects on the activation of NLRP3 inflammasome activation so the role of

cholesterol in inflammasome activation is still unclear [377]. Whether the scramblase activity of VMP1 is involved in exacerbated inflammatory responses is unknown, but it seems possible that it may be involved although perhaps indirectly.

Our data demonstrated that there was increased mitochondrial dysfunction and release of mtDNA in VMP1 KO cells (Fig. 18 and 21), yet we have not measured the levels of mtROS which are likely elevated in VMP1 KO cells. Following mitochondrial damage mtROS can be produced and oxidize mtDNA to activate the NLRP3 inflammasome [221]. It has been shown that ATP can induce the production of mtROS to activate the inflammasome [378]. Yet several studies have found that mtROS is dispensable for NLRP3 inflammasome activation where serum β -amyloid can induce activation through mtROS-dependent and mtROS-independent mechanisms [379]. In contrast, some viruses can activate the inflammasome in a mtROS-independent manner [227, 380]. Overall, it remains controversial whether mtROS is essential for NLRP3 inflammasome activation. Another source of signals that activate the inflammasome and may be affected in VMP1 KO cells are derived from lysosomal permeabilization. LPS and ATP induce lysosomal destabilization, and cathepsin B, a lysosomal cysteine protease, has been found to be required for caspase-1 activation, ASC speck formation, and IL-1 β production [345]. In VMP1 KO cells, there was increased cathepsin B activity in untreated cells that was increased compared to control untreated cells (Fig. 22). Perhaps the increased levels of cathepsin B in VMP1 KO cells may contribute to increased basal inflammatory responses in VMP1 KO cells. It would be interesting to further characterize the function of the lysosome in VMP1 KO cells and

more specifically elucidate whether it contributes to elevated inflammatory responses in VMP1 KO cells. Given that several signals that can induce NLRP3 inflammasome activation are elevated in VMP1 KO cells, but not all of them are required, it would be interesting to tease apart which ones are required for increased inflammasome activation in these cells. It can sometimes be difficult to inhibit these signals directly without off target effects, but it would help to define the mechanism for how the host protein, VMP1, negatively regulates inflammatory responses.

In summary, we showed that in VMP1 KO cells in response to inflammatory stimuli there was increased release of IL-1 β , IL-6, and gal-3. In VMP1 KO cells, there was increased NLRP3 inflammasome and caspase-1 activation. Due to inhibition of SERCA activity in VMP1 KO cells, there were elevated levels of cytoplasmic [Ca²⁺] and increased influx and decreased efflux rates of Ca²⁺ from mitochondria upon ATP stimulation which caused a loss of membrane potential in almost all mitochondria and increased the release of mtDNA. VMP1 KO impaired autophagic flux at the stage of autophagosome/lysosome fusion which likely prevented the cells from degrading damaged mitochondria further exacerbating inflammatory responses. Taken together, our findings identify a novel negative regulatory role for VMP1 in inflammatory responses. VMP1 restricts NLRP3 inflammasome activation through its modulation of SERCA activity and autophagy. In the broader context, decreased expression of VMP1 has been identified in the monocytes of patients with Primary-Progressive MS and in the PBMCs of PD patients [40, 90]. The progression of these neurologic diseases is characterized by dysregulated inflammatory responses that contribute to devastating

disease sequelae. Our findings support a potentially critical role for VMP1 in the progression of inflammatory responses in these diseases that perhaps can one day be targeted therapeutically.

Concluding Remarks.

In this work, for the first time, the function of VMP1 was characterized in macrophages specifically how it can regulate inflammatory responses was outlined. Depletion of VMP1 resulted in increased basal release of IL-1 β along with elevated levels of proinflammatory cytokines and gal-3 being released in response to proinflammatory stimuli. In part, this exacerbated inflammatory response was mediated by increased NLRP3 inflammasome activation. In connection with disease, VMP1 KO cells treated with LPS and α -syn fibrils released more IL-1 β compared to control cells suggesting that PD patients with decreased expression of VMP1 would have increased inflammatory responses with exposure to inflammatory stimuli but also due to α -syn fibrils characteristic of disease pathology. It would be interesting to determine if there are other diseases associated with decreased VMP1 expression and to further characterize the function of VMP1 in additional immune cell types both in the periphery and the CNS.

This work demonstrated that in VMP1 KO macrophages there was decreased SERCA activity and impaired autophagic flux consistent with what was observed previously [5, 31]. Regulation of [Ca²⁺] and autophagy both likely contributed to increased inflammasome activation. The data showed that elevated [Ca²⁺] in response to ATP increased [Ca²⁺] in the mitochondria which led to loss of membrane potential

and the release of mtDNA. Additionally, impaired autophagy would prevent the degradation of damaged mitochondria as well as the removal of activated inflammasome components which likely further exacerbate inflammatory responses over the long-term. Further studies will need to be done to address to what extent each function of VMP1 contributes to regulating inflammatory responses especially given the pleiotropic role of VMP1. With this work as the foundation, many questions remain about how VMP1 may be regulating cellular responses in immune cells. Future work needs to be done to characterize the mechanisms underlying how VMP1 regulates inflammatory responses broadly but also more specifically in the context of PPMS and PD. Ultimately, it would be useful for a therapeutic to be developed that could fine-tune the expression of VMP1 in different disease states with it potentially being able to mitigate excessive and unwanted inflammatory responses that typically contribute to disease progression in PPMS and PD until cures for these diseases can be developed.

REFERENCE LIST.

1. Gay, N.J., et al., *Assembly and localization of Toll-like receptor signalling complexes*. Nature Reviews Immunology, 2014. **14**(8): p. 546-558.
2. Meléndez, A. and B. Levine, *Autophagy in C. elegans*. WormBook: the online review of C. elegans biology, 2009: p. 1-26.
3. Pajares, M., et al., *Inflammation in Parkinson's disease: mechanisms and therapeutic implications*. Cells, 2020. **9**(7): p. 1687.
4. Song, Y., Y. Zhou, and X. Zhou, *The role of mitophagy in innate immune responses triggered by mitochondrial stress*. Cell Communication and Signaling, 2020. **18**(1): p. 1-14.
5. Zhao, Y.G., et al., *The ER-localized transmembrane protein EPG-3/VMP1 regulates SERCA activity to control ER-isolation membrane contacts for autophagosome formation*. Molecular cell, 2017. **67**(6): p. 974-989. e6.
6. Kong, F., et al., *The crosstalk between pattern-recognition receptor signaling and calcium signaling*. International Journal of Biological Macromolecules, 2021. **192**: p. 745-756.
7. Celarain, N. and J. Tomas-Roig, *Aberrant DNA methylation profile exacerbates inflammation and neurodegeneration in multiple sclerosis patients*. Journal of neuroinflammation, 2020. **17**(1): p. 1-17.
8. Huang, Y., W. Xu, and R. Zhou, *NLRP3 inflammasome activation and cell death*. Cellular & Molecular Immunology, 2021. **18**(9): p. 2114-2127.
9. Dusetti, N.J., et al., *Cloning and expression of the rat vacuole membrane protein 1 (VMP1), a new gene activated in pancreas with acute pancreatitis, which promotes vacuole formation*. Biochemical and biophysical research communications, 2002. **290**(2): p. 641-649.

10. Ropolo, A., et al., *The pancreatitis-induced vacuole membrane protein 1 triggers autophagy in mammalian cells*. Journal of Biological Chemistry, 2007. **282**(51): p. 37124-37133.
11. Schneider, W.M., et al., *Genome-scale identification of SARS-CoV-2 and pan-coronavirus host factor networks*. Cell, 2021. **184**(1): p. 120-132. e14.
12. Morita, K., et al., *Genome-wide CRISPR screen identifies TMEM41B as a gene required for autophagosome formation*. Journal of Cell Biology, 2018. **217**(11): p. 3817-3828.
13. Morita, K., Y. Hama, and N. Mizushima, *TMEM41B functions with VMP1 in autophagosome formation*. Autophagy, 2019. **15**(5): p. 922-923.
14. Li, Y.E., et al., *TMEM41B and VMP1 are scramblases and regulate the distribution of cholesterol and phosphatidylserine*. Journal of Cell Biology, 2021. **220**(6): p. e202103105.
15. Tábara, L.-C.E., Ricardo, *VMP1 establishes ER-microdomains that regulate membrane contact sites and autophagy*. PloS one, 2016. **11.11**.
16. Calvo-Garrido, J., et al., *Vacuole membrane protein 1 is an endoplasmic reticulum protein required for organelle biogenesis, protein secretion, and development*. Molecular biology of the cell, 2008. **19**(8): p. 3442-3453.
17. Wang, P., et al., *KMS1 and KMS2, two plant endoplasmic reticulum proteins involved in the early secretory pathway*. The Plant Journal, 2011. **66**(4): p. 613-628.
18. Tenenboim, H., et al., *VMP1-deficient Chlamydomonas exhibits severely aberrant cell morphology and disrupted cytokinesis*. BMC plant biology, 2014. **14**(1): p. 1-13.
19. Bard, F., et al., *Functional genomics reveals genes involved in protein secretion and Golgi organization*. Nature, 2006. **7076**: p. 604-607.
20. Michelangeli, F. and J.M. East, *A diversity of SERCA Ca²⁺ pump inhibitors*. Biochemical Society Transactions, 2011. **39**(3): p. 789-797.
21. Zhao, Y.G. and H. Zhang, *The ER-localized autophagy protein EPG-3/VMP1 regulates ER contacts with other organelles by modulating ATP2A/SERCA activity*. Autophagy, 2018. **14**(2): p. 362-363.

22. Prinz, W.A., *Bridging the gap: membrane contact sites in signaling, metabolism, and organelle dynamics*. Journal of Cell Biology, 2014. **205**(6): p. 759-769.
23. Raiborg, C., E.M. Wenzel, and H. Stenmark, *ER-endosome contact sites: molecular compositions and functions*. The EMBO journal, 2015. **34**(14): p. 1848-1858.
24. Phillips, M.J. and G.K. Voeltz, *Structure and function of ER membrane contact sites with other organelles*. Nature reviews Molecular cell biology, 2016. **17**(2): p. 69-82.
25. Giordano, F., et al., *PI (4, 5) P2-dependent and Ca²⁺-regulated ER-PM interactions mediated by the extended synaptotagmins*. Cell, 2013. **153**(7): p. 1494-1509.
26. Yi, M., D. Weaver, and G.r. Hajnóczky, *Control of mitochondrial motility and distribution by the calcium signal: a homeostatic circuit*. The Journal of cell biology, 2004. **167**(4): p. 661-672.
27. MacLennan, D.H. and E.G. Kranias, *Phospholamban: a crucial regulator of cardiac contractility*. Nature reviews Molecular cell biology, 2003. **4**(7): p. 566-577.
28. Feng, Y., et al., *The machinery of macroautophagy*. Cell research, 2014. **24**(1): p. 24-41.
29. Lamb, C.A., T. Yoshimori, and S.A. Tooze, *The autophagosome: origins unknown, biogenesis complex*. Nature reviews Molecular cell biology, 2013. **14**(12): p. 759-774.
30. Tian, Y., et al., *C. elegans screen identifies autophagy genes specific to multicellular organisms*. Cell, 2010. **141**(6): p. 1042-1055.
31. Wang, P., et al., *Essential role for autophagy protein VMP1 in maintaining neuronal homeostasis and preventing axonal degeneration*. Cell death & disease, 2021. **12**(1): p. 1-14.
32. Kimura, S., T. Noda, and T. Yoshimori, *Dissection of the autophagosome maturation process by a novel reporter protein, tandem fluorescent-tagged LC3*. Autophagy, 2007. **3**(5): p. 452-460.
33. Lin, W., et al., *VMP1, a novel prognostic biomarker, contributes to glioma development by regulating autophagy*. Journal of Neuroinflammation, 2021. **18**(1): p. 1-15.

34. Zheng, L., et al., *TMEM49-related apoptosis and metastasis in ovarian cancer and regulated cell death*. Molecular and cellular biochemistry, 2016. **416**(1): p. 1-9.
35. Folkerts, H., et al., *Elevated VMP1 expression in acute myeloid leukemia amplifies autophagy and is protective against venetoclax-induced apoptosis*. Cell death & disease, 2019. **10**(6): p. 1-12.
36. Guo, L., et al., *Novel roles of Vmp1: Inhibition metastasis and proliferation of hepatocellular carcinoma*. Cancer science, 2012. **103**(12): p. 2110-2119.
37. Qian, Q., et al., *VMP1 related autophagy and apoptosis in colorectal cancer cells: VMP1 regulates cell death*. Biochemical and biophysical research communications, 2014. **443**(3): p. 1041-1047.
38. Dauer, W. and S. Przedborski, *Parkinson's disease: mechanisms and models*. Neuron, 2003. **39**(6): p. 889-909.
39. Reeve, A., E. Simcox, and D. Turnbull, *Ageing and Parkinson's disease: why is advancing age the biggest risk factor?* Ageing research reviews, 2014. **14**: p. 19-30.
40. Al-Nusaif, M., et al., *Abnormal Vacuole Membrane Protein-1 Expression in Parkinson's Disease Patients*. Frontiers in neuroscience, 2022. **16**.
41. Surmeier, D.J., J.A. Obeso, and G.M. Halliday, *Selective neuronal vulnerability in Parkinson disease*. Nature Reviews Neuroscience, 2017. **18**(2): p. 101-113.
42. Jankovic, J. and E.K. Tan, *Parkinson's disease: Etiopathogenesis and treatment*. Journal of Neurology, Neurosurgery & Psychiatry, 2020. **91**(8): p. 795-808.
43. Wirdefeldt, K., et al., *Epidemiology and etiology of Parkinson's disease: a review of the evidence*. European journal of epidemiology, 2011. **26**(1): p. 1-58.
44. Brodacki, B., et al., *Serum interleukin (IL-2, IL-10, IL-6, IL-4), TNF α , and INF γ concentrations are elevated in patients with atypical and idiopathic parkinsonism*. Neuroscience letters, 2008. **441**(2): p. 158-162.
45. Reale, M., et al., *Peripheral cytokines profile in Parkinson's disease*. Brain, behavior, and immunity, 2009. **23**(1): p. 55-63.
46. Braak, H., et al., *Idiopathic Parkinson's disease: possible routes by which vulnerable neuronal types may be subject to neuroinvasion by an unknown pathogen*. Journal of neural transmission, 2003. **110**(5): p. 517-536.

47. Chen, Z. and B.D. Trapp, *Microglia and neuroprotection*. Journal of neurochemistry, 2016. **136**: p. 10-17.
48. Blum-Degen, D., et al., *Interleukin-1 β and interleukin-6 are elevated in the cerebrospinal fluid of Alzheimer's and de novo Parkinson's disease patients*. Neuroscience letters, 1995. **202**(1-2): p. 17-20.
49. Grozdanov, V., et al., *Inflammatory dysregulation of blood monocytes in Parkinson's disease patients*. Acta neuropathologica, 2014. **128**(5): p. 651-663.
50. Fan, Z., et al., *Systemic activation of NLRP3 inflammasome and plasma α -synuclein levels are correlated with motor severity and progression in Parkinson's disease*. Journal of neuroinflammation, 2020. **17**(1): p. 1-10.
51. Panicker, N., et al., *Fyn kinase regulates misfolded α -synuclein uptake and NLRP3 inflammasome activation in microglia*. Journal of Experimental Medicine, 2019. **216**(6): p. 1411-1430.
52. Earls, R.H., et al., *Intrastriatal injection of preformed alpha-synuclein fibrils alters central and peripheral immune cell profiles in non-transgenic mice*. Journal of Neuroinflammation, 2019. **16**(1): p. 1-15.
53. Kuhbandner, K., et al., *alpha-Synuclein: a modulator during inflammatory CNS demyelination*. Journal of Molecular Neuroscience, 2020. **70**(7): p. 1038-1049.
54. da Silva, D.J., et al., *Decreased toll-like receptor 2 and toll-like receptor 7/8-induced cytokines in Parkinson's disease patients*. Neuroimmunomodulation, 2016. **23**(1): p. 58-66.
55. Drouin-Ouellet, J., et al., *Toll-like receptor expression in the blood and brain of patients and a mouse model of Parkinson's disease*. International Journal of Neuropsychopharmacology, 2015. **18**(6).
56. Kim, C., et al., *Neuron-released oligomeric α -synuclein is an endogenous agonist of TLR2 for paracrine activation of microglia*. Nature communications, 2013. **4**(1): p. 1-12.
57. Dzamko, N., et al., *Toll-like receptor 2 is increased in neurons in Parkinson's disease brain and may contribute to alpha-synuclein pathology*. Acta neuropathologica, 2017. **133**(2): p. 303-319.
58. Kouli, A., C. Horne, and C. Williams-Gray, *Toll-like receptors and their therapeutic potential in Parkinson's disease and α -synucleinopathies*. Brain, behavior, and immunity, 2019. **81**: p. 41-51.

59. Hughes, C.D., et al., *Picomolar concentrations of oligomeric alpha-synuclein sensitizes TLR4 to play an initiating role in Parkinson's disease pathogenesis*. *Acta neuropathologica*, 2019. **137**(1): p. 103-120.
60. Shin, W.-H., et al., *Induction of microglial toll-like receptor 4 by prothrombin kringle-2: a potential pathogenic mechanism in Parkinson's disease*. *Scientific reports*, 2015. **5**(1): p. 1-14.
61. Heidari, A., N. Yazdanpanah, and N. Rezaei, *The role of Toll-like receptors and neuroinflammation in Parkinson's disease*. *Journal of Neuroinflammation*, 2022. **19**(1): p. 1-21.
62. Perez-Pardo, P., et al., *Role of TLR4 in the gut-brain axis in Parkinson's disease: a translational study from men to mice*. *Gut*, 2019. **68**(5): p. 829-843.
63. Komatsu, M., et al., *Homeostatic levels of p62 control cytoplasmic inclusion body formation in autophagy-deficient mice*. *Cell*, 2007. **131**(6): p. 1149-1163.
64. Nezis, I.P., et al., *Ref (2) P, the Drosophila melanogaster homologue of mammalian p62, is required for the formation of protein aggregates in adult brain*. *The Journal of cell biology*, 2008. **180**(6): p. 1065-1071.
65. Pankiv, S., et al., *p62/SQSTM1 binds directly to Atg8/LC3 to facilitate degradation of ubiquitinated protein aggregates by autophagy*. *Journal of biological chemistry*, 2007. **282**(33): p. 24131-24145.
66. Bjørkøy, G., T. Lamark, and T. Johansen, *p62/SQSTM1: a missing link between protein aggregates and the autophagy machinery*. *Autophagy*, 2006. **2**(2): p. 138-139.
67. Müller-Taubenberger, A., A. Kortholt, and L. Eichinger, *Simple system—substantial share: the use of Dictyostelium in cell biology and molecular medicine*. *European journal of cell biology*, 2013. **92**(2): p. 45-53.
68. Calvo-Garrido, J. and R. Escalante, *Autophagy dysfunction and ubiquitin-positive protein aggregates in Dictyostelium cells lacking Vmp1*. *Autophagy*, 2010. **6**(1): p. 100-109.
69. Clarelli, F., et al., *Contribution of rare and low-frequency variants to multiple sclerosis susceptibility in the Italian continental population*. *Frontiers in genetics*, 2021: p. 2507.

70. Consortium*†, I.M.S.G., et al., *Multiple sclerosis genomic map implicates peripheral immune cells and microglia in susceptibility*. *Science*, 2019. **365**(6460): p. eaav7188.
71. Briggs, F., L. Leung, and L. Barcellos, *Annotation of functional variation within non-MHC MS susceptibility loci through bioinformatics analysis*. *Genes & Immunity*, 2014. **15**(7): p. 466-476.
72. Oksenberg, J. and L. Barcellos, *Multiple sclerosis genetics: leaving no stone unturned*. *Genes & Immunity*, 2005. **6**(5): p. 375-387.
73. Bjornevik, K., et al., *Longitudinal analysis reveals high prevalence of Epstein-Barr virus associated with multiple sclerosis*. *Science*, 2022. **375**(6578): p. 296-301.
74. Ghasemi, N., S. Razavi, and E. Nikzad, *Multiple sclerosis: pathogenesis, symptoms, diagnoses and cell-based therapy*. *Cell Journal (Yakhteh)*, 2017. **19**(1): p. 1.
75. Gandhi, R., A. Laroni, and H.L. Weiner, *Role of the innate immune system in the pathogenesis of multiple sclerosis*. *Journal of neuroimmunology*, 2010. **221**(1-2): p. 7-14.
76. Young, H.A. and K.J. Hardy, *Role of interferon- γ in immune cell regulation*. *Journal of leukocyte biology*, 1995. **58**(4): p. 373-381.
77. Sattler, A., et al., *Cytokine-induced human IFN- γ -secreting effector-memory Th cells in chronic autoimmune inflammation*. *Blood, The Journal of the American Society of Hematology*, 2009. **113**(9): p. 1948-1956.
78. Takeshita, Y. and R.M. Ransohoff, *Inflammatory cell trafficking across the blood-brain barrier: chemokine regulation and in vitro models*. *Immunological reviews*, 2012. **248**(1): p. 228-239.
79. Leech, S., et al., *Persistent endothelial abnormalities and blood-brain barrier leak in primary and secondary progressive multiple sclerosis*. *Neuropathology and applied neurobiology*, 2007. **33**(1): p. 86-98.
80. Larochelle, C., J.I. Alvarez, and A. Prat, *How do immune cells overcome the blood-brain barrier in multiple sclerosis?* *FEBS letters*, 2011. **585**(23): p. 3770-3780.
81. Cao, Y., et al., *Functional inflammatory profiles distinguish myelin-reactive T cells from patients with multiple sclerosis*. *Science translational medicine*, 2015. **7**(287): p. 287ra74-287ra74.

82. Chitnis, T., *The role of CD4 T cells in the pathogenesis of multiple sclerosis*. International review of neurobiology, 2007. **79**: p. 43-72.
83. Correale, J. and M.F. Farez, *The role of astrocytes in multiple sclerosis progression*. Frontiers in neurology, 2015. **6**: p. 180.
84. Guerrero, B.L. and N.L. Sicotte, *Microglia in multiple sclerosis: friend or foe?* Frontiers in immunology, 2020. **11**: p. 374.
85. Denic, A., B. Wootla, and M. Rodriguez, *CD8+ T cells in multiple sclerosis*. Expert opinion on therapeutic targets, 2013. **17**(9): p. 1053-1066.
86. Krumbholz, M., et al., *B cells and antibodies in multiple sclerosis pathogenesis and therapy*. Nature Reviews Neurology, 2012. **8**(11): p. 613-623.
87. Jelcic, I., et al., *Memory B cells activate brain-homing, autoreactive CD4+ T cells in multiple sclerosis*. Cell, 2018. **175**(1): p. 85-100. e23.
88. Consortium, I.I.G., et al., *Analysis of immune-related loci identifies 48 new susceptibility variants for multiple sclerosis*. Nature genetics, 2013. **45**(11): p. 1353-1360.
89. Ruhrmann, S., et al., *Hypermethylation of MIR21 in CD4+ T cells from patients with relapsing-remitting multiple sclerosis associates with lower miRNA-21 levels and concomitant up-regulation of its target genes*. Multiple Sclerosis Journal, 2018. **24**(10): p. 1288-1300.
90. Kaufmann, M., et al., *Identifying CNS-colonizing T cells as potential therapeutic targets to prevent progression of multiple sclerosis*. Med, 2021. **2**(3): p. 296-312. e8.
91. Soares, J.L., E.M. Oliveira, and A. Pontillo, *Variants in NLRP3 and NLRC4 inflammasome associate with susceptibility and severity of multiple sclerosis*. Multiple sclerosis and related disorders, 2019. **29**: p. 26-34.
92. Ming, X., et al., *Caspase-1 expression in multiple sclerosis plaques and cultured glial cells*. Journal of the neurological sciences, 2002. **197**(1-2): p. 9-18.
93. Kawana, N., et al., *Reactive astrocytes and perivascular macrophages express NLRP 3 inflammasome in active demyelinating lesions of multiple sclerosis and necrotic lesions of neuromyelitis optica and cerebral infarction*. Clinical and Experimental Neuroimmunology, 2013. **4**(3): p. 296-304.

94. Keane, R.W., W.D. Dietrich, and J.P. de Rivero Vaccari, *Inflammasome proteins as biomarkers of multiple sclerosis*. *Frontiers in neurology*, 2018. **9**: p. 135.
95. Malhotra, S., et al., *NLRP3 inflammasome as prognostic factor and therapeutic target in primary progressive multiple sclerosis patients*. *Brain*, 2020. **143**(5): p. 1414-1430.
96. McKenzie, B.A., et al., *Caspase-1 inhibition prevents glial inflammasome activation and pyroptosis in models of multiple sclerosis*. *Proceedings of the National Academy of Sciences*, 2018. **115**(26): p. E6065-E6074.
97. Medzhitov, R., *Origin and physiological roles of inflammation*. *Nature*, 2008. **454**(7203): p. 428-435.
98. Wang, Z., et al., *NLRP3 inflammasome and inflammatory diseases*. *Oxidative medicine and cellular longevity*, 2020. **2020**.
99. Voet, S., M. Prinz, and G. van Loo, *Microglia in central nervous system inflammation and multiple sclerosis pathology*. *Trends in molecular medicine*, 2019. **25**(2): p. 112-123.
100. Brikos, C. and L.A. O'Neill, *Signalling of toll-like receptors*. *Toll-like receptors (TLRs) and innate immunity*, 2008: p. 21-50.
101. Zhang, Y. and C. Liang, *Innate recognition of microbial-derived signals in immunity and inflammation*. *Science China Life Sciences*, 2016. **59**(12): p. 1210-1217.
102. Schaefer, L., *Complexity of danger: the diverse nature of damage-associated molecular patterns*. *Journal of Biological Chemistry*, 2014. **289**(51): p. 35237-35245.
103. Kawasaki, T. and T. Kawai, *Toll-like receptor signaling pathways*. *Frontiers in immunology*, 2014: p. 461.
104. Medzhitov, R., P. Preston-Hurlburt, and C.A. Janeway, *A human homologue of the Drosophila Toll protein signals activation of adaptive immunity*. *Nature*, 1997. **388**(6640): p. 394-397.
105. Park, B.S. and J.-O. Lee, *Recognition of lipopolysaccharide pattern by TLR4 complexes*. *Experimental & molecular medicine*, 2013. **45**(12): p. e66-e66.

106. Leonard, J.N., et al., *The TLR3 signaling complex forms by cooperative receptor dimerization*. Proceedings of the National Academy of Sciences, 2008. **105**(1): p. 258-263.
107. Burns, K., et al., *Inhibition of interleukin 1 receptor/Toll-like receptor signaling through the alternatively spliced, short form of MyD88 is due to its failure to recruit IRAK-4*. The Journal of experimental medicine, 2003. **197**(2): p. 263-268.
108. Cusson-Hermance, N., et al., *Rip1 mediates the Trif-dependent toll-like receptor 3-and 4-induced NF- κ B activation but does not contribute to interferon regulatory factor 3 activation*. Journal of Biological Chemistry, 2005. **280**(44): p. 36560-36566.
109. Li, X., S. Jiang, and R.I. Tapping, *Toll-like receptor signaling in cell proliferation and survival*. Cytokine, 2010. **49**(1): p. 1-9.
110. Kumar, H., T. Kawai, and S. Akira, *Pathogen recognition by the innate immune system*. International reviews of immunology, 2011. **30**(1): p. 16-34.
111. Moresco, E.M.Y., D. LaVine, and B. Beutler, *Toll-like receptors*. Current Biology, 2011. **21**(13): p. R488-R493.
112. Schroder, K. and J. Tschopp, *The inflammasomes*. cell, 2010. **140**(6): p. 821-832.
113. Place, D.E. and T.-D. Kanneganti, *Recent advances in inflammasome biology*. Current opinion in immunology, 2018. **50**: p. 32-38.
114. He, Y., H. Hara, and G. Núñez, *Mechanism and regulation of NLRP3 inflammasome activation*. Trends in biochemical sciences, 2016. **41**(12): p. 1012-1021.
115. Lu, A., et al., *Unified polymerization mechanism for the assembly of ASC-dependent inflammasomes*. Cell, 2014. **156**(6): p. 1193-1206.
116. Martinon, F., K. Burns, and J. Tschopp, *The inflammasome: a molecular platform triggering activation of inflammatory caspases and processing of proIL- β* . Molecular cell, 2002. **10**(2): p. 417-426.
117. Lei, Q., T. Yi, and C. Chen, *NF- κ B-Gasdermin D (GSDMD) axis couples oxidative stress and NACHT, LRR and PYD domains-containing protein 3 (NLRP3) inflammasome-mediated cardiomyocyte pyroptosis following myocardial infarction*. Medical Science Monitor: international medical journal of experimental and clinical research, 2018. **24**: p. 6044.

118. Shi, J., et al., *Cleavage of GSDMD by inflammatory caspases determines pyroptotic cell death*. Nature, 2015. **526**(7575): p. 660-665.
119. He, W.-t., et al., *Gasdermin D is an executor of pyroptosis and required for interleukin-1 β secretion*. Cell research, 2015. **25**(12): p. 1285-1298.
120. Leffler, H., et al., *Introduction to galectins*. Glycoconjugate journal, 2002. **19**(7): p. 433-440.
121. Nakahara, S. and A. Raz, *On the role of galectins in signal transduction*. Methods in enzymology, 2006. **417**: p. 273-289.
122. Delacour, D., A. Koch, and R. Jacob, *The role of galectins in protein trafficking*. Traffic, 2009. **10**(10): p. 1405-1413.
123. Boscher, C., J.W. Dennis, and I.R. Nabi, *Glycosylation, galectins and cellular signaling*. Current opinion in cell biology, 2011. **23**(4): p. 383-392.
124. Yang, R.-Y., G.A. Rabinovich, and F.-T. Liu, *Galectins: structure, function and therapeutic potential*. Expert reviews in molecular medicine, 2008. **10**.
125. Domic, J., S. Dabelic, and M. Flögel, *Galectin-3: an open-ended story*. Biochimica et Biophysica Acta (BBA)-General Subjects, 2006. **1760**(4): p. 616-635.
126. Funasaka, T., A. Raz, and P. Nangia-Makker. *Nuclear transport of galectin-3 and its therapeutic implications*. in *Seminars in cancer biology*. 2014. Elsevier.
127. Huflejt, M., et al., *L-29, a soluble lactose-binding lectin, is phosphorylated on serine 6 and serine 12 in vivo and by casein kinase I*. Journal of Biological Chemistry, 1993. **268**(35): p. 26712-26718.
128. Yang, R.-Y., et al., *Role of the carboxyl-terminal lectin domain in self-association of galectin-3*. Biochemistry, 1998. **37**(12): p. 4086-4092.
129. Mehul, B., et al., *Structure of baby hamster kidney carbohydrate-binding protein CBP30, an S-type animal lectin*. Journal of Biological Chemistry, 1994. **269**(27): p. 18250-18258.
130. Hsu, D.K., R.I. Zuberi, and F.-T. Liu, *Biochemical and biophysical characterization of human recombinant IgE-binding protein, an S-type animal lectin*. Journal of Biological Chemistry, 1992. **267**(20): p. 14167-14174.

131. Menon, R.P. and R.C. Hughes, *Determinants in the N-terminal domains of galectin-3 for secretion by a novel pathway circumventing the endoplasmic reticulum–Golgi complex*. European journal of biochemistry, 1999. **264**(2): p. 569-576.
132. Menon, R.P., M. Strom, and R.C. Hughes, *Interaction of a novel cysteine and histidine-rich cytoplasmic protein with galectin-3 in a carbohydrate-independent manner*. FEBS letters, 2000. **470**(3): p. 227-231.
133. Lukyanov, P., V. Furtak, and J. Ochieng, *Galectin-3 interacts with membrane lipids and penetrates the lipid bilayer*. Biochemical and biophysical research communications, 2005. **338**(2): p. 1031-1036.
134. Chen, Y., et al., *Gasdermin D drives the nonexosomal secretion of galectin-3, an insulin signal antagonist*. The Journal of Immunology, 2019. **203**(10): p. 2712-2723.
135. Burguillos, M.A., et al., *Microglia-secreted galectin-3 acts as a toll-like receptor 4 ligand and contributes to microglial activation*. Cell reports, 2015. **10**(9): p. 1626-1638.
136. Starossom, S.C., et al., *Galectin-1 deactivates classically activated microglia and protects from inflammation-induced neurodegeneration*. Immunity, 2012. **37**(2): p. 249-263.
137. Sirko, S., et al., *Astrocyte reactivity after brain injury—: the role of galectins 1 and 3*. Glia, 2015. **63**(12): p. 2340-2361.
138. Yan, Y.-P., et al., *Galectin-3 mediates post-ischemic tissue remodeling*. Brain research, 2009. **1288**: p. 116-124.
139. Lalancette-Hébert, M., et al., *Galectin-3 is required for resident microglia activation and proliferation in response to ischemic injury*. Journal of Neuroscience, 2012. **32**(30): p. 10383-10395.
140. Pasquini, L.A., et al., *Galectin-3 drives oligodendrocyte differentiation to control myelin integrity and function*. Cell Death & Differentiation, 2011. **18**(11): p. 1746-1756.
141. Siew, J.J. and Y. Chern, *Microglial lectins in health and neurological diseases*. Frontiers in molecular neuroscience, 2018. **11**: p. 158.

142. de Jong, C.G., H.-J. Gabius, and W. Baron, *The emerging role of galectins in (re) myelination and its potential for developing new approaches to treat multiple sclerosis*. Cellular and Molecular Life Sciences, 2020. **77**(7): p. 1289-1317.
143. Rahimian, R., L.-C. Béland, and J. Kriz, *Galectin-3: mediator of microglia responses in injured brain*. Drug discovery today, 2018. **23**(2): p. 375-381.
144. Rahimian, R., et al., *Delayed galectin-3-mediated reprogramming of microglia after stroke is protective*. Molecular Neurobiology, 2019. **56**(9): p. 6371-6385.
145. Nishikawa, H. and H. Suzuki, *Possible role of inflammation and galectin-3 in brain injury after subarachnoid hemorrhage*. Brain sciences, 2018. **8**(2): p. 30.
146. Boza-Serrano, A., et al., *Galectin-3, a novel endogenous TREM2 ligand, detrimentally regulates inflammatory response in Alzheimer's disease*. Acta neuropathologica, 2019. **138**(2): p. 251-273.
147. Tao, C.-C., et al., *Galectin-3 promotes A β oligomerization and A β toxicity in a mouse model of Alzheimer's disease*. Cell Death & Differentiation, 2020. **27**(1): p. 192-209.
148. Li, Y., et al., *Galectin-3 is a negative regulator of lipopolysaccharide-mediated inflammation*. The Journal of Immunology, 2008. **181**(4): p. 2781-2789.
149. Sharma, M. and E. de Alba, *Structure, activation and regulation of NLRP3 and AIM2 inflammasomes*. International Journal of Molecular Sciences, 2021. **22**(2): p. 872.
150. Vanasco, V., et al., *Mitochondrial Dynamics and VMP1-Related Selective Mitophagy in Experimental Acute Pancreatitis*. Frontiers in Cell and Developmental Biology, 2021. **9**: p. 498.
151. Lind, N.A., et al., *Regulation of the nucleic acid-sensing Toll-like receptors*. Nature Reviews Immunology, 2022. **22**(4): p. 224-235.
152. Gavin, A.L., et al., *PLD3 and PLD4 are single-stranded acid exonucleases that regulate endosomal nucleic-acid sensing*. Nature immunology, 2018. **19**(9): p. 942-953.
153. Pisitkun, P., et al., *Autoreactive B cell responses to RNA-related antigens due to TLR7 gene duplication*. Science, 2006. **312**(5780): p. 1669-1672.

154. Subramanian, S., et al., *A Tlr7 translocation accelerates systemic autoimmunity in murine lupus*. Proceedings of the National Academy of Sciences, 2006. **103**(26): p. 9970-9975.
155. Deane, J.A., et al., *Control of toll-like receptor 7 expression is essential to restrict autoimmunity and dendritic cell proliferation*. Immunity, 2007. **27**(5): p. 801-810.
156. Marshak-Rothstein, A., *Toll-like receptors in systemic autoimmune disease*. Nature Reviews Immunology, 2006. **6**(11): p. 823-835.
157. Lande, R., et al., *Plasmacytoid dendritic cells sense self-DNA coupled with antimicrobial peptide*. Nature, 2007. **449**(7162): p. 564-569.
158. Gilliet, M. and R. Lande, *Antimicrobial peptides and self-DNA in autoimmune skin inflammation*. Current opinion in immunology, 2008. **20**(4): p. 401-407.
159. Leadbetter, E.A., et al., *Chromatin-IgG complexes activate B cells by dual engagement of IgM and Toll-like receptors*. Nature, 2002. **416**(6881): p. 603-607.
160. Sun, H., et al., *A nuclear export signal is required for cGAS to sense cytosolic DNA*. Cell Reports, 2021. **34**(1): p. 108586.
161. Meng, L., et al., *Toll-like receptor 3 upregulation in macrophages participates in the initiation and maintenance of pristane-induced arthritis in rats*. Arthritis research & therapy, 2010. **12**(3): p. 1-12.
162. de Oliveira, R.T.G., et al., *ERVs-TLR3-IRF axis is linked to myelodysplastic syndrome pathogenesis*. Medical Oncology, 2021. **38**(3): p. 1-12.
163. Ospelt, C., et al., *Overexpression of toll-like receptors 3 and 4 in synovial tissue from patients with early rheumatoid arthritis: toll-like receptor expression in early and longstanding arthritis*. Arthritis & Rheumatism: Official Journal of the American College of Rheumatology, 2008. **58**(12): p. 3684-3692.
164. Zhang, Z., et al., *Upregulation of HMGB1-TLR4 inflammatory pathway in focal cortical dysplasia type II*. Journal of neuroinflammation, 2018. **15**(1): p. 1-11.
165. Bruce, J.I. and A.D. James, *Targeting the calcium signalling machinery in cancer*. Cancers, 2020. **12**(9): p. 2351.
166. Marchi, S., et al., *Ca²⁺ fluxes and cancer*. Molecular cell, 2020. **78**(6): p. 1055-1069.

167. Trebak, M. and J.-P. Kinet, *Calcium signalling in T cells*. Nature Reviews Immunology, 2019. **19**(3): p. 154-169.
168. Sun, Y., et al., *Inhibition of store-operated calcium entry in microglia by helminth factors: implications for immune suppression in neurocysticercosis*. Journal of neuroinflammation, 2014. **11**(1): p. 1-12.
169. Chen, X.-X., et al., *TRPC3-mediated Ca²⁺ entry contributes to mouse airway smooth muscle cell proliferation induced by lipopolysaccharide*. Cell Calcium, 2016. **60**(4): p. 273-281.
170. Tauseef, M., et al., *TLR4 activation of TRPC6-dependent calcium signaling mediates endotoxin-induced lung vascular permeability and inflammation*. Journal of Experimental Medicine, 2012. **209**(11): p. 1953-1968.
171. Boonen, B., et al., *Differential effects of lipopolysaccharide on mouse sensory TRP channels*. Cell calcium, 2018. **73**: p. 72-81.
172. Yamashiro, K., et al., *Role of transient receptor potential vanilloid 2 in LPS-induced cytokine production in macrophages*. Biochemical and biophysical research communications, 2010. **398**(2): p. 284-289.
173. Li, M., et al., *Transient receptor potential vanilloid 4 is a critical mediator in LPS mediated inflammation by mediating calcineurin/NFATc3 signaling*. Biochemical and biophysical research communications, 2019. **513**(4): p. 1005-1012.
174. Schappe, M.S., et al., *Chanzyme TRPM7 mediates the Ca²⁺ influx essential for lipopolysaccharide-induced toll-like receptor 4 endocytosis and macrophage activation*. Immunity, 2018. **48**(1): p. 59-74. e5.
175. Liu, X., et al., *CaMKII promotes TLR-triggered proinflammatory cytokine and type I interferon production by directly binding and activating TAK1 and IRF3 in macrophages*. Blood, The Journal of the American Society of Hematology, 2008. **112**(13): p. 4961-4970.
176. Zhang, Q., M.J. Lenardo, and D. Baltimore, *30 years of NF- κ B: a blossoming of relevance to human pathobiology*. Cell, 2017. **168**(1-2): p. 37-57.
177. Qiu, X., K. Dong, and R. Sun, *STIM1 Regulates Endothelial Calcium Overload and Cytokine Upregulation During Sepsis*. Journal of Surgical Research, 2021. **263**: p. 236-244.

178. Li, S., et al., *Increasing extracellular Ca²⁺ sensitizes TNF-alpha-induced vascular cell adhesion molecule-1 (VCAM-1) via a TRPC1/ERK1/2/NFκB-dependent pathway in human vascular endothelial cells*. *Biochimica et Biophysica Acta (BBA)-Molecular Cell Research*, 2017. **1864**(10): p. 1566-1577.
179. Liu, L., et al., *TRPC6 attenuates cortical astrocytic apoptosis and inflammation in cerebral ischemic/reperfusion injury*. *Frontiers in Cell and Developmental Biology*, 2021. **8**: p. 594283.
180. Sang, L.-j., et al., *LncRNA CamK-A regulates Ca²⁺-signaling-mediated tumor microenvironment remodeling*. *Molecular cell*, 2018. **72**(1): p. 71-83. e7.
181. Song, T., et al., *Canonical transient receptor potential 3 channels activate NF-κB to mediate allergic airway disease via PKC-α/IκB-α and calcineurin/IκB-β pathways*. *The FASEB Journal*, 2016. **30**(1): p. 214-229.
182. Martin, T.P., et al., *CaMKIIδ interacts directly with IKKβ and modulates NF-κB signalling in adult cardiac fibroblasts*. *Cellular Signalling*, 2018. **51**: p. 166-175.
183. Jeon, S., et al., *Clozapine reduces Toll-like receptor 4/NF-κB-mediated inflammatory responses through inhibition of calcium/calmodulin-dependent Akt activation in microglia*. *Progress in Neuro-Psychopharmacology and Biological Psychiatry*, 2018. **81**: p. 477-487.
184. Pu, Y., et al., *The immunomodulatory effect of Poria cocos polysaccharides is mediated by the Ca²⁺/PKC/p38/NF-κB signaling pathway in macrophages*. *International Immunopharmacology*, 2019. **72**: p. 252-257.
185. Wang, Y.-X., L. Wang, and Y.-M. Zheng, *Canonical transient potential receptor-3 channels in normal and diseased airway smooth muscle cells*. *Calcium Signaling*, 2020: p. 471-487.
186. Liu, X., et al., *T cell receptor-induced nuclear factor κB (NF-κB) signaling and transcriptional activation are regulated by STIM1-and Orai1-mediated calcium entry*. *Journal of Biological Chemistry*, 2016. **291**(16): p. 8440-8452.
187. Riquelme, D., et al., *High-frequency field stimulation of primary neurons enhances ryanodine receptor-mediated Ca²⁺ release and generates hydrogen peroxide, which jointly stimulate NF-κB activity*. *Antioxidants & redox signaling*, 2011. **14**(7): p. 1245-1259.
188. Lee, G.-S., et al., *The calcium-sensing receptor regulates the NLRP3 inflammasome through Ca²⁺ and cAMP*. *Nature*, 2012. **492**(7427): p. 123-127.

189. Murakami, T., et al., *Critical role for calcium mobilization in activation of the NLRP3 inflammasome*. Proceedings of the National Academy of Sciences, 2012. **109**(28): p. 11282-11287.
190. Karmakar, M., et al., *Neutrophil P2X7 receptors mediate NLRP3 inflammasome-dependent IL-1 β secretion in response to ATP*. Nature communications, 2016. **7**(1): p. 1-13.
191. Zhong, Z., et al., *TRPM2 links oxidative stress to NLRP3 inflammasome activation*. Nature communications, 2013. **4**(1): p. 1-11.
192. Compan, V., et al., *Cell volume regulation modulates NLRP3 inflammasome activation*. Immunity, 2012. **37**(3): p. 487-500.
193. Wang, M., et al., *Roles of TRPA1 and TRPV1 in cigarette smoke-induced airway epithelial cell injury model*. Free Radical Biology and Medicine, 2019. **134**: p. 229-238.
194. Triantafilou, K., et al., *The complement membrane attack complex triggers intracellular Ca $^{2+}$ fluxes leading to NLRP3 inflammasome activation*. Journal of cell science, 2013. **126**(13): p. 2903-2913.
195. Chun, J. and A. Prince, *Ca $^{2+}$ signaling in airway epithelial cells facilitates leukocyte recruitment and transepithelial migration*. Journal of leukocyte biology, 2009. **86**(5): p. 1135-1144.
196. Chiang, C.-Y., et al., *Phospholipase C γ -2 and intracellular calcium are required for lipopolysaccharide-induced Toll-like receptor 4 (TLR4) endocytosis and interferon regulatory factor 3 (IRF3) activation*. Journal of Biological Chemistry, 2012. **287**(6): p. 3704-3709.
197. Jäger, E., et al., *Calcium-sensing receptor-mediated NLRP3 inflammasome response to calciprotein particles drives inflammation in rheumatoid arthritis*. Nature communications, 2020. **11**(1): p. 1-17.
198. Rossol, M., et al., *Extracellular Ca $^{2+}$ is a danger signal activating the NLRP3 inflammasome through G protein-coupled calcium sensing receptors*. Nature communications, 2012. **3**(1): p. 1-9.
199. Li, C., et al., *A mini-review on ion fluxes that regulate NLRP3 inflammasome activation*. Acta Biochimica et Biophysica Sinica, 2021. **53**(2): p. 131-139.
200. Liu, Q., et al., *The role of mitochondria in NLRP3 inflammasome activation*. Molecular immunology, 2018. **103**: p. 115-124.

201. Di, A., et al., *The TWIK2 potassium efflux channel in macrophages mediates NLRP3 inflammasome-induced inflammation*. *Immunity*, 2018. **49**(1): p. 56-65. e4.
202. Katsnelson, M.A., et al., *K⁺ efflux agonists induce NLRP3 inflammasome activation independently of Ca²⁺ signaling*. *The Journal of Immunology*, 2015. **194**(8): p. 3937-3952.
203. Srinivasan, S., et al., *Mitochondrial dysfunction and mitochondrial dynamics-The cancer connection*. *Biochimica et Biophysica Acta (BBA)-Bioenergetics*, 2017. **1858**(8): p. 602-614.
204. Adebayo, M., et al., *Mitochondrial fusion and fission: The fine-tune balance for cellular homeostasis*. *The FASEB Journal*, 2021. **35**(6): p. e21620.
205. Chan, D.C., *Mitochondrial fusion and fission in mammals*. *Annual review of cell and developmental biology*, 2006. **22**: p. 79-99.
206. Tondera, D., et al., *SLP-2 is required for stress-induced mitochondrial hyperfusion*. *The EMBO journal*, 2009. **28**(11): p. 1589-1600.
207. Rambold, A.S., et al., *Tubular network formation protects mitochondria from autophagosomal degradation during nutrient starvation*. *Proceedings of the National Academy of Sciences*, 2011. **108**(25): p. 10190-10195.
208. Gomes, L.C., G.D. Benedetto, and L. Scorrano, *During autophagy mitochondria elongate, are spared from degradation and sustain cell viability*. *Nature cell biology*, 2011. **13**(5): p. 589-598.
209. De Brito, O.M. and L. Scorrano, *Mitofusin 2 tethers endoplasmic reticulum to mitochondria*. *Nature*, 2008. **456**(7222): p. 605-610.
210. Leboucher, G.P., et al., *Stress-induced phosphorylation and proteasomal degradation of mitofusin 2 facilitates mitochondrial fragmentation and apoptosis*. *Molecular cell*, 2012. **47**(4): p. 547-557.
211. Chen, Y. and G.W. Dorn, *PINK1-phosphorylated mitofusin 2 is a Parkin receptor for culling damaged mitochondria*. *Science*, 2013. **340**(6131): p. 471-475.
212. Westermann, B., *Mitochondrial fusion and fission in cell life and death*. *Nature reviews Molecular cell biology*, 2010. **11**(12): p. 872-884.

213. Elgass, K., et al., *Recent advances into the understanding of mitochondrial fission*. Biochimica et Biophysica Acta (BBA)-Molecular Cell Research, 2013. **1833**(1): p. 150-161.
214. Detmer, S.A. and D.C. Chan, *Functions and dysfunctions of mitochondrial dynamics*. Nature reviews Molecular cell biology, 2007. **8**(11): p. 870-879.
215. Machiela, E., et al., *Disruption of mitochondrial dynamics increases stress resistance through activation of multiple stress response pathways*. The FASEB Journal, 2020. **34**(6): p. 8475-8492.
216. Chakrabarti, R., et al., *INF2-mediated actin polymerization at the ER stimulates mitochondrial calcium uptake, inner membrane constriction, and division*. Journal of Cell Biology, 2018. **217**(1): p. 251-268.
217. Zhou, R., et al., *A role for mitochondria in NLRP3 inflammasome activation*. Nature, 2011. **469**(7329): p. 221-225.
218. Zhang, Q., et al., *Circulating mitochondrial DAMPs cause inflammatory responses to injury*. Nature, 2010. **464**(7285): p. 104-107.
219. de Torre-Minguela, C., et al., *Gasdermins mediate cellular release of mitochondrial DNA during pyroptosis and apoptosis*. The FASEB Journal, 2021. **35**(8): p. e21757.
220. Zhong, Z., et al., *New mitochondrial DNA synthesis enables NLRP3 inflammasome activation*. Nature, 2018. **560**(7717): p. 198-203.
221. Shimada, K., et al., *Oxidized mitochondrial DNA activates the NLRP3 inflammasome during apoptosis*. Immunity, 2012. **36**(3): p. 401-414.
222. Nakahira, K., et al., *Autophagy proteins regulate innate immune response by inhibiting NALP3 inflammasome-mediated mitochondrial DNA release*. Nature immunology, 2011. **12**(3): p. 222.
223. Lemasters, J.J., et al., *Mitochondrial calcium and the permeability transition in cell death*. Biochimica et Biophysica Acta (BBA)-Bioenergetics, 2009. **1787**(11): p. 1395-1401.
224. Allam, R., et al., *Mitochondrial apoptosis is dispensable for NLRP 3 inflammasome activation but non-apoptotic caspase-8 is required for inflammasome priming*. EMBO reports, 2014. **15**(9): p. 982-990.

225. Subramanian, N., et al., *The adaptor MAVS promotes NLRP3 mitochondrial localization and inflammasome activation*. Cell, 2013. **153**(2): p. 348-361.
226. Dudek, J., *Role of cardiolipin in mitochondrial signaling pathways*. Frontiers in cell and developmental biology, 2017. **5**: p. 90.
227. Iyer, S.S., et al., *Mitochondrial cardiolipin is required for Nlrp3 inflammasome activation*. Immunity, 2013. **39**(2): p. 311-323.
228. Elliott, E.I., et al., *Cutting edge: mitochondrial assembly of the NLRP3 inflammasome complex is initiated at priming*. The Journal of Immunology, 2018. **200**(9): p. 3047-3052.
229. Chen, J. and Z.J. Chen, *PtdIns4P on dispersed trans-Golgi network mediates NLRP3 inflammasome activation*. Nature, 2018. **564**(7734): p. 71-76.
230. Yu, L. and P. Liu, *Cytosolic DNA sensing by cGAS: regulation, function, and human diseases*. Signal Transduction and Targeted Therapy, 2021. **6**(1): p. 1-15.
231. Ishikawa, H. and G.N. Barber, *STING is an endoplasmic reticulum adaptor that facilitates innate immune signalling*. Nature, 2008. **455**(7213): p. 674-678.
232. Sun, L., et al., *Cyclic GMP-AMP synthase is a cytosolic DNA sensor that activates the type I interferon pathway*. Science, 2013. **339**(6121): p. 786-791.
233. Hornung, V., et al., *AIM2 recognizes cytosolic dsDNA and forms a caspase-1-activating inflammasome with ASC*. Nature, 2009. **458**(7237): p. 514-518.
234. Fernandes-Alnemri, T., et al., *AIM2 activates the inflammasome and cell death in response to cytoplasmic DNA*. Nature, 2009. **458**(7237): p. 509-513.
235. Gaidt, M.M., et al., *The DNA inflammasome in human myeloid cells is initiated by a STING-cell death program upstream of NLRP3*. Cell, 2017. **171**(5): p. 1110-1124. e18.
236. Yu, C.-H., et al., *TDP-43 triggers mitochondrial DNA release via mPTP to activate cGAS/STING in ALS*. Cell, 2020. **183**(3): p. 636-649. e18.
237. Axe, E.L., et al., *Autophagosome formation from membrane compartments enriched in phosphatidylinositol 3-phosphate and dynamically connected to the endoplasmic reticulum*. The Journal of cell biology, 2008. **182**(4): p. 685-701.

238. Graef, M., et al., *ER exit sites are physical and functional core autophagosome biogenesis components*. Molecular biology of the cell, 2013. **24**(18): p. 2918-2931.
239. Hamasaki, M., et al., *Autophagosomes form at ER-mitochondria contact sites*. Nature, 2013. **495**(7441): p. 389-393.
240. Hayashi-Nishino, M., et al., *A subdomain of the endoplasmic reticulum forms a cradle for autophagosome formation*. Nature cell biology, 2009. **11**(12): p. 1433-1437.
241. Ylä-Anttila, P., et al., *3D tomography reveals connections between the phagophore and endoplasmic reticulum*. Autophagy, 2009. **5**(8): p. 1180-1185.
242. Ktistakis, N.T. and S.A. Tooze, *Digesting the expanding mechanisms of autophagy*. Trends in cell biology, 2016. **26**(8): p. 624-635.
243. Ganley, I.G., et al., *Distinct autophagosomal-lysosomal fusion mechanism revealed by thapsigargin-induced autophagy arrest*. Molecular cell, 2011. **42**(6): p. 731-743.
244. Engedal, N., et al., *Modulation of intracellular calcium homeostasis blocks autophagosome formation*. Autophagy, 2013. **9**(10): p. 1475-1490.
245. Vandecaetsbeek, I., et al., *The Ca²⁺ pumps of the endoplasmic reticulum and Golgi apparatus*. Cold Spring Harbor perspectives in biology, 2011. **3**(5): p. a004184.
246. Romero-Garcia, S. and H. Prado-Garcia, *Mitochondrial calcium: Transport and modulation of cellular processes in homeostasis and cancer*. International Journal of Oncology, 2019. **54**(4): p. 1155-1167.
247. Imbert, N., et al., *Abnormal calcium homeostasis in Duchenne muscular dystrophy myotubes contracting in vitro*. Cell calcium, 1995. **18**(3): p. 177-186.
248. Budd, S. and D. Nicholls, *A reevaluation of the role of mitochondria in neuronal Ca²⁺ homeostasis*. Journal of neurochemistry, 1996. **66**(1): p. 403-411.
249. Hartmann, J. and A. Verkhratsky, *Relations between intracellular Ca²⁺ stores and store-operated Ca²⁺ entry in primary cultured human glioblastoma cells*. The Journal of Physiology, 1998. **513**(2): p. 411-424.

250. Jouaville, L.S., et al., *Regulation of mitochondrial ATP synthesis by calcium: evidence for a long-term metabolic priming*. Proceedings of the National Academy of Sciences, 1999. **96**(24): p. 13807-13812.
251. Rizzuto, R., et al., *Close contacts with the endoplasmic reticulum as determinants of mitochondrial Ca²⁺ responses*. Science, 1998. **280**(5370): p. 1763-1766.
252. Gomez-Suaga, P., et al., *The ER-mitochondria tethering complex VAPB-PTPIP51 regulates autophagy*. Current Biology, 2017. **27**(3): p. 371-385.
253. Ohshima, Y., et al., *Disrupting mitochondrial Ca²⁺ homeostasis causes tumor-selective TRAIL sensitization through mitochondrial network abnormalities*. International Journal of Oncology, 2017. **51**(4): p. 1146-1158.
254. Hajnóczky, G., et al., *Decoding of cytosolic calcium oscillations in the mitochondria*. Cell, 1995. **82**(3): p. 415-424.
255. Nicholls, D.G., *Mitochondria and calcium signaling*. Cell calcium, 2005. **38**(3-4): p. 311-317.
256. Rizzuto, R., et al., *Mitochondria as biosensors of calcium microdomains*. Cell calcium, 1999. **26**(5): p. 193-200.
257. Robb-Gaspers, L.D., et al., *Integrating cytosolic calcium signals into mitochondrial metabolic responses*. The EMBO journal, 1998. **17**(17): p. 4987-5000.
258. Rutter, G.A., et al., *Subcellular imaging of intramitochondrial Ca²⁺ with recombinant targeted aequorin: significance for the regulation of pyruvate dehydrogenase activity*. Proceedings of the National Academy of Sciences, 1996. **93**(11): p. 5489-5494.
259. Jouaville, L.S., F. Ichas, and J.-P. Mazat, *Modulation of cell calcium signals by mitochondria*, in *Bioenergetics of the Cell: Quantitative Aspects*. 1998, Springer. p. 371-376.
260. Raaflaub, J., *Swelling of isolated mitochondria of the liver and their susceptibility to physicochemical influences*. Helvetica physiologica et pharmacologica acta, 1953. **11**(2): p. 142-156.
261. Hunter Jr, F.E. and L. Ford, *Inactivation of oxidative and phosphorylative systems in mitochondria by preincubation with phosphate and other ions*. Journal of Biological Chemistry, 1955. **216**(1): p. 357-369.

262. Karch, J. and J.D. Molkenin, *Identifying the components of the elusive mitochondrial permeability transition pore*. Proceedings of the National Academy of Sciences, 2014. **111**(29): p. 10396-10397.
263. Halestrap, A.P., S.J. Clarke, and S.A. Javadov, *Mitochondrial permeability transition pore opening during myocardial reperfusion—a target for cardioprotection*. Cardiovascular research, 2004. **61**(3): p. 372-385.
264. Gelmetti, V., et al., *PINK1 and BECN1 relocate at mitochondria-associated membranes during mitophagy and promote ER-mitochondria tethering and autophagosome formation*. Autophagy, 2017. **13**(4): p. 654-669.
265. Narendra, D., et al., *Parkin is recruited selectively to impaired mitochondria and promotes their autophagy*. The Journal of cell biology, 2008. **183**(5): p. 795-803.
266. Narendra, D.P., et al., *PINK1 is selectively stabilized on impaired mitochondria to activate Parkin*. PLoS biology, 2010. **8**(1): p. e1000298.
267. Vincow, E.S., et al., *The PINK1–Parkin pathway promotes both mitophagy and selective respiratory chain turnover in vivo*. Proceedings of the National Academy of Sciences, 2013. **110**(16): p. 6400-6405.
268. Ponpuak, M., et al., *Secretory autophagy*. Current opinion in cell biology, 2015. **35**: p. 106-116.
269. Rabouille, C., V. Malhotra, and W. Nickel, *Diversity in unconventional protein secretion*. Journal of cell science, 2012. **125**(22): p. 5251-5255.
270. Dupont, N., et al., *Autophagy-based unconventional secretory pathway for extracellular delivery of IL-1 β* . The EMBO journal, 2011. **30**(23): p. 4701-4711.
271. Jiang, S., et al., *Secretory versus degradative autophagy: unconventional secretion of inflammatory mediators*. Journal of innate immunity, 2013. **5**(5): p. 471-479.
272. Tan, H.W.S., et al., *A degradative to secretory autophagy switch mediates mitochondria clearance in the absence of the mATG8-conjugation machinery*. Nature Communications, 2022. **13**(1): p. 1-17.
273. Välimäki, E., et al., *Calpain activity is essential for ATP-driven unconventional vesicle-mediated protein secretion and inflammasome activation in human macrophages*. The Journal of Immunology, 2016. **197**(8): p. 3315-3325.

274. Välimäki, E., et al., *Monosodium urate activates Src/Pyk2/PI3 kinase and cathepsin dependent unconventional protein secretion from human primary macrophages*. *Molecular & Cellular Proteomics*, 2013. **12**(3): p. 749-763.
275. Cypryk, W., et al., *Proteomic and bioinformatic characterization of extracellular vesicles released from human macrophages upon influenza A virus infection*. *Journal of Proteome Research*, 2017. **16**(1): p. 217-227.
276. Cypryk, W., et al., *Quantitative proteomics of extracellular vesicles released from human monocyte-derived macrophages upon β -glucan stimulation*. *Journal of Proteome Research*, 2014. **13**(5): p. 2468-2477.
277. Lorey, M.B., et al., *Global characterization of protein secretion from human macrophages following non-canonical caspase-4/5 inflammasome activation*. *Molecular & Cellular Proteomics*, 2017. **16**(4): p. S187-S199.
278. Singhto, N., et al., *Roles of macrophage exosomes in immune response to calcium oxalate monohydrate crystals*. *Frontiers in immunology*, 2018. **9**: p. 316.
279. Bänfer, S., et al., *Molecular mechanism to recruit galectin-3 into multivesicular bodies for polarized exosomal secretion*. *Proceedings of the National Academy of Sciences*, 2018. **115**(19): p. E4396-E4405.
280. Welton, J.L., et al., *Proteomics analysis of bladder cancer exosomes*. *Molecular & cellular proteomics*, 2010. **9**(6): p. 1324-1338.
281. Théry, C., et al., *Proteomic analysis of dendritic cell-derived exosomes: a secreted subcellular compartment distinct from apoptotic vesicles*. *The Journal of Immunology*, 2001. **166**(12): p. 7309-7318.
282. Fei, F., et al., *B-cell precursor acute lymphoblastic leukemia and stromal cells communicate through Galectin-3*. *Oncotarget*, 2015. **6**(13): p. 11378.
283. Aarreberg, L.D., et al., *Interleukin-1 β induces mtDNA release to activate innate immune signaling via cGAS-STING*. *Molecular cell*, 2019. **74**(4): p. 801-815. e6.
284. Wang, S., et al., *Loss of acinar cell VMP1 triggers spontaneous pancreatitis in mice*. *Autophagy*, 2021: p. 1-11.
285. Ko, J.H., et al., *Rapamycin regulates macrophage activation by inhibiting NLRP3 inflammasome-p38 MAPK-NF κ B pathways in autophagy-and p62-dependent manners*. *Oncotarget*, 2017. **8**(25): p. 40817.

286. Bousset, L., et al., *Structural and functional characterization of two alpha-synuclein strains*. Nature communications, 2013. **4**(1): p. 1-13.
287. Sanjana, N.E., O. Shalem, and F. Zhang, *Improved vectors and genome-wide libraries for CRISPR screening*. Nature methods, 2014. **11**(8): p. 783-784.
288. Vermeire, J., et al., *Quantification of reverse transcriptase activity by real-time PCR as a fast and accurate method for titration of HIV, lenti-and retroviral vectors*. PloS one, 2012. **7**(12): p. e50859.
289. Zufferey, R., et al., *Self-inactivating lentivirus vector for safe and efficient in vivo gene delivery*. Journal of virology, 1998. **72**(12): p. 9873-9880.
290. Talley, S., et al., *A caspase-1 biosensor to monitor the progression of inflammation in vivo*. The Journal of Immunology, 2019. **203**(9): p. 2497-2507.
291. Burbidge, K., et al., *LGALS3 (galectin 3) mediates an unconventional secretion of SNCA/ α -synuclein in response to lysosomal membrane damage by the autophagic-lysosomal pathway in human midbrain dopamine neurons*. Autophagy, 2021: p. 1-29.
292. Luo, W. and C. Brouwer, *Pathview: an R/Bioconductor package for pathway-based data integration and visualization*. Bioinformatics, 2013. **29**(14): p. 1830-1831.
293. Kaja, S., et al., *Quantification of lactate dehydrogenase for cell viability testing using cell lines and primary cultured astrocytes*. Current protocols in toxicology, 2017. **72**(1): p. 2.26. 1-2.26. 10.
294. Böhler, P., et al., *The mycotoxin phomoxanthone A disturbs the form and function of the inner mitochondrial membrane*. Cell death & disease, 2018. **9**(3): p. 1-17.
295. Akimzhanov, A.M. and D. Boehning, *Monitoring dynamic changes in mitochondrial calcium levels during apoptosis using a genetically encoded calcium sensor*. JoVE (Journal of Visualized Experiments), 2011(50): p. e2579.
296. Rosa, H. and A.N. Malik, *Accurate Measurement of Cellular and Cell-Free Circulating Mitochondrial DNA Content from Human Blood Samples Using Real-Time Quantitative PCR*, in *Mitochondrial Medicine*. 2021, Springer. p. 247-268.
297. Rabinovich, G.A. and M.A. Toscano, *Turning'sweet'on immunity: galectin-glycan interactions in immune tolerance and inflammation*. Nature Reviews Immunology, 2009. **9**(5): p. 338-352.

298. Rabinovich, G.A., *Galectins: an evolutionarily conserved family of animal lectins with multifunctional properties; a trip from the gene to clinical therapy*. Cell Death & Differentiation, 1999. **6**(8): p. 711-721.
299. Perillo, N., M.E. Marcus, and L.G. Baum, *Galectins: versatile modulators of cell adhesion, cell proliferation, and cell death*. Journal of molecular medicine, 1998. **76**(6): p. 402-412.
300. Barrionuevo, P., et al., *A novel function for galectin-1 at the crossroad of innate and adaptive immunity: galectin-1 regulates monocyte/macrophage physiology through a nonapoptotic ERK-dependent pathway*. The Journal of Immunology, 2007. **178**(1): p. 436-445.
301. Rabinovich, G.A., et al., *Galectins and their ligands: amplifiers, silencers or tuners of the inflammatory response?* Trends in immunology, 2002. **23**(6): p. 313-320.
302. Brinchmann, M.F., D.M. Patel, and M.H. Iversen, *The role of galectins as modulators of metabolism and inflammation*. Mediators of inflammation, 2018. **2018**.
303. Kim, S.-J. and K.-H. Chun, *Non-classical role of Galectin-3 in cancer progression: translocation to nucleus by carbohydrate-recognition independent manner*. BMB reports, 2020. **53**(4): p. 173.
304. Flavin, W.P., et al., *Endocytic vesicle rupture is a conserved mechanism of cellular invasion by amyloid proteins*. Acta neuropathologica, 2017. **134**(4): p. 629-653.
305. Hughes, R.C., *Secretion of the galectin family of mammalian carbohydrate-binding proteins*. Biochimica et Biophysica Acta (BBA)-General Subjects, 1999. **1473**(1): p. 172-185.
306. García-Revilla, J., et al., *Reformulating pro-oxidant microglia in neurodegeneration*. Journal of Clinical Medicine, 2019. **8**(10): p. 1719.
307. Keller, M., et al., *Active caspase-1 is a regulator of unconventional protein secretion*. Cell, 2008. **132**(5): p. 818-831.
308. MacKinnon, A.C., et al., *Regulation of alternative macrophage activation by galectin-3*. The Journal of Immunology, 2008. **180**(4): p. 2650-2658.
309. Jia, J., et al., *Galectin-3 coordinates a cellular system for lysosomal repair and removal*. Developmental cell, 2020. **52**(1): p. 69-87. e8.

310. Freeman, D., et al., *Alpha-synuclein induces lysosomal rupture and cathepsin dependent reactive oxygen species following endocytosis*. PloS one, 2013. **8**(4): p. e62143.
311. Stewart, S.E., et al., *A genome-wide CRISPR screen reconciles the role of N-linked glycosylation in galectin-3 transport to the cell surface*. Journal of cell science, 2017. **130**(19): p. 3234-3247.
312. Schneider, D., et al., *Trafficking of galectin-3 through endosomal organelles of polarized and non-polarized cells*. European journal of cell biology, 2010. **89**(11): p. 788-798.
313. Harris, J., et al., *Autophagy controls IL-1 β secretion by targeting pro-IL-1 β for degradation*. Journal of Biological Chemistry, 2011. **286**(11): p. 9587-9597.
314. Andrei, C., et al., *The secretory route of the leaderless protein interleukin 1 β involves exocytosis of endolysosome-related vesicles*. Molecular biology of the cell, 1999. **10**(5): p. 1463-1475.
315. Andrei, C., et al., *Phospholipases C and A2 control lysosome-mediated IL-1 β secretion: implications for inflammatory processes*. Proceedings of the National Academy of Sciences, 2004. **101**(26): p. 9745-9750.
316. Xu, Y., et al., *Toll-like receptor 4 is a sensor for autophagy associated with innate immunity*. Immunity, 2007. **27**(1): p. 135-144.
317. Shi, C.-S. and J.H. Kehrl, *MyD88 and Trif target Beclin 1 to trigger autophagy in macrophages*. Journal of Biological Chemistry, 2008. **283**(48): p. 33175-33182.
318. Shi, C.-S., et al., *Activation of autophagy by inflammatory signals limits IL-1 β production by targeting ubiquitinated inflammasomes for destruction*. Nature immunology, 2012. **13**(3): p. 255-263.
319. Delgado, M.A., et al., *Toll-like receptors control autophagy*. The EMBO journal, 2008. **27**(7): p. 1110-1121.
320. Kayagaki, N., et al., *Caspase-11 cleaves gasdermin D for non-canonical inflammasome signalling*. Nature, 2015. **526**(7575): p. 666-671.
321. Suzuki, T., et al., *Differential regulation of caspase-1 activation, pyroptosis, and autophagy via Ipaf and ASC in Shigella-infected macrophages*. PLoS pathogens, 2007. **3**(8): p. e111.

322. Lamkanfi, M. and V.M. Dixit, *Mechanisms and functions of inflammasomes*. Cell, 2014. **157**(5): p. 1013-1022.
323. Willingham, S.B., et al., *NLRP3 (NALP3, Cryopyrin) facilitates in vivo caspase-1 activation, necrosis, and HMGB1 release via inflammasome-dependent and-independent pathways*. The Journal of Immunology, 2009. **183**(3): p. 2008-2015.
324. Lamkanfi, M., et al., *Inflammasome-dependent release of the alarmin HMGB1 in endotoxemia*. The Journal of immunology, 2010. **185**(7): p. 4385-4392.
325. Rajan, J.V., et al., *Activation of the NLRP3 inflammasome by intracellular poly I: C*. FEBS letters, 2010. **584**(22): p. 4627-4632.
326. Burbidge, K., et al., *Cargo and cell-specific differences in extracellular vesicle populations identified by multiplexed immunofluorescent analysis*. Journal of extracellular vesicles, 2020. **9**(1): p. 1789326.
327. Mizenko, R.R., et al., *Tetraspanins are unevenly distributed across single extracellular vesicles and bias sensitivity to multiplexed cancer biomarkers*. Journal of nanobiotechnology, 2021. **19**(1): p. 1-17.
328. Lombardi, M., et al., *Role of ATP in extracellular vesicle biogenesis and dynamics*. Frontiers in Pharmacology, 2021. **12**: p. 654023.
329. Vijayan, V., et al., *Human and murine macrophages exhibit differential metabolic responses to lipopolysaccharide-A divergent role for glycolysis*. Redox biology, 2019. **22**: p. 101147.
330. Schroder, K., et al., *Conservation and divergence in Toll-like receptor 4-regulated gene expression in primary human versus mouse macrophages*. Proceedings of the National Academy of Sciences, 2012. **109**(16): p. E944-E953.
331. Ma, H., et al., *Differential Macrophage Phenotype Rewired by Hantaan Virus Constrains the Magnitude of Inflammatory Responses in Murine versus Humans*. 2022.
332. Ventham, N., et al., *Integrative epigenome-wide analysis demonstrates that DNA methylation may mediate genetic risk in inflammatory bowel disease*. Nature communications, 2016. **7**(1): p. 1-14.
333. Amirfallah, A., et al., *High expression of the vacuole membrane protein 1 (VMP1) is a potential marker of poor prognosis in HER2 positive breast cancer*. PloS one, 2019. **14**(8): p. e0221413.

334. Mogensen, T.H., et al., *Activation of NF- κ B in virus-infected macrophages is dependent on mitochondrial oxidative stress and intracellular calcium: downstream involvement of the kinases TGF- β -activated kinase 1, mitogen-activated kinase/extracellular signal-regulated kinase kinase 1, and I κ B kinase*. The Journal of Immunology, 2003. **170**(12): p. 6224-6233.
335. Chauhan, A., et al., *M1 macrophage polarization is dependent on TRPC1-mediated calcium entry*. Iscience, 2018. **8**: p. 85-102.
336. Shoemaker, C.J., et al., *CRISPR screening using an expanded toolkit of autophagy reporters identifies TMEM41B as a novel autophagy factor*. PLoS biology, 2019. **17**(4): p. e2007044.
337. Shi, J., et al., *Inflammatory caspases are innate immune receptors for intracellular LPS*. Nature, 2014. **514**(7521): p. 187-192.
338. Coll, R.C., et al., *A small-molecule inhibitor of the NLRP3 inflammasome for the treatment of inflammatory diseases*. Nature medicine, 2015. **21**(3): p. 248-255.
339. Rayamajhi, M., Y. Zhang, and E.A. Miao, *Detection of pyroptosis by measuring released lactate dehydrogenase activity*, in *The Inflammasome*. 2013, Springer. p. 85-90.
340. Franceschini, A., et al., *The P2X7 receptor directly interacts with the NLRP3 inflammasome scaffold protein*. The FASEB Journal, 2015. **29**(6): p. 2450-2461.
341. Muñoz-Planillo, R., et al., *K⁺ efflux is the common trigger of NLRP3 inflammasome activation by bacterial toxins and particulate matter*. Immunity, 2013. **38**(6): p. 1142-1153.
342. Zhong, Z., et al., *NF- κ B restricts inflammasome activation via elimination of damaged mitochondria*. Cell, 2016. **164**(5): p. 896-910.
343. Youle, R.J. and A.M. Van Der Bliek, *Mitochondrial fission, fusion, and stress*. Science, 2012. **337**(6098): p. 1062-1065.
344. Lowes, H., et al., *Post-mortem ventricular cerebrospinal fluid cell-free-mtDNA in neurodegenerative disease*. Scientific reports, 2020. **10**(1): p. 1-10.
345. Chevriaux, A., et al., *Cathepsin B is required for NLRP3 inflammasome activation in macrophages, through NLRP3 interaction*. Frontiers in Cell and Developmental Biology, 2020. **8**: p. 167.

346. Junho, C.V.C., et al., *An overview of the role of calcium/calmodulin-dependent protein kinase in cardiorenal syndrome*. *Frontiers in Physiology*, 2020: p. 735.
347. Zhang, W., et al., *Cytosolic escape of mitochondrial DNA triggers cGAS-STING-NLRP3 axis-dependent nucleus pulposus cell pyroptosis*. *Experimental & molecular medicine*, 2022. **54**(2): p. 129-142.
348. Buratta, S., et al., *Lysosomal exocytosis, exosome release and secretory autophagy: the autophagic-and endo-lysosomal systems go extracellular*. *International journal of molecular sciences*, 2020. **21**(7): p. 2576.
349. Li, P., M. Gu, and H. Xu, *Lysosomal ion channels as decoders of cellular signals*. *Trends in Biochemical Sciences*, 2019. **44**(2): p. 110-124.
350. Yadati, T., et al., *The ins and outs of cathepsins: physiological function and role in disease management*. *Cells*, 2020. **9**(7): p. 1679.
351. Deretic, V. and B. Levine, *Autophagy balances inflammation in innate immunity*. *Autophagy*, 2018. **14**(2): p. 243-251.
352. Evavold, C.L., et al., *The pore-forming protein gasdermin D regulates interleukin-1 secretion from living macrophages*. *Immunity*, 2018. **48**(1): p. 35-44. e6.
353. Baroja-Mazo, A., et al., *Early endosome autoantigen 1 regulates IL-1 β release upon caspase-1 activation independently of gasdermin D membrane permeabilization*. *Scientific reports*, 2019. **9**(1): p. 1-10.
354. Manderson, A.P., et al., *Subcompartments of the macrophage recycling endosome direct the differential secretion of IL-6 and TNF α* . *The Journal of cell biology*, 2007. **178**(1): p. 57-69.
355. Xia, Y., et al., *The macrophage-specific V-ATPase subunit ATP6V0D2 restricts inflammasome activation and bacterial infection by facilitating autophagosome-lysosome fusion*. *Autophagy*, 2019. **15**(6): p. 960-975.
356. Saitoh, T., et al., *Loss of the autophagy protein Atg16L1 enhances endotoxin-induced IL-1 β production*. *Nature*, 2008. **456**(7219): p. 264-268.
357. Murray, R.Z. and J.L. Stow, *Cytokine secretion in macrophages: SNAREs, Rabs, and membrane trafficking*. *Frontiers in immunology*, 2014. **5**: p. 538.
358. Lopez-Castejon, G. and D. Brough, *Understanding the mechanism of IL-1 β secretion*. *Cytokine & growth factor reviews*, 2011. **22**(4): p. 189-195.

359. Popa, S.J., S.E. Stewart, and K. Moreau. *Unconventional secretion of annexins and galectins*. in *Seminars in cell & developmental biology*. 2018. Elsevier.
360. Swanson, K.V., M. Deng, and J.P.-Y. Ting, *The NLRP3 inflammasome: molecular activation and regulation to therapeutics*. *Nature Reviews Immunology*, 2019. **19**(8): p. 477-489.
361. Schinder, A.F., et al., *Mitochondrial dysfunction is a primary event in glutamate neurotoxicity*. *Journal of Neuroscience*, 1996. **16**(19): p. 6125-6133.
362. Bernardi, P., et al., *The mitochondrial permeability transition from in vitro artifact to disease target*. *The FEBS journal*, 2006. **273**(10): p. 2077-2099.
363. Elrod, J.W. and J.D. Molkenin, *Physiologic functions of cyclophilin D and the mitochondrial permeability transition pore*. *Circulation Journal*, 2013: p. CJ-13-0321.
364. Rottenberg, H. and J.B. Hoek, *The path from mitochondrial ROS to aging runs through the mitochondrial permeability transition pore*. *Aging cell*, 2017. **16**(5): p. 943-955.
365. Ding, Z., et al., *LOX-1, mtDNA damage, and NLRP3 inflammasome activation in macrophages: implications in atherogenesis*. *Cardiovascular research*, 2014. **103**(4): p. 619-628.
366. Yu, J., et al., *Inflammasome activation leads to Caspase-1–dependent mitochondrial damage and block of mitophagy*. *Proceedings of the National Academy of Sciences*, 2014. **111**(43): p. 15514-15519.
367. Bruchard, M., et al., *Chemotherapy-triggered cathepsin B release in myeloid-derived suppressor cells activates the Nlrp3 inflammasome and promotes tumor growth*. *Nature medicine*, 2013. **19**(1): p. 57-64.
368. Kimura, T., et al., *Dedicated SNARE s and specialized TRIM cargo receptors mediate secretory autophagy*. *The EMBO journal*, 2017. **36**(1): p. 42-60.
369. Hamilton, C. and P.K. Anand, *Right place, right time: localisation and assembly of the NLRP3 inflammasome*. *F1000Research*, 2019. **8**.
370. Misawa, T., et al., *Microtubule-driven spatial arrangement of mitochondria promotes activation of the NLRP3 inflammasome*. *Nature immunology*, 2013. **14**(5): p. 454-460.

371. Zhang, T., et al., *TMEM41B and VMP1 are phospholipid scramblases*. *Autophagy*, 2021. **17**(8): p. 2048-2050.
372. Gao, M., et al., *The biogenesis of lipid droplets: lipids take center stage*. *Progress in Lipid Research*, 2019. **75**: p. 100989.
373. Joshi, A.S., H. Zhang, and W.A. Prinz, *Organelle biogenesis in the endoplasmic reticulum*. *Nature cell biology*, 2017. **19**(8): p. 876-882.
374. Duewell, P., et al., *NLRP3 inflammasomes are required for atherogenesis and activated by cholesterol crystals*. *Nature*, 2010. **464**(7293): p. 1357-1361.
375. Dang, E.V., et al., *Oxysterol restraint of cholesterol synthesis prevents AIM2 inflammasome activation*. *Cell*, 2017. **171**(5): p. 1057-1071. e11.
376. Youm, Y.-H., et al., *The Nlrp3 inflammasome promotes age-related thymic demise and immunosenescence*. *Cell reports*, 2012. **1**(1): p. 56-68.
377. Guo, C., et al., *Cholesterol homeostatic regulator SCAP-SREBP2 integrates NLRP3 inflammasome activation and cholesterol biosynthetic signaling in macrophages*. *Immunity*, 2018. **49**(5): p. 842-856. e7.
378. Cruz, C.M., et al., *ATP activates a reactive oxygen species-dependent oxidative stress response and secretion of proinflammatory cytokines in macrophages*. *Journal of Biological Chemistry*, 2007. **282**(5): p. 2871-2879.
379. Jabaut, J., et al., *Mitochondria-targeted drugs enhance Nlrp3 inflammasome-dependent IL-1 β secretion in association with alterations in cellular redox and energy status*. *Free Radical Biology and Medicine*, 2013. **60**: p. 233-245.
380. Ichinohe, T., et al., *Mitochondrial protein mitofusin 2 is required for NLRP3 inflammasome activation after RNA virus infection*. *Proceedings of the National Academy of Sciences*, 2013. **110**(44): p. 17963-17968.

VITA

Stephanie Zack was born in Hinsdale, Illinois, on June 12, 1994 to Steven and Linda Zack. She earned her Bachelor of Arts degree in Chemistry from Carthage College in Kenosha, Wisconsin, in May 2016. During her undergraduate studies, Stephanie worked in the laboratory of Dr. Kevin Morris, studying chiral recognition by molecular micelles with molecular dynamics simulations.

After graduation, Stephanie then matriculated into the Loyola University Chicago Stritch School Infectious Disease and Immunology Graduate Program under the mentorship of Dr. Edward Campbell. Stephanie's thesis work focused on understanding how lidocaine and Zep peptides attenuate inflammatory responses. In 2018, Stephanie matriculated into the Loyola University Chicago Interdisciplinary Program in Biomedical Sciences. She joined the Department of Microbiology and Immunology and continued under the mentorship of Dr. Edward Campbell studying how the protein, vacuole membrane protein 1 (VMP1), regulates inflammatory responses. This work was supported by the T32 Immunology Training Grant awarded to Dr. Katherine Knight.

After completion of her graduate studies, Stephanie will continue to pursue her interest in scientific research and begin a postdoctoral position at the University of Illinois Chicago in the laboratory of Dr. Shiva Shahrara. She will investigate Notch signaling in rheumatoid arthritis.

